JET PROPULSION

Journal of the
AMERICAN ROCKET SOCIETY

Rocketry . . . . . Jet Propulsion Sciences . . . . . Astronautics

VOLUME 27 JULY 1957 **NUMBER 7**

Technical Notes

Cluster of three Hawks, Army's newest surface-to-air missiles, for use against low altitude attackers, are shown mounted on launcher

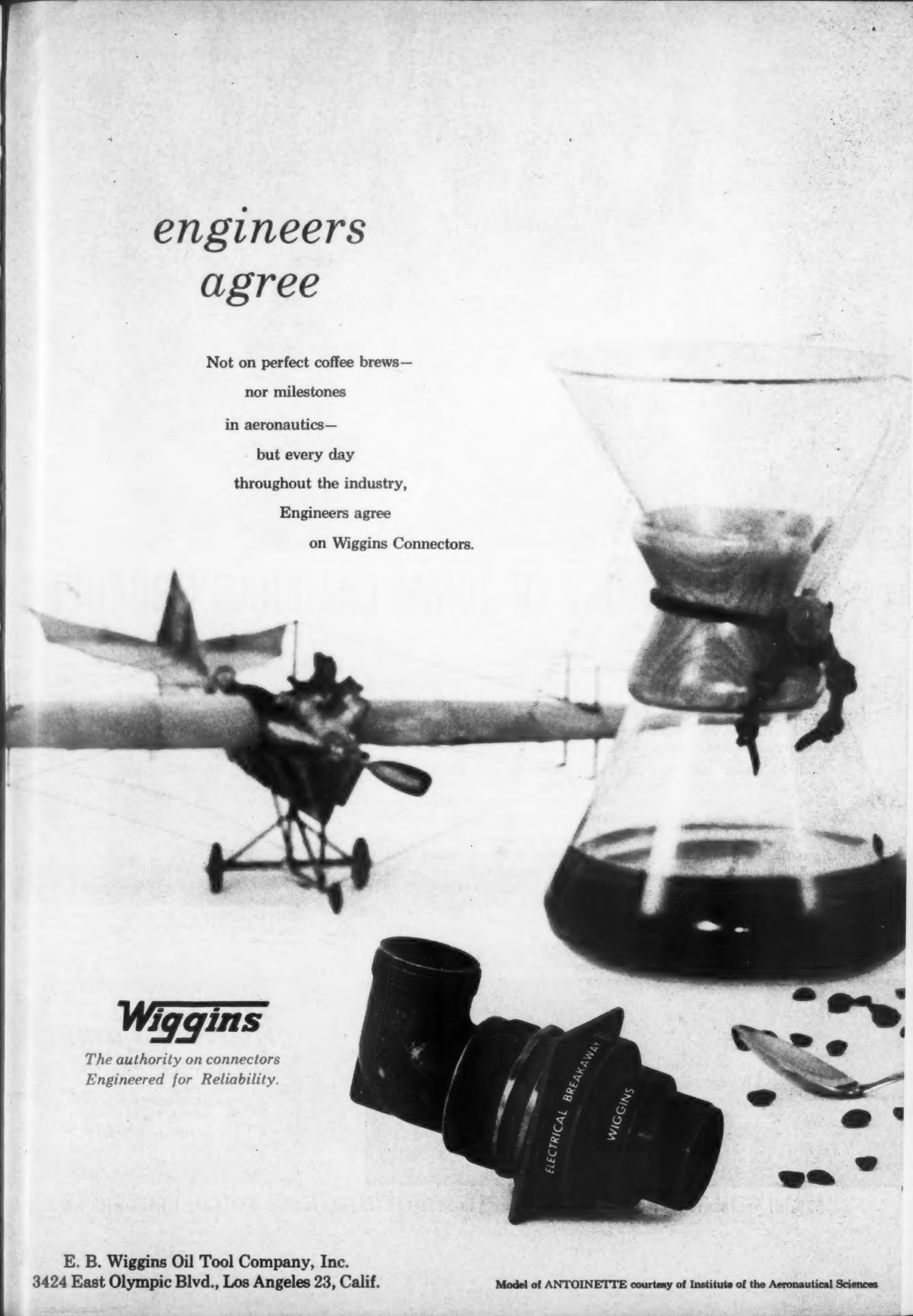
engineers
agree
Not on perfect coffee brews—
nor milestones
in aeronautics—
but every day
throughout the industry,
Engineers agree
on Wiggins Connectors.
Wiggins
The authority on connectors
Engineered for Reliability.
ELECTRICAL BREAKAWAY
WIGGINS
E. B. Wiggins Oil Tool Company, Inc.
3424 East Olympic Blvd., Los Angeles 23, Calif.
Model of ANTOINETTE courtesy of Institute of the Aeronautical Sciences

Scope of JET PROPULSION

JET PROPULSION, the Journal of the American Rocket Society, is devoted to the advancement of the field of jet propulsion through the publication of original papers disclosing new knowledge and new developments. The term "jet propulsion" as used herein is understood to embrace all engines that develop thrust by rearward discharge of a jet through a nozzle or duct; and thus it includes systems utilizing atmospheric air and underwater systems, as well as rocket engines. JET PROPULSION is open to contributions, either fundamental or applied, dealing with specialized aspects of jet and rocket propulsion, such as fuels and propellants, combustion, heat transfer, high temperature materials, mechanical design analyses, flight mechanics of jet-propelled vehicles, astronautics, and so forth. JET PROPULSION endeavors, also, to keep its subscribers informed of the affairs of the Society and of outstanding events in the rocket and jet propulsion field.

Limitation of Responsibility

Statements and opinions expressed in JET PROPULSION are to be understood as the individual expressions of the authors and do not necessarily reflect the views of the Editors or the Society.

Subscription Rates

One year for members (twelve monthly issues)	\$6.25
One year for nonmembers (twelve monthly issues)	\$12.50
Foreign countries, additional postage ... add	.50
Single copies	1.25
Special issues, single copies	2.50
Back numbers	2.00

Change of Address

Notices of change of address should be sent to the Secretary of the Society at least 30 days prior to the date of publication.

Information for Authors

Preparation of Manuscripts

Manuscripts must be double spaced on one side of paper only with wide margins to allow for instructions to printer. Submit two copies: original and first carbon. Include a 100–200 word abstract of paper. The title of the paper should be brief to simplify indexing. The author's name should be given without title, degree, or honor. A footnote on the first page should indicate the author's position and affiliation. Include only essential illustrations, tables, and mathematics. References should be grouped at the end of the manuscript; footnotes are reserved for comments on the text. Use American Standard symbols and abbreviations published by the American Standards Association. Greek letters should be identified clearly for the printer. References should be given as follows: For Journal Articles: Authors, Title, Journal, Volume, Year, Page Numbers. For Books: Author, Title, Publisher, City, Edition, Year, Page Numbers. Line drawings must be made with India ink on white paper or tracing cloth. Lettering on drawings should be large enough to permit reduction to standard one-column width, except for unusually complex drawings where such reduction would be prohibitive. Photographs should be clear, glossy prints. Legends must accompany each illustration submitted and should be listed in order on a separate sheet of paper.

Security Clearance

Manuscripts must be accompanied by written assurance as to security clearance in the event the subject matter of the manuscript is considered to lie in a classified area. Alternatively, written assurance that clearance is unnecessary should be submitted. Full responsibility for obtaining authoritative clearance rests with the author.

Submission of Manuscripts

Manuscripts should be submitted in duplicate to the Technical Editor, Martin Summerfield, Professor of Aeronautical Engineering, Princeton University, Princeton, N. J.

Manuscripts Presented at ARS Meetings

A manuscript submitted to the ARS Program Chairman and accepted for presentation at a national meeting will automatically be referred to the Editors for consideration for publication in JET PROPULSION, unless a contrary request is made by the author.

To Order Reprints

Prices for reprints will be sent to the author with the galley proof, and orders should accompany the corrected galley when it is returned to the Assistant Editor.

JET PROPULSION

Journal of the
AMERICAN ROCKET SOCIETY

JET PROPULSION, the Journal of the American Rocket Society and the American Interplanetary Society, published monthly by the American Rocket Society at 20th and Northampton Streets, Easton, Pa., U.S.A. The Editorial Office is located at 500 5th Ave., New York 36, N. Y. Price \$1.25 per copy, \$12.50 per year for nonmembers, \$6.25 per year for members: Entered as second-class matter at the Post Office at Easton, Pa., under the Act of March 3, 1879.

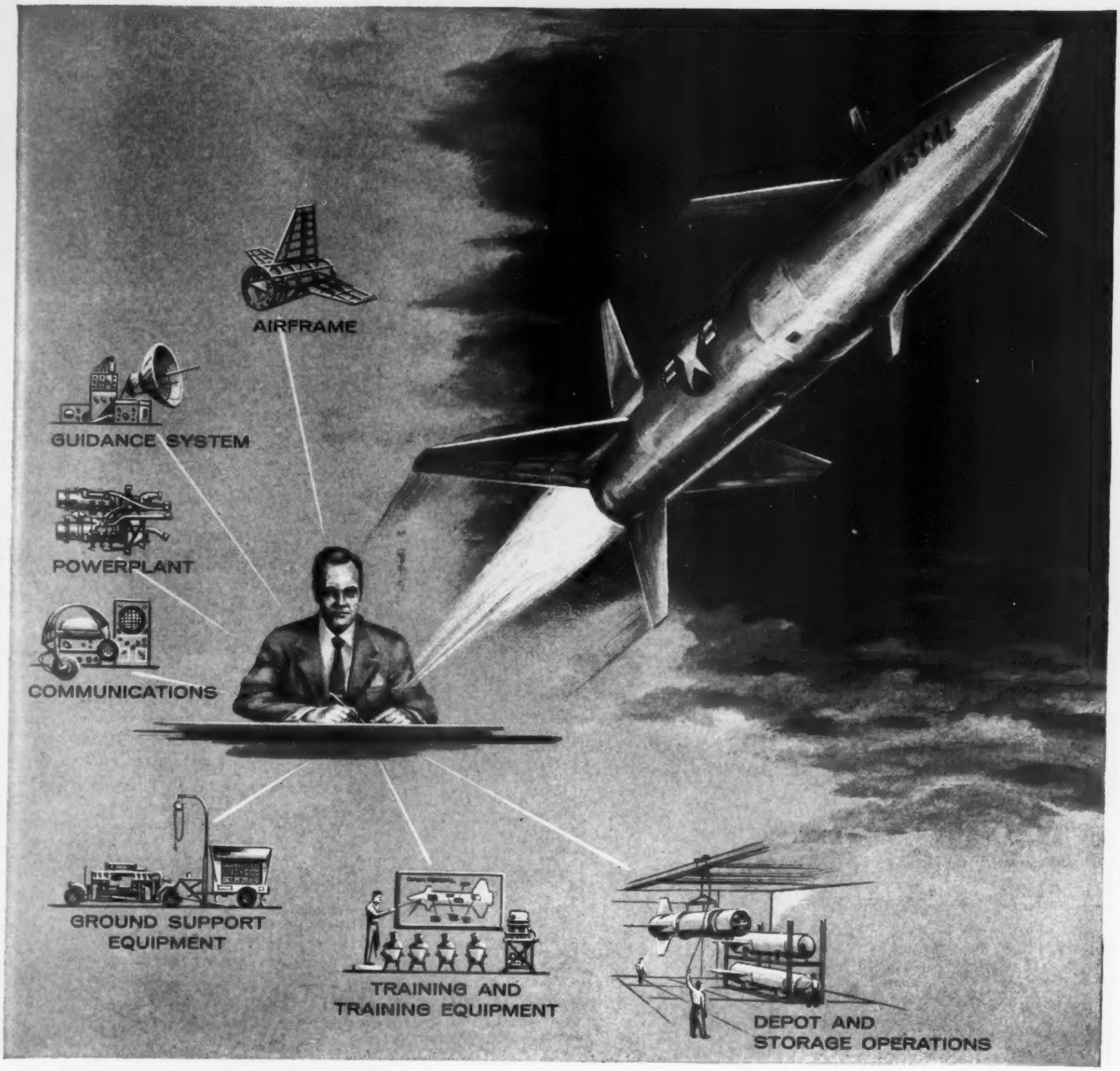

Weapon Systems Management

.....IS OUR BUSINESS

The air-to-surface GAM-63 "Rascal" of the USAF has already clearly demonstrated the capabilities of Bell Aircraft Corporation's *Guided Missiles Division* for the complete and highly efficient management of any weapon systems program.

This large and diversified team of specialists has the skills and experience necessary to follow a system through from the idea stage until it is operational. Each step—each phase is closely coordinated with time an ever essential consideration. Airframe, power plant and avionics are interrelated. Test and training devices, personnel training, ground support equipment and auxiliary systems follow in their proper sequence. The system comes into being under unified, centralized management—with dispatch and efficiency not possible in assembling component units which have been produced under a divided responsibility.

Some 100,000 man years of experience in this field have been logged by the men in the *Guided Missiles Division.* Their past is history worthy—their future important in our national defense.

BELL
Aircraft CORP.

Guided Missiles Div.
BUFFALO, N. Y.

VERSATILE TYPE 6885

PRESSURE SWITCH

ONE BASIC DESIGN

COVERS THE FULL RANGE

OF APPLICATIONS

PRESSURE ADJUSTMENT RANGE	15 to 25 psia	0.25 to 4 psi	2 - 10 psi	10 - 50 psi	50 - 150 psi	150 - 500 psi	500 - 800 psi	600 to 3,000 psi	DUAL VERSION
ACCURACY OF SETTING (Under all test conditions)	±1 psi	±0.3 psi at 2.5 psi setting	±0.5 psi at 5 psi setting	±4% at 50 psi setting	±3% at 100 psi setting	±4% at 500 psi setting	±4% at 800 psi setting	±60 psi at 3000 psi setting	According to selected ranges
PROOF PRESSURE (Without setpoint drift)	500 psi	100 psi	750 or 4,500 psi (as required)	750 or 4,500 psi (as required)	750 or 4,500 psi (as required)	750 or 4,500 psi (as required)	4,500 psi	4,500 psi	250 psi
BURST PRESSURE	750 psi	450 psi	1,000 or 7,500 psi (as required)					7,500 psi	450 psi
TEMPERATURE RANGE	−75° F. to +250° F.								
VIBRATION	Up to 2,000 cps at 40 g. Exceeds MIL-E-5272A Procedure I								
OVERALL DIMENSIONS	Switch Proper—2" Diameter; Length 4⅜". Mounting Bracket to Suit Application								3½" wide 4⅜" long
WEIGHT	9 Ounces							10.5 Ounces	16 Ounces
ELECTRICAL RATING	30 Volts, 2.5 Amperes Inductive Load at 50,000 Feet								

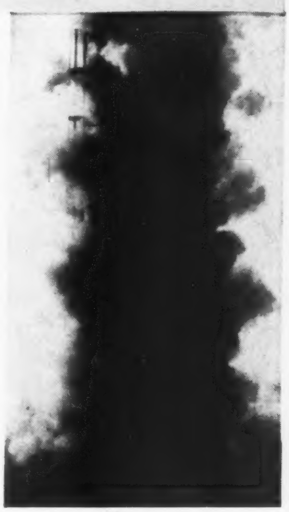

This pressure actuated switch is particularly designed for aircraft, rockets and missiles to control electrical circuits whenever the system pressure deviates from a specified value.

Integral vibration isolation between mounting bracket and switch body contributes greatly to exceptional performance under vibration and shock conditions. Switch performance remains well within the tolerance limits given in the above table.

The Type 6885 incorporates an enclosed snap-action switch, actuated by the movement of a limp diaphragm. *External* adjustment of the control set-point is easy with the unit installed for operation. Mounting position does not affect calibration, nor can pressures above the switch adjustment range deflect the diaphragm. The switch is immune to standard aircraft fluids and to corrosive media like oxidizers, rocket fuels, or Mil-O-7808 oil. Only Teflon and aluminum contact the pressure medium.

An alternate Type 6885 Pressure Switch has two independent sensing and switch elements inside two housings with a single electrical connector and one pressure port. The Type 6885 can also be supplied with two electrical switches for double-pole, double-throw, non-simultaneous actuation.

The wide range of operating pressures and functional perfection under vibration obtainable with the Type 6885 Pressure Switch recommends it for a variety of airborne applications. For engineering counsel, please address your inquiry to our headquarters plant, Danbury, Conn.

MAXWELL MANNING M&M & MOORE INC. TRADE MARK

MANNING, MAXWELL & MOORE, INC.

AIRCRAFT PRODUCTS DIVISION · DANBURY, CONNECTICUT · INGLEWOOD, CALIFORNIA

OUR AIRCRAFT PRODUCTS INCLUDE: TURBOJET ENGINE TEMPERATURE CONTROL AMPLIFIERS • ELECTRONIC AMPLIFIERS PRESSURE SWITCHES FOR ROCKETS, JET ENGINE AND AIRFRAME APPLICATIONS • PRESSURE GAUGES • THERMOCOUPLES HYDRAULIC VALVES • JET ENGINE AFTERBURNER CONTROL SYSTEMS.

We have many reasons for suggesting Firestone's Guided Missile Division as the likeliest spot for nurturing your brainstorms. Most important is our small-project approach to large-scale engineering problems. This select-team effort gives the highest possible ceiling for individual creativity. Within a reasonable framework of intelligent guidance, it makes the most of every man's potential, keeps frustrations and lost motion at a minimum.

You'll find a maximum of professional opportunity whether you join Firestone's development program for the Army's Corporal in Los Angeles...or the new Engineering Lab in idyllic Monterey—Carmel-by-the-Sea. In either spot, your family (and you) will fall in love with the Golden State of living!

Please write us today if you are brainstorming in these fields:

Aeronautics
Structures Air Frame
Stress Analysis
Propulsion System &
Component Design
Materials & Process

Firestone/GUIDED MISSILE DIVISION
RESEARCH • DEVELOPMENT • MANUFACTURE

FIND YOUR FUTURE AT FIRESTONE • LOS ANGELES • MONTEREY

WRITE: DIRECTOR OF ENGINEERING STAFF, LOS ANGELES 54, CALIFORNIA

FACTS

about

NEW DEPARTURE BALL BEARINGS

BALL BEARINGS MAKE GOOD PRODUCTS BETTER

NEW DEPARTURE • DIVISION OF GENERAL MOTORS • BRISTOL, CONN.


Getting them there
• on the button
• with maximum efficiency
• with perfect control
Typical FICo Systems and Instruments
FICo ASN-7 Course and Distance Computer System — indicator and control are shown. Can be provided with polar capabilities.
FICo Viewfinder Computing Timer — controls up to five aerial cameras simultaneously. Highly compact.
FICo Exhaust Temperature Indicator — range 200°C to 1000°C with ±5° accuracy. 6" long x 2" diam.
FICo Wind Memory Computer — an aid when navigational systems operate with Doppler.
FICo Magnetic Variation Computer — precludes need for manual correction in aero navigation.
FICo ASN-6 Present Position Computer System — indicator and control are shown.
No missile systems can be illustrated because of the level of classification. FICo is doing extensive work in ABMA's Redstone and Jupiter programs, in the Navy's Tartar and Terrier programs, and in other projects.
FICo Test Set — for flight line check out of navigational system. Self-contained and portable.
FICo Analog-to-Digital Converter — for airborne sensing system for traffic control.

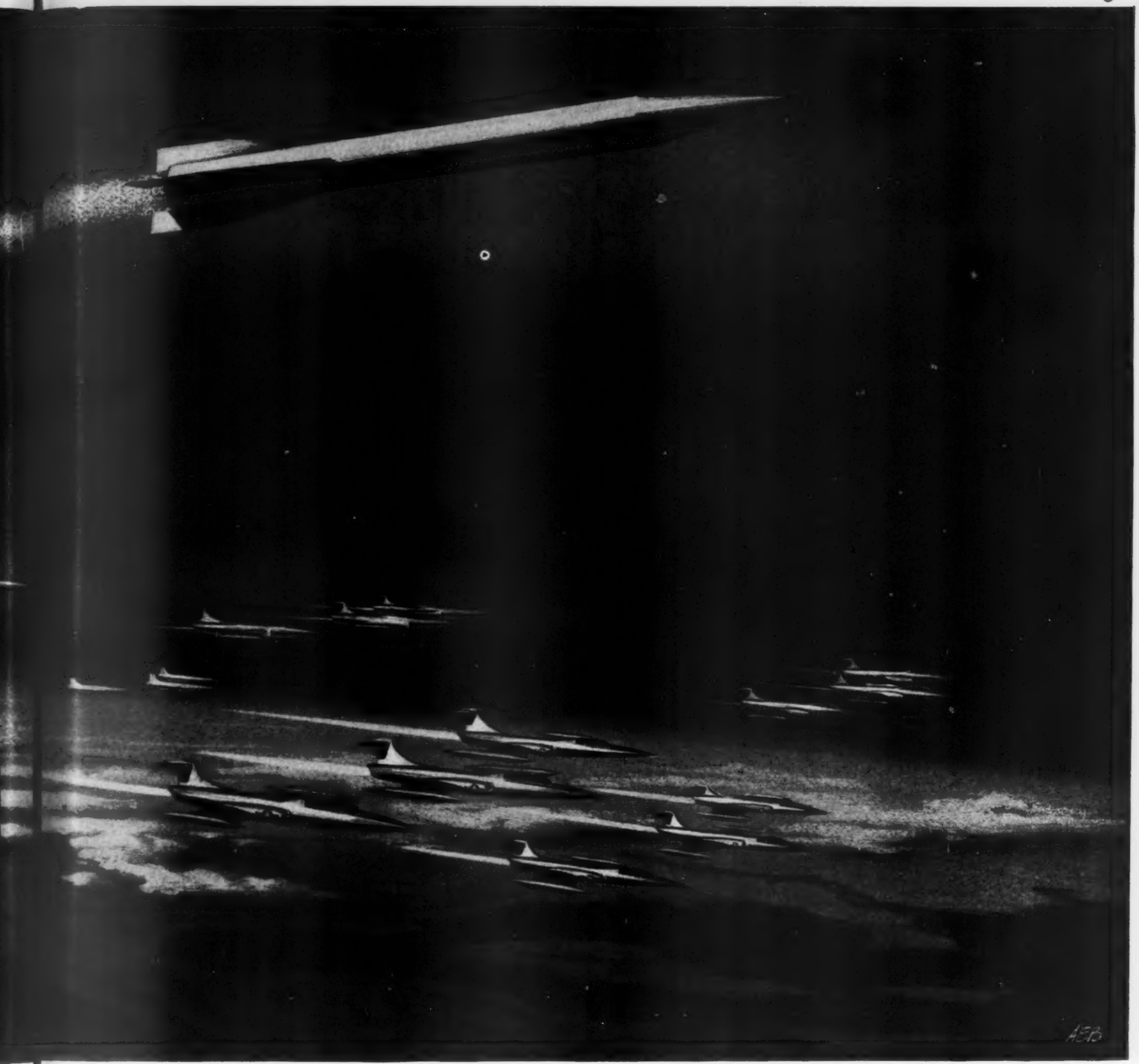

C

THE STORY BEHIND THE STORY

MISSILE CRUISER–Problem: To launch a missile 1500 miles from target. An error of only 1 degree in launching information would cause a 25-mile target miss.

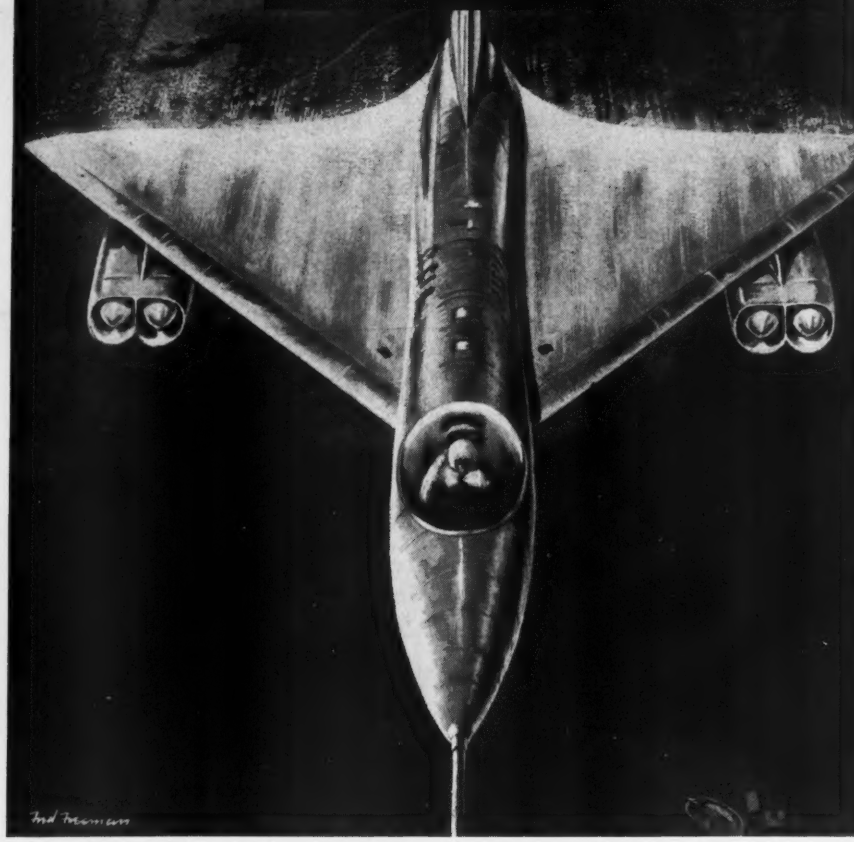

SUPERSONIC BOMBER–Problem: To navigate undetected for thousands of miles to exact position in space for release of bombs or missiles.

INERTIAL NAVIGATION:

In Its Accuracy Lies Power for Peace

ATOMIC SUBMARINE– Problem: To travel submerged for days and know exact spot to surface for missile firing.

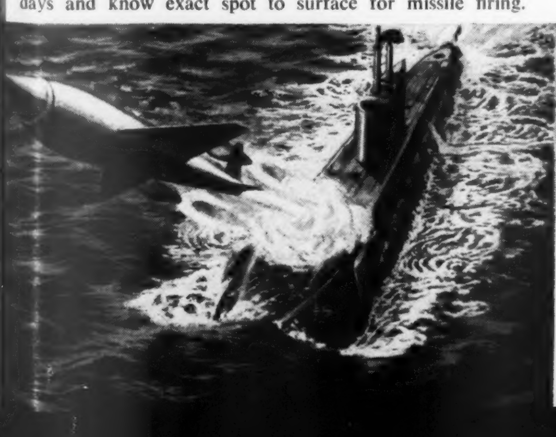

U. S. strategy for maintaining peace by making aggression unprofitable is based on our ability to deliver a crushing retaliatory blow anywhere in the world. Accurate means of directing such blows at long range, high speeds and extreme altitudes make would-be aggressors wary of breaking the peace.

To be effective, weapon carriers must know at all times *exactly* where they are. For example, the long-range bomber with its pinpoint target or the pitching cruiser launching missiles far at sea must navigate with great accuracy.

Solving such problems is the task of Inertial Navigation systems which furnish all data required *automatically*. Completely self-contained within the bomber, ship, submarine or missile, these Inertial Navigation systems require no contact with ground stations. This is extremely important when military missions must be carried on without chance of detection.

To design and engineer Inertial Navigation systems involves a complex combination of engineering skills—gyroscopics, computation, electronics, servomechanics and more. Their production calls for laboratory precision at every stage. For example, the gyroscopes which form the heart of Inertial Navigation systems must be many times more accurate than those used in commercial navigation.

At Sperry, Inertial Navigation systems are being produced for a wide variety of military applications.

SPERRY GYROSCOPE COMPANY
Great Neck, New York

DIVISION OF SPERRY RAND CORPORATION

JULY 1957 JET PROPULSION Journal of the AMERICAN ROCKET SOCIETY VOLUME 27 NUMBER 7

Instrumentation to Measure Gas-Phase Composition of High Velocity, Two-Phase, Two-Component Flows

K. R. WADLEIGH[1] and R. A. OMAN[2]

Massachusetts Institute of Technology, Cambridge Mass.

The problems associated with the measurement of the properties of high velocity flows of liquid droplets suspended in gases are discussed. Particular emphasis is placed on the flow of liquid water droplets suspended in air-water vapor mixtures, with water-air mass ratios up to 0.3 and flow velocities from 350 to 600 fps. The mechanism of operation and the development of special probes to remove "true point samples" of the gas phase alone are described, as well as the devices for analyzing the composition of samples removed by these probes.

Nomenclature

a = acceleration
C_D = coefficient of drag
d = diameter of sampling tube
D = diameter of boundary layer suction tube
$\mathfrak{D}$ = $\delta/\bar{\delta}$
E = computed error
F_D = drag force
g_0 = proportionality factor in Newton's second law
G = mass velocity, $G = \omega/A$
h = projection of sampling tube beyond boundary layer suction tube
m = mass
n = number of droplets in a unit volume of diameter equal to or less than δ
p = pressure
R = Reynolds number
t = time
T = temperature
V = velocity
W = molecular weight
x, y = distance in Cartesian coordinates
δ = diameter of liquid drop
ρ = density
μ = viscosity
ω = mass rate of flow
Ω = specific humidity

Subscripts

1 = at entrance section of tunnel
01 = stagnation at entrance section of tunnel
2 = at sampling section in tunnel
02 = stagnation at sampling section in tunnel
a = air
av = air and water vapor
A = analyzer
BL = boundary layer
e = error
m = maximum
r = relative
rot = caused by rotation
S = sample
v = water vapor
W = hot wire
x = x direction, normal to probe shank
ω = liquid water

1 Introduction

PROCESSES which involve the evaporation of liquids from suspended droplet surfaces into surrounding gaseous media have long been of considerable industrial importance. More recently, interest has been focused upon evaporation processes carried out at high stream velocities wherein the problems of gas sampling, temperature and pressure measurement, etc., are more difficult than for the corresponding semistatic processes.

The work described herein was first stimulated by interest in the Aerothermopressor project at the Massachusetts Institute of Technology (1).[3] The Aerothermopressor is a device which produces a rise in stagnation pressure of a high velocity, high temperature gas stream by virtue of the effect on the gas stream of the evaporative cooling caused by injected liquid water. More recently, a number of similar evaporation-cooling processes have been under study for application to aircraft. Finally, the evaporation processes which precede combustion are of a similar nature.

In processes such as these, the measurement of many properties is necessary to define completely the local state of the liquid-vapor mixture. If, for instance, it is desired to measure in a macroscopic sense the local state of a steady[4] flow of liquid water droplets suspended in an air-water vapor mixture, values of seven properties must be obtained: (a) Gas velocity, (b) average liquid velocity, (c) gas composition (specific humidity), (d) stream composition (mass ratio of liquid to gas), (e) static pressure, (f) liquid temperature and (g) gas temperature.

If, as is often permissible, the average liquid velocity may be assumed essentially equal to the gas velocity, the number of required properties is reduced to six. If, however, additional data are desired on what might be called submacroscopic properties, such as local drop size spectra, it is ap-

Presented at the ARS 11th Annual Meeting, New York, N. Y., Nov. 26–30, 1956.
[1] Associate Professor of Mechanical Engineering.
[2] Fellow, Mechanical Engineering Department.

[3] Numbers in parentheses indicate References at end of paper.
[4] "The word "steady" is used only in the macroscopic sense since the presence of discrete droplets cause small scale fluctuations with time.

parent that the measurement problem becomes even more complex.

Previous workers have developed or suggested means of measuring several properties of the flow. Dussourd (2) has developed a probe which measures the local gas-phase stagnation pressure and local mass velocity of the liquid phase. The use of this probe (called a "deceleration probe") as a mean drop-size measuring device is now being studied at MIT. In addition, numerous means for measuring droplet size (3) have been developed and a means for measuring gas phase temperatures by sonic velocity techniques (4) is under consideration.

This paper describes in detail the current state of development of a probe designed to measure the local water vapor-air mass flow ratio (specific humidity). Probes to measure the local total water-air mass flow and local gas phase stagnation temperature have also been under development and will be reported upon at a later data.

This work is in progress at the Gas Turbine Laboratory of the MIT Mechanical Engineering Department; a portion has been sponsored by the Office of Naval Research and the remainder under a grant-in-aid from Pratt and Whitney Aircraft. The work has formed the basis for several undergraduate and graduate theses (5–8).

2 Measurement of Local Value of Specific Humidity

A. The Over-all Problem

The ratio of the mass rate of flow of water vapor to the mass rate of flow of air at any "point" in a steadily flowing stream is defined as the specific humidity of the air-vapor mixture

$$\Omega = \frac{\omega_v}{\omega_a} \qquad [1]$$

With the assumption that the water vapor exists at a sufficiently low pressure to obey the perfect gas equation of state, Equation [1] may be written in terms of pressure (9) as

$$\Omega = \frac{\omega_v}{\omega_a} = \frac{W_\omega p_v}{W_a p_a} = 0.622 \frac{p_v}{p - p_v} \qquad [2]$$

If a means is found to withdraw a true sample of the vapor phase and to measure the partial pressure of the water vapor p_v at some static pressure p of the sample, an adequate technique of measuring the local specific humidity of the flow has been established.

B. The Sampling Problem

To remove a true point sample of only the gaseous phase of a flow of liquid droplets suspended in gas, it is necessary to insure that:

1 A negligible portion of the liquid droplets traveling near the probe enter with the sample stream.

2 None of the liquid film which exists in the boundary layer on the outer surface of the probe flows into the sample stream.

3 The disturbances in the flow pattern caused by the presence of the probe are sufficiently small so that local spurious high evaporation rates do not appreciably alter the humidity of the sample.

Fortunately, the application under consideration for the "humidity probe" is at rather high stream velocity levels. Therefore, a droplet "shedding" characteristic can be obtained if that portion of the gas flow to be removed as a sample is caused to negotiate a path of very high curvature upon sampling. Since the droplets are in general of higher density than the gas phase (in the experimental case, liquid water compared to water vapor-air mixtures) and since in most evaporative processes the major portion of the droplets are rather large (say, a volume surface mean diameter range of 10 to 100 μ or more), the major portion of the droplets can be caused to be "shed" from the sample flow. Inevitably, a few very small droplets will negotiate the path of the gas and enter the probe, but the actual mass rate of flow of liquid associated with these very small drops may be negligible compared to the average mass rates of flow of liquid past the sampling section.

Of course, the actual flow pattern in the region of any sampling probe is so complex that exact mathematical analysis is impossible. However, in the Appendix a very rough approximation to the flow pattern is devised and the resulting trajectories of the liquid droplets are studied so that the error associated with the very small droplets which do enter the sample port may be approximated. This analysis indicates that the shedding effectiveness is determined primarily by the parameter

$$\bar{R} = \frac{\rho_\omega V_x(\bar{\delta})^2}{18\,\mu_{av} x_S}$$

For high values of $\bar{R}$ (high velocity, large liquid density, large droplets, small sampling hole, etc.) the computed error is extremely small.

The most promising solution for requirement 1 above is therefore to cause the sample stream to negotiate a sharp turn before entering the probe. One might therefore conclude that a good vapor sampling probe would be one in which the flow is caused to turn 180 deg, e.g., a Pitot tube turned downstream. Actual experimental work with such a probe has shown that it is very unsatisfactory, and the reason is described by requirement 2. Since liquid will impinge on the surface of the sampling probe (because only the extremely small droplets can negotiate the gas path around the probe), there will in general be a liquid film in the boundary layer on the probe. This liquid film will very easily flow into a sample port if there is a pressure gradient in that direction. For a Pitot-like tube turned downstream, such a pressure gradient along the surface of the probe to the sampling port exists, and a larger error is caused by the entrainment of this boundary layer liquid in the sample.

The means taken in this development for eliminating the boundary layer liquid entrainment was suggested by A. H. Shapiro of MIT (5) and involves the provision of a boundary layer suction port to remove such liquid prior to its entrainment in the sample.

Finally, to minimize the effects of high local rates of evaporation caused by the presence of the probe (requirement 3) it is necessary to make the size of the probe as small as possible and to eliminate special auxiliary shedding devices in the flow path upstream of the probe position.

C. General Features of Vapor-Sampling Probe Design

A few probe geometries were built and tested (5) prior to the selection of the design discussed in this paper. The present design consists essentially of a small sample suction tube located concentrically inside a larger tube so that the annular area thus formed may be used for boundary layer suction (Fig. 1). The end of the sample tube projects slightly beyond the outer tube for reasons which are discussed below. In operation the tube axis is placed normal to the flow direction so that the sampled gas negotiates a turn of 90 deg upon entering the sample tube.

The sketches in Fig. 2 are intended to illustrate the manner in which sampling errors are effected by changing operating conditions.

Recall that all surfaces which face upstream are covered with a film of "boundary layer liquid" which can flow along the surface either by virtue of the shear stress between the liquid and the gas flowing over it or by virtue of a pressure gradient along the surface.

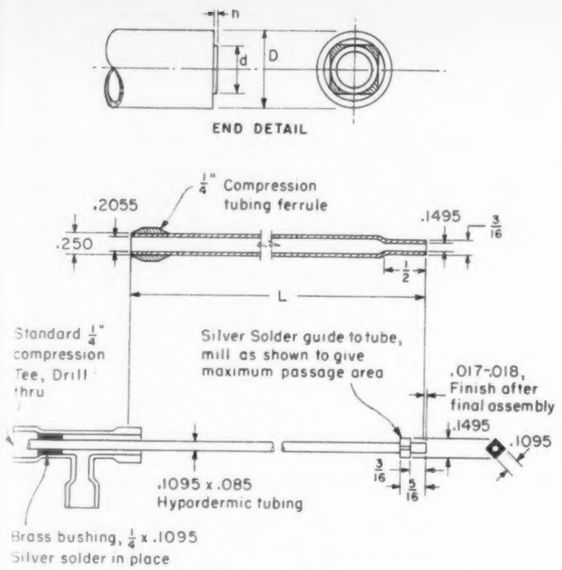

Fig. 1 Assembly views of basic humidity probe

Figs. 2(a) and 2(b) show the general pattern of streamlines which exists if there is no boundary layer suction. In each case, boundary layer liquid will be sucked into the sampling port. When the boundary layer suction is properly adjusted (Fig. 2(c)), boundary layer liquid from the outer tube and the outer surface of the inner tube are prevented from entering the sample port because an adverse pressure gradient is created by the boundary layer suction. In addition, the direction of the streamline reaching a stagnation point at the forward face of the inner tube is such that there is no shedding tendency to shed droplets from below into the sample stream. Although an increase in the boundary layer flow above this optimum will not permit boundary layer liquid to enter the sample, it will cause a decrease in the curvature of the sample flow streamlines, thereby decreasing the shedding effect. Too large values of sample flow rate will have the same effect.

The effect of the projection h of the inner tube of diameter d beyond the outer tube of diameter D is shown in Figs. 2(d) and 2(e). If the projection is too small, liquid will be shed from the outer tube wall into the sample stream, whereas if the projection is too large, it is not possible to maintain the desired sample streamline curvature, and the inner tube behaves like an unprotected tube with no boundary layer suction at all.

On the basis of this physical picture of vapor-sampling probe operation, the experimental work was devoted to the establishment of the optimum geometry and optimum values of flow parameters. It is again emphasized that the flow pattern is so complex that a complete theoretical treatment is impossible.

D. Equipment for Calibration of Vapor-Sampling Probe

The calibration of the vapor-sampling or "humidity" probe required (a) the production of a high velocity, liquid-gas stream from which the sample could be withdrawn and (b) a means for measuring the specific humidity of the sample so taken. The latter measurement was accomplished by a specially developed device called the "Humidity Analyzer" which is described in Section 3.

Because there are in existence no methods of measuring the humidity of high speed flows other than those under study here, it was necessary to resort to semianalytical predictions of the measured humidity for calibration purposes. The high velocity liquid water-vapor water-air mixtures were produced in a special $2\frac{1}{8}$-in. $\times$ $6\frac{1}{2}$-ft cylindrical tunnel supplied with humid air from an atmospheric combustion chamber and powered by a steam ejector. These tunnels have been built at MIT for two-phase, high velocity work and are described in detail in (1, 5). Suffice it to say that provisions are made for measuring stagnation temperature T_{01} and stagnation pressure p_{01} at the bell-mouth entrance of the tunnel, static pressure p_1 at the exit of the bell-mouth and entrance to the cylindrical tunnel section, and the pressure distribution along the tunnel to the probe position at which the static pressure is p_2. In addition, means for measuring the water flow rate $\omega_{\omega 1}$ which is injected at the exit of the bell-mouth are provided.

Detailed experimental and theoretical studies of the flow process inside the tunnel have been carried out (1). These studies indicate that, for the range of operating conditions used in this work, the flow is always saturated at the sampling position (position 2). The equations of momentum, continuity, and energy then permit the prediction of the state of the stream at the probe from the measured properties. In this way, the gas and liquid velocities, $V_{av2} = V_{\omega 2}$, the local mass rates of flow of gas ω_{va2} and water $\omega_{\omega 2}$ and the local specific humidity Ω_2 were predicted at the sampling "point."

E. Calibration Parameters

The composition of the sample removed from the flow at position 2 was measured by the humidity analyzer as a specific humidity Ω_A. The index of performance was then computed as

$$\frac{\Delta\Omega}{(\omega_\omega/\omega_{av})_2} = \frac{\Omega_A - \Omega_2}{(\omega_\omega/\omega_{av})_2}$$

This index is actually the ratio of the mass rate of flow of liquid per unit mass rate of flow of gas which enters the probe to the total mass rate of flow of liquid per unit mass

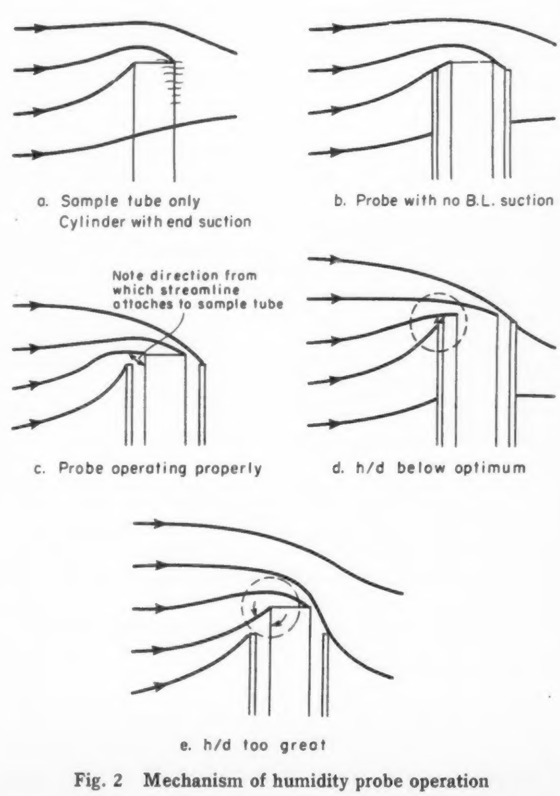

Fig. 2 Mechanism of humidity probe operation

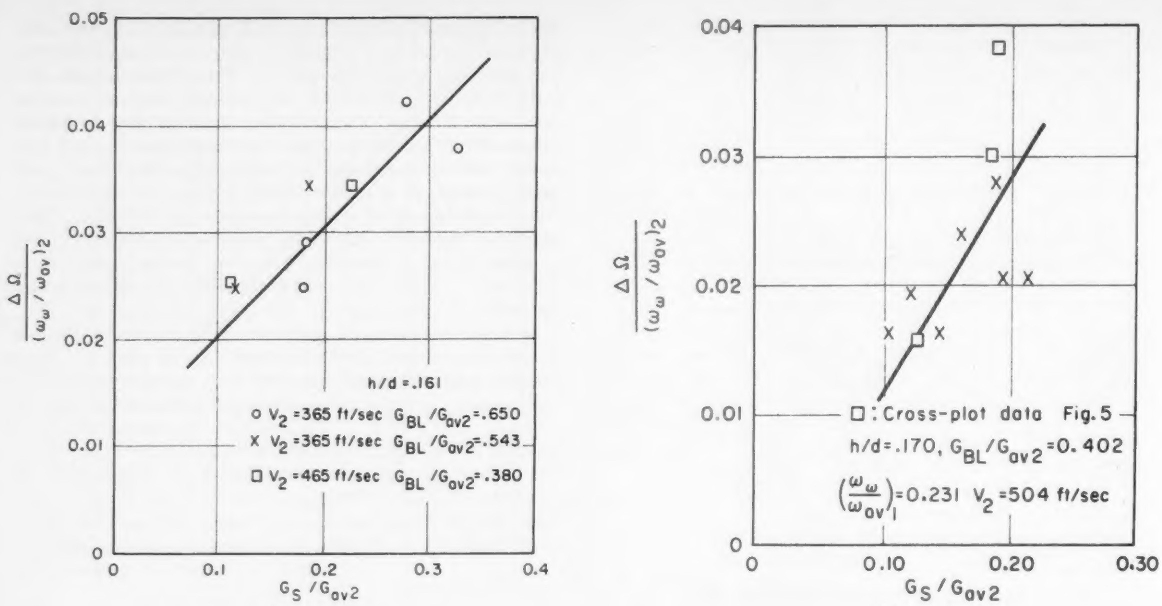

Fig. 3 Effect of G_S/G_{av2} on performance of humidity probe

rate of flow of gas in the main stream at the sampling position. This index is therefore a measure of the liquid separating performance of the probe, and is identical to the error E defined for the simplified flow system treated theoretically in the Appendix.

Under most test conditions, the probe was "deluged" with water; that is, the amount of water in liquid droplets was much greater than in the vapor phase. Attempts to operate at very low flow rates of water were not successful because it was no longer valid to assume saturated conditions at the sampling position, and therefore the calibration technique broke down. Nevertheless, there is every reason to believe that the performance of the probe should be best at low water flow rates when the amount of boundary layer liquid is less.

As an independent parameter representing the boundary layer and sample flow conditions, the ratios of the mass velocities G_S/G_{av2} and G_{BL}/G_{av2} were chosen because the considerations of probe operation outlined in Section 2C indicate that streamline shapes are of paramount importance.

To study the effects of probe geometry, the ratio of h/d (Fig. 1) was varied, but the ratio d/D was held fixed at a reasonable design value. In addition, the effect of misalignment with the stream direction was studied by testing a probe which had a 30 deg bend $\frac{5}{8}$-in. below the tip. By rotating this probe about an axis normal to the stream, various angles of attack were achieved. (The sine of the angle of attack equals the sine of the bend angle multiplied by the sine of the angle of rotation.)

It may be possible to extend the use of the vapor-sampling probe to measure gas phase stagnation temperature. The fact that most of the liquid is removed in the sampling process may permit the application of hot wire techniques for this purpose. This extension is now under study at MIT.

F. Results of Calibration Tests of Humidity Probe

Effect of Sample Suction Rate

The effect of varying sample flow rate is shown in Figs. 3(a) and 3(b). At high values of the sample flow, there is a sufficient "sucking in" so that the streamline shapes above the probe are reduced in curvature and thus this droplet shedding performance is impaired. Fig. 4 is a plot of similar data for tests in which the value of h/d was too great and consequently the boundary layer suction was not sufficient to prevent entrainment of boundary layer liquid in the sampling stream. The value of the optimum sample flow rate was therefore established as a minimum value consistent with resonable response times in the humidity analyzer system.

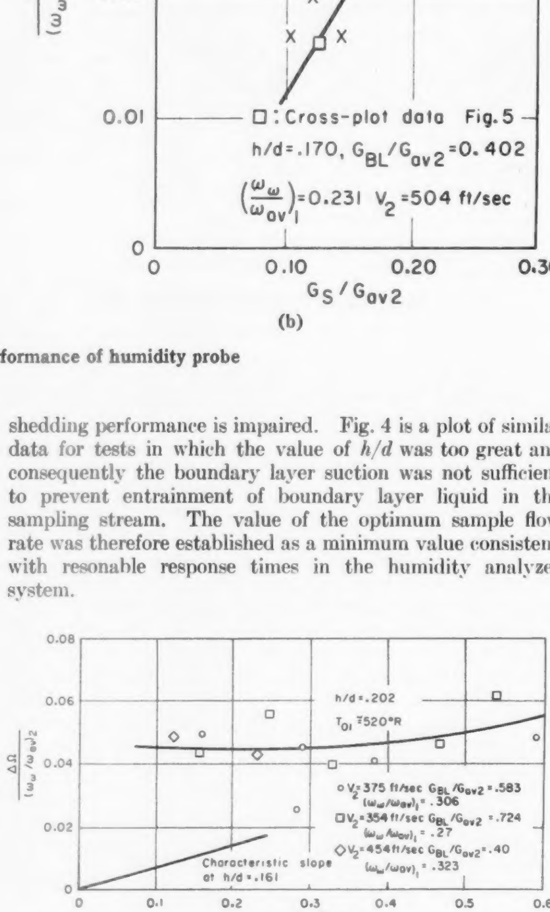

Fig. 4 Effect of G_S/G_{av2} on performance of humidity probe at high h/d ratios

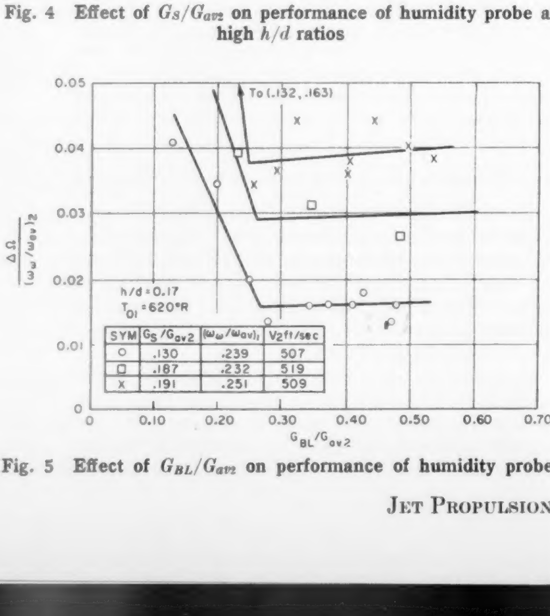

Fig. 5 Effect of G_{BL}/G_{av2} on performance of humidity probe

Effect of Boundary Layer Flow Rate

The effect of changing the boundary layer flow rate for three constant values of the sample flow rate is shown in Fig. 5. When no boundary layer suction is applied, a large quantity of boundary layer liquid is entrained in the sample stream. As the boundary layer suction is increased from zero, the error gradually falls as the flow pattern approaches the optimum condition sketched in Fig. 2(b). Finally, as the suction is increased beyond the optimum value, there is a gradual rise in error caused, not by entrainment of boundary layer liquid, but by the lessened shedding effectiveness resulting from the decrease in curvature of the sample streamlines.

Effect of Geometry—h/d Ratio

A range of h/d ratios (Fig. 1) from 0 to 0.5 was tested; the results are shown in Fig. 6.

For values of h/d which are too small, there is entrainment of the boundary layer liquid which runs along the outside probe surface (Fig. 2(d)). For large extensions of the inner sample tube beyond the outer boundary layer tube (h/d too large), the behavior of the sampling probe approaches the behavior of a probe with no boundary layer suction, and boundary layer water is again entrained in the sample flow.

Effect of Geometry—Angle of Attack

A probe with a sampling head exactly like the basic humdity probe of Fig. 1, but with the axis of the probe head inclined at an angle of 30 deg with the probe shank, was tested to determine the effect of misalignment of the sampling port with the stream direction (Fig. 7). Angles of attack, defined by the sketch in Fig. 7, were varied by rotating the probe around the shank axis. This rotation placed the plane of the sampling port at different transverse positions in the duct, and resulting differences in flow, caused probably by non-one-dimensional flow conditions in the duct, were observed. The influence of angle of attack on performance was measured in terms of $\Delta\Omega_{rot}/(\omega_\omega/\omega_{av})_2$ where $\Delta\Omega_{rot}$ is the difference between the measured humidity and the measured humidity at zero angle of attack.

Limitations imposed by flow conditions in the humidity analyzer made it necessary to run these tests at a value of G_{BL}/G_{av2} slightly lower than the optimum, and some additional error resulted.

As expected, the error is large for negative angles of attack, where a projection of the sampling port area faces upstream. As the angle of attack is increased from zero, the error increases more gradually as the shearing action of the free stream carries boundary layer water off the top of the outer tube into the sample stream. This error might have been counteracted to a certain extent had the boundary layer flow rate not been limited by restrictions in humidity analyzer flow conditions.

Recommended Operating Conditions for Humidity Probe

As is indicated by the discussion in Section 2C and the approximate theoretical analysis of the Appendix, the vapor sampling or humidity probe described here is a dynamic sampling instrument which depends upon high stream velocities to permit the "shedding" of liquid droplets from the gaseous sample stream. High values of the parameter $\bar{R}$ are favorable for this action, but ultimate determination of performance requires experimental calibration. Based upon the tests carried out with water-air mixtures, in which the volume surface mean drop size is estimated to be at about 25 to 50 μ, the following values are recommended:

$d/D = 0.585$; $h/d = 0.16$; $V_2 = 350$ to 650 fps; $G_S/G_{av2} = 0.1$ to 0.2; $G_{BL}/G_{av2} = 0.35$ to 0.65.

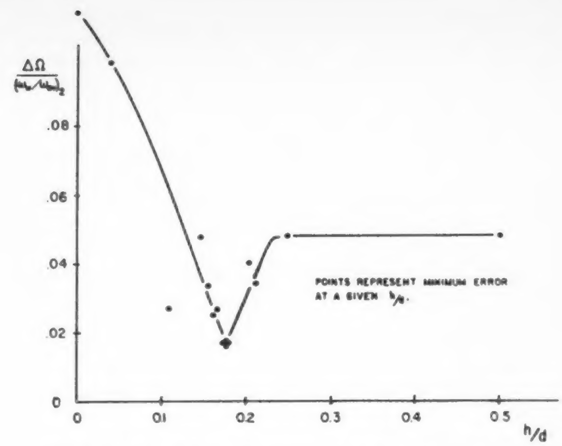

Fig. 6 Effect of h/d on performance of humidity probe

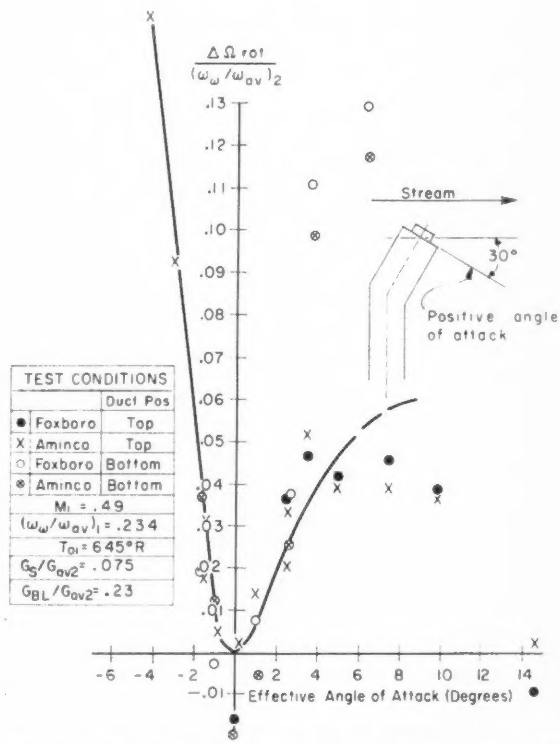

Fig. 7 Effect of angle of attack on performance of humidity probe

3 The Humidity Analyzer

A. The Problem of Analysis of the Sample

Assuming that the vapor-sampling probe or a probe designed to sample any other composition property actually removes a true sample from the stream as desired, there remains the problem of accurately determining the mass ratio of the two components in the sample flow. In the case of the probes and experimental apparatus used in this work, the desired characteristics of the analyzing device were (a) continuous instantaneous readings with a reasonably short response time, (b) broad range of permissible compositions (humidity values), (c) reliability and (d) low cost.

Several methods of measuring the specific humidity of the

sample water-air flow were considered. The usual wet bulb-dry bulb psychrometer techniques were discarded because of uncertainty in available calibrations at the required low pressure levels and high humidity conditions (as compared to normal atmospheric air conditions). Absorption or adsorption devices were not used because they are not continuous reading and would require the expenditure of a large time interval to get accurate values. Commercially available dew point meters of the mirror-condensation type suitable for the desired range of operating conditions were found to be very expensive.

Continuous condensation at low temperature was attempted, and although such a device might have been developed to a satisfactory state, this technique was discarded in favor of the final form of the humidity analyzer described below—in which the Foxboro Dewcel or the American Instrument Company Electric Hygrometer was the primary measuring element.

B. Description of Humidity Analyzer

The humidity analyzer used in this work is refined from the product of several student theses at the Massachusetts Institute of Technology (5–7). The primary measuring element used is either the Foxboro Dewcel or the Aminco Electric Hygrometer, both commercially available instruments. Each instrument measures the dew point temperature of the water vapor-air atmosphere in which it is immersed. Knowledge of this dew point temperature permits the determination of the partial pressure of the water vapor in the surrounding atmosphere p_v(12). This partial pressure together with the measured static pressure p permits the determination of the specific humidity from Equation [2].

The Dewcel consists essentially of a spiral winding of resistance wire, each turn of which is separated from the adjacent turns by a glass fibre tape impregnated with lithium chloride. In operation, if the temperature of the windings is sufficiently low compared to the surrounding gaseous medium, water may combine with the LiCl, causing a reduction in electrical resistance by a "short-circuit" effect of the resistance wire. As a result, the electric current flow increases and the heating causes the "drying" of the impregnated tape. The process continues until an equilibrium temperature attains. Since the LiCl-H_2O equilibrium is well understood, this equilibrium temperature may be converted to the equivalent dew point temperature of the surrounding gaseous mixtures.

The Dewcel proved to be reliable and rugged over a broad range of operating conditions, but the time response for changes in operating conditions was not rapid (a few minutes). The Aminco unit was therefore used for certain tests in which rapid time response was desired. This latter device depends upon the measurement of resistance changes in a hygroscopic film containing LiBr and LiCl with changing water content. Permanent damage to the film occurs if condensation occurs, and this characteristic proved a limitation in the application of the Aminco unit.

The apparatus in which the Dewcel or Aminco unit ("sensing elements") was used is shown schematically in Fig. 8. Also incorporated in this apparatus were the heat exchangers, flow measuring nozzles, control valves and suction devices necessary to handle both sample and boundary layer streams. The boundary layer stream passed through a boiling water heat exchanger to evaporate all liquid[5] so that the total mass rate of flow, $\omega_{BL} = G_{BL}A_{BL}$, could be measured by a small flow nozzle.[6] The stream was then exhausted through an air ejector.

The sample was conducted to the boiling water exchanger

[5] Note that all pressure levels in the main tunnel and measuring apparatus were subatmospheric.

[6] This flow measurement involved minor approximations in predicting the properties of the gaseous mixtures of water vapor and air.

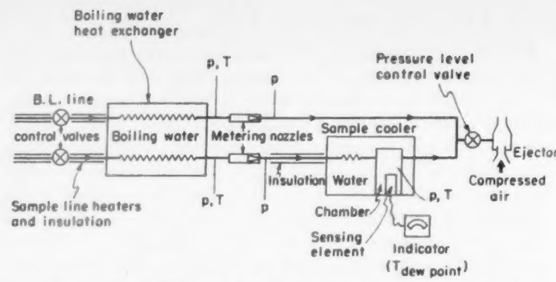

Fig. 8 Flow diagram of humidity measuring apparatus

through an electrically heated line to prevent condensation which might cause local unsteady effects. The mass rate of flow of the sample was measured by a flow metering nozzle, $\omega_S = G_SA_S$. The sample was then passed into another heat exchanger in which warm water was used to bring the sample to the temperature required for the Dewcel or Aminco measurement. The pressure and dew point temperature were measured in the sensing element chamber, and the sample was then exhausted through an air ejector.

Absolute calibration was not possible, but the instruments were checked against psychrometer measurements in the range of normal psychrometer operation. Excellent agreement was found in these checks. The nature of the calculation of Ω (Equation [2]) is such that small errors in dew point temperature and pressure measurement can cause large errors in specific humidity, particularly at very low values of pressures and high values of the dew point. These errors account for the major errors in the entire probe calibration procedure.

APPENDIX

Approximate Evaluation of Errors in Droplet 'Shedding' Process of Vapor-Sampling Probe

The exact mathematical solution of the gas-liquid flow in the neighborhood of the vapor-sampling probe ("humidity probe") is at present impossible. However, for purposes of estimating the magnitude of the error caused by the entrance of small liquid droplets with the sample gas stream, the following approximate analysis has been carried out:

Consider the gas flow in the neighborhood of the sampling port to be two-dimensional and to have a velocity V_a normal to the axis of the probe at all regions ahead of the probe; while in the region over the probe the velocity is such that the component normal to the probe, V_X, is equal to V_a, and the component parallel to the axis of the probe is V_S (see Fig. 9).

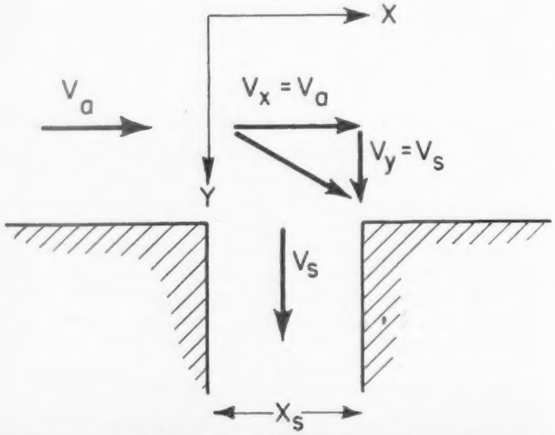

Fig. 9 Schematic picture of idealized flow at sampling port

The flow before the probe is thus defined by $x \leq 0$, $y = y$, and the flow over the probe is defined by $x \geq 0$, $y = y$. The liquid droplets are assumed to travel at the gas velocity at $x = 0$. Over the probe, the droplets continue to travel at V_a in the x direction, but they are acted upon by drag forces caused by the assumed transverse velocity component, V_S. The problem of predicting the error in the vapor sampling performance of the probe is thus reduced to predicting the fraction of the total mass rate of flow of water passing $x = 0$ which will pass into the probe of axial length x_S because the droplet trajectories are curved downward. The problem is complicated by the fact that the liquid droplets are not of uniform size and, therefore, of all the droplets crossing $x = 0$ at any given value of y, certain small drops will enter the probe while larger drops will not.

The equation of motion of a spherical droplet of diameter δ may be written by combining Newton's second law and the definition of the drag coefficient

$$F_D = C_D \frac{\rho_{av} V_r^2 \pi \delta^2}{8 g_0} = \frac{m}{g_0} a$$

or

$$a = \frac{\pi \delta^2 \rho_{av} V_r^2}{8m} C_D \ldots\ldots\ldots\ldots\ldots\ldots [A1]$$

Introducing the assumption that the relative Reynolds number is sufficiently small so that Stoke's law holds, we have

$$C_D = \frac{24 \mu_{av}}{\rho_{av} V_r \delta} \ldots\ldots\ldots\ldots\ldots\ldots [A2]$$

Since

$$m = \frac{\pi \delta^3}{6} \rho_\omega \ldots\ldots\ldots\ldots\ldots\ldots [A3]$$

combination of [A1, A2, and A3] yields

$$a = 18 \frac{V_r \mu_{av}}{\rho_\omega \delta^2} \ldots\ldots\ldots\ldots\ldots\ldots [A4]$$

If we recall that it is assumed that $V_x = V_a =$ const, we may rewrite Equation [A4] as

$$a = \frac{d^2 y}{dt^2} = \frac{18 \mu_{av} V_r}{\rho_\omega \delta^2} = \frac{18 \mu_{av}}{\rho_\omega \delta^2}\left(V_S - \frac{dy}{dt}\right) \ldots\ldots [A5]$$

Equation [A5] when integrated twice gives

$$y = V_s t - R \frac{V_S}{V_x} \delta \left[1 - e^{-V_x t / R\delta}\right] \ldots\ldots\ldots [A6]$$

where $R = \rho_\omega V_x \delta / 18 \mu_{av}$, and y is the distance the drop travels in the direction of the probe axis from the position at the line $x = 0$. During the same time interval, the distance traveled in the x direction is $V_x t$. Thus, Equation [A6] may be written as

$$\frac{y}{x} = \frac{V_S}{V_x}\left[1 - R \frac{\delta}{x}\left(1 - e^{-x_S / R\delta}\right)\right] \ldots\ldots\ldots [A7]$$

Equation [A7] is the basic equation which explains the "shedding" characteristic of the vapor sampling probe. Suppose the probe size $x = x_S$, V_x, ρ_ω and μ_{av} are fixed, then Equation [A7] predicts the value of the maximum drop diameter δ' which will enter the probe as a function of the distance y above the probe at which the drop crossed $x = 0$

$$\frac{y}{x_S} = \frac{V_S}{V_x}\left[1 - R' \frac{\delta'}{x_S}\left(1 - e^{-x_S / R'\delta'}\right)\right] \ldots\ldots [A7a]$$

Thus, for a unit depth of flow, the infinitesimal mass rate of flow of liquid which passes through the infinitesimal height dy at $y = y$, $x = 0$, and which will be sufficiently deflected to enter the probe will be

$$d\omega_e = \left[\frac{\pi}{6} \rho_\omega V_x \int_0^{\delta'} \delta^3 \left(\frac{dn}{d\delta}\right) d\delta\right] dy \ldots\ldots [A8]$$

where n is the number of drops per unit volume whose diameter is equal to or less than δ. The total mass rate of flow of liquid water passing through the same elemental height dy at $x = 0$ is given by

$$d\omega_\omega = \left[\frac{\pi}{6} \rho_\omega V_x \int_0^{\infty} \delta^3 \left(\frac{dn}{d\delta}\right) d\delta\right] dy \ldots\ldots [A9]$$

The sampling error E may thus be defined as the ratio of the mass rate of flow of water which enters the probe to the total free stream mass rate of flow of water at $x = 0$

$$E = \frac{\int d\omega_e}{\int d\omega_\omega} = \frac{\int_0^{y_m} \int_0^{\delta'} \delta^3 \left(\frac{dn}{d\delta}\right) d\delta\, dy}{\int_0^{y_m} \int_0^{\infty} \delta^3 \left(\frac{dn}{d\delta}\right) d\delta\, dy} \ldots\ldots [A10]$$

The upper limit y_m on the y integration in Equation [A10] corresponds to the maximum value of y at $x = 0$ for which an entering drop whose diameter is zero can enter the probe at x_S. This limit may be computed from Equation [A7a] by setting $\delta = 0$

$$\frac{y_m}{x_S} = \frac{V_S}{V_x} \ldots\ldots\ldots\ldots\ldots\ldots [A7b]$$

Physically, it is obvious that this must be the value of y_m since a drop of size approaching zero will have a velocity vector identical to that of the gas flow, and the gas flow in this region has been assumed to have the velocity components V_x and V_S which are respectively constant.

It should be noted that the sampling error E, defined by Equation [A10] is for the special case under consideration identical to the parameter used as an index of performance throughout the test work

$$\frac{\Delta\Omega}{(\omega_\omega/\omega_{av})_2}$$

Equations [A7a, A7b, A10] provide a means for estimating the sampling error provided the droplet size distribution is known. The following Nukiyama-Tanasawa correlation (11) represents to very good accuracy the distribution of droplet sizes found in air atomization

$$\frac{dn}{d(\delta/\bar{\delta})} = \frac{125\, n_0}{2}\left(\frac{\delta}{\bar{\delta}}\right)^2 e^{-5(\delta/\bar{\delta})} \ldots\ldots\ldots [A11]$$

where n_0 is the total number of drops per unit volume, and

$$\bar{\delta} = \frac{\int_0^\infty \delta^3 \frac{dn}{d\delta} d\delta}{\int_0^\infty \delta^2 \frac{dn}{d\delta} d\delta}$$

is the volume-surface mean diameter.

For the droplet size distribution of Equation [A11], and with the limit specified by Equation [A7b], the denominator of Equation [A10] may be evaluated

$$\int_0^{y_m} \int_0^{\infty} \delta^3 \left(\frac{dn}{d\delta}\right) d\delta\, dy = \frac{12}{25} n_0 \frac{V_S}{V_x} x_S (\bar{\delta})^3 \ldots [A10a]$$

The evaluation of the numerator of Equation [A10] for the drop size distribution of Equation [A11] is more difficult. The variable y may be replaced with the variable δ' by direct differentiation of Equation [A7a], and the numerator may be written as

(Continued on page 783)

Heat Transfer to Fluids in the Region of the Critical Temperature[1]

WALTER B. POWELL[2]

Jet Propulsion Laboratory, California Institute of Technology, Pasadena 3, Calif.

Heat transfer by forced convection in the region of the critical temperature has been studied experimentally, using oxygen at supercritical and at subcritical pressures. Near the critical temperature there exists a minimum in the heat transfer coefficient which is appreciably lower than the value at lower or at higher temperatures. This phenomenon will limit the use of this liquefied gas as a heat transfer fluid.

Nomenclature

A = parameter in Appendix A
A_{tube} = cross-sectional area of tube wall
B = parameter in Appendix A
C_p = specific heat at constant pressure
d = diameter of tube
e = potential along axis of tube
F = parameter in Appendix A
G = mass flow per unit area
h = heat transfer coefficient of fluid film = $q/(T_W - T_B)$
h' = generalized heat transfer coefficient = $q(d^{0.20}/G^{0.80})/(T_W - T_B)$
h'' = $0.023 \left[\frac{C_{pf}^{0.40}\, k_f^{0.60}}{\mu_f^{0.40}}\right] \frac{1}{(\rho_B/\rho_f)^{0.80}}$
H = enthalpy; constant in Appendix A
I = total current through tube
J = conversion factor: 0.7376 (ft lb/watt sec)
k = thermal conductivity
l = length of heater tube
Nu = Nusselt number = hd/k
P = pressure
Pr = Prandtl number = $C_p\mu/k$
q = heat flux per unit area
r = radius
R = resistivity; gas constant
Re = Reynolds number = $\rho Vd/\mu = dG/\mu$
s = radial position parameter = $(1 - r/r_2)$, Appendix A
T = temperature
V = velocity
γ = ratio of specific heats of gas
δ = external heat loss parameter, Appendix A
μ = viscosity
ρ = density

Subscripts

$(\ )_1$ = quantity at inside radius of tube
$(\ )_2$ = quantity at outside radius of tube
$(\ )_W$ = quantity at temperature of inside wall of tube
$(\ )_f$ = quantity at reference temperature: $T_B < T_f < T_W$
$(\ )_B$ = quantity at temperature of bulk of fluid within tube
$(\ )_{cr}$ = quantity at critical point of fluid

Introduction

THE possible use of liquefied gases as coolants for regeneratively cooled rocket motor combustion chambers requires that some information on the heat transfer characteristics of typical fluids be obtained, particularly in the region of the critical temperature.

An experimental program in which hydrogen, nitrogen and oxygen were used as the test fluids was undertaken with the object of obtaining data which would permit the formulation of useful relationships between the variables most important in the region of possible application.

Only the work with oxygen is reported here.

Experimental Equipment and Procedure

The experimental equipment consisted of an electrically heated tube through which the fluid being tested was forced from a pressurized supply reservoir. Schematic fluid flow and electrical circuit diagrams are given in Fig. 1. The fluid flow rate, pressure and temperature, the electrical current and voltage drops, and the tube wall temperature were among the data measured and recorded.

The heat transfer element used was a short length of type-347 stainless steel tubing with nominal dimensions of $\frac{1}{4}$-in. OD 0.028-in. wall thickness. This heater tube was used in lengths varying from 6 to 72 in. A portion of the tube with its end flange is shown in Fig. 2.

The inlet and outlet fluid flow adapters had a 7-deg included angle conical transition from the $\frac{1}{2}$-in.-diam tube inlet line to the $\frac{1}{4}$-in.-diam heater tube. These adapters were separated from the flanges by an insulating gasket and held down by insulated bolts, as shown in Fig. 2, so that none of the fluid circuit tubing, except the heater itself, was electrically "hot" at any time.

Electric power for the heater was supplied from a 100-kva transformer mounted on the roof of the test cell directly above the heater assembly. Notable features of the power supply were the wide range of voltage over which the full 100-kva output could be delivered and the fine control which the operator could exercise over the output at any time.

The fluids were supplied to the heater from a regulated pressure source. A general schematic diagram of the fluid flow circuit and instrumentation is given in Fig. 1. The incoming fluid passed in succession through a flowmetering device, a temperature equalizer, the heater tube, a downstream temperature equalizer, a manually controlled throttle valve and a vent to atmosphere.

The temperatures on the outside surface of the tube were obtained by measuring the output of chromel-alumel thermocouple junctions, formed by pulse-welding the two component wires to the surface of the tube very close to each other. The thermocouple wires used were No. 28 gage (0.0125-in. diam). Because of the small wire size and the fact that each wire was bonded to the hot tube wall, the indicated output was used without further correction in the determination of the tube outerwall temperature.

One modified thermocouple installation technique was tried a few times. It consisted of welding a single pair of No. 36 (0.005-in.) wires to the tube as before, and then wrapping them $1\frac{1}{2}$ turns around the tube, using a thin sheet of mica (approximately 0.002 in. thick) to prevent electrical contact between the wires and the tube except at the welded junction. The entire assembly was held together by a pair of

Received Nov. 30, 1956.

[1] This paper presents one phase of research carried out at the Jet Propulsion Laboratory, California Institute of Technology, under Contract No. DA-04-495-Ord 18, sponsored by the Department of the Army, Ordnance Corps.

[2] Engineering Specialist, Power Plant Research Section. Mem. ARS.

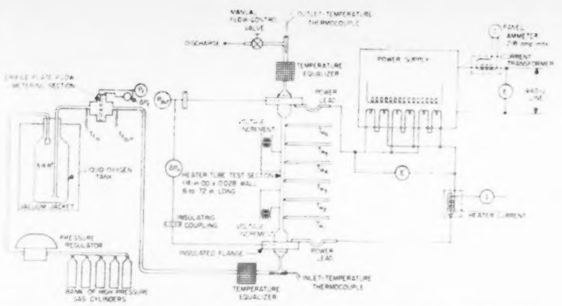

Fig. 1 **Schematic fluid flow, electrical power and instrumentation diagram**

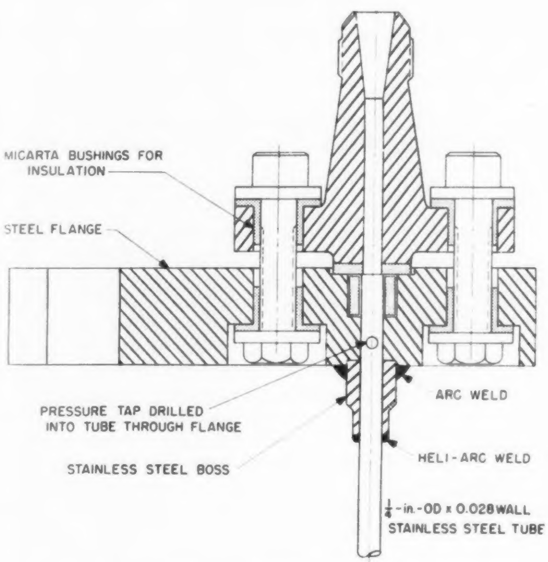

Fig. 2 **Assembly of tube and fluid flow adapter showing insulation**

grooved clamp blocks, made of diatomaceous earth supported by a metal backing. This assembly had several potential advantages, but it prevented observation of the tube and interfered with installation of the voltage pickup clamps. A comparative test, in which both types of thermocouples were mounted on a single tube, failed to show any significant differences in output, so the original type of installation was retained.

Voltage increments across 2-in. lengths of the heater tube were picked up by clamps having spring-loaded points. These voltage signals were rectified and recorded on potentiometers.

The orifice plate flowmeter was mounted near the outlet of the insulated tank which was used for the liquefied gases, and the flowmeter differential pressure transducer was mounted nearby and at the same elevation. A horizontal pancake coil of copper tubing was inserted in the interconnecting lines so that the transducer was protected from extreme temperature changes when cold fluid was passing through the flowmeter. The flowmeter was calibrated with water as the calibrating fluid; the orifice dimensions were corrected for contraction resulting from cooling before using the calibration in computing the flow of liquid oxygen. Fluid densities needed in the flow computations were determined from the measured pressure and temperature at the flowmeter in accordance with the best available physical data.

The electrical resistivity of the tube material as a function of temperature was determined by passing a small direct current from a battery supply through a 3-ft specimen of the tube which was immersed in a constant-temperature oven. Precision hand-balancing instruments were used to measure the current and voltage drop, and the temperature was determined from the output of a platinum vs. platinum + 10 per cent rhodium thermocouple previously calibrated by the Bureau of Standards. Concurrently with the resistivity determination, the output of typical thermocouple junctions (formed by welding the No. 28 chromel and alumel wires to the wall of the tube) was measured, and the corresponding temperatures were found to agree closely with those determined from the platinum thermocouple.

The thermal conductivity of the type-347 stainless steel was obtained from manufacturers' data sheets and handbook sources. It was necessary to extrapolate from the data available in order to cover the range of temperatures encountered in the test program.

All data were recorded throughout each test on recording-type potentiometers. A chronograph pen was installed on each potentiometer to mark a time signal in the margin of the chart so that all the records could be synchronized, and a manual override switch was available to the test-cell operators so that a distinctive signal could be introduced when it was desired to mark the time at which a particular set of data was being recorded.

Reduction of Test Data

The following procedures were used in obtaining the desired information from the primary data:

1 Flow rate was computed using the orifice-plate calibration, the measured differential pressure and a density corresponding to the measured temperature and pressure. It was assumed that the density of the liquid at elevated pressure was the same as that at the saturation pressure corresponding to the measured bulk temperature.

2 Local values of fluid bulk temperature and pressure were estimated by linear interpolation between the measured values at the inlet and outlet ends of the tube. The mixed fluid temperatures were measured in areas of enlarged cross section near each end of the tube, and, hence, they approximated the stagnation temperature of the fluid. The pressure taps were located in the bosses at the ends of the tube, about two diameters from the tube inlet and outlet, respectively; thus, the measured pressure drop across the tube was the static pressure drop due to both friction and the acceleration of the fluid in the tube.

3 The tube dimensions and the variation with temperature of the thermal conductivity and electrical resistivity of the tube material being known, the local heat flux and the temperature of the tube wall at the fluid interface were computed from the measured values of the outer wall temperature and the electric current carried by the tube. Appendix A presents the equations used in computing this part of the data.

In the derivation of the equations used in computing the inside wall temperature, it is assumed that the axial temperature gradient in the tube is negligible in comparison with the radial temperature gradient. Inspection of typical data indicates that the axial gradients are less than 5 per cent of the radial gradients, except in regions where the fluid bulk temperature is very close to the critical temperature of the fluid; therefore, the equations can be considered valid in all except these limited regions.

It is also possible to have appreciable axial temperature gradients in the tube next to the flange, but calculations indicate that this effect should be negligible at a distance of $\frac{1}{2}$ in. (18 wall thicknesses) from the attachment point; furthermore, only measurements made 2 in. or more from the flanges were used in compiling the data, in order to minimize entrance effects.

The calculation of the inside wall temperature and of the heat flux to the fluid involved a parameter δ, which was proportional to the heat flux to the air at the outer surface of the tube (Equations [A-8–A-14]). This heat flux was evaluated using the standard equations for radiative and convective heat transfer from the exterior of a hot pipe; it was found that the terms which involved δ in these equations were completely negligible unless the wall temperature was near 2000 R.

Results of Test

Theoretical Considerations and Basis of Correlation

Eckert (1)[3] shows by dimensional analysis that heat transfer phenomena can be correlated in terms of functions of certain dimensionless variables. Thus, for the simple case of heat transfer to a perfect fluid by convection only, $Nu = f(Re, Pr)$. When the flow is in the range where convective processes predominate, and where gravitational and Mach number effects are negligible, but where the temperature differences are moderate and the fluid properties vary with the temperature to some power, the heat transfer equation can be written as

$$Nu = f\left(Re, Pr, \frac{T_W}{T_B}\right) \quad [1]$$

Dimensional analysis cannot tell the form of the function; it can only tell which dimensionless variables are important. Various functional relationships of the above variables have been proposed and used to correlate experimental data. A commonly used equation for fully developed heat transfer with low flux is

$$Nu = 0.023\,(Re)^{0.80}(Pr)^{0.40} \quad [2]$$

Other more complicated functional forms have been found to be useful over wider ranges of values of the variables.

Humble, Lowdermilk and Desmon (2) have studied heat transfer to air near atmospheric pressure over a wide range of fluid and surface temperatures, all above 500 R; they found that the data can be correlated by an equation of simple form

$$\frac{h_{avg}d}{k_f} = 0.023\left(\frac{\rho_f V_B d}{\mu_f}\right)^{0.80}\left(\frac{C_{pf}\mu_f}{k_f}\right)^{0.40}\frac{1.48}{(l/d)^{0.10}} \quad [3]$$

Here, h_{avg} is an average heat transfer coefficient over the whole length of the heat transfer tube, including the first few diameters, where the local heat transfer coefficients are usually considerably higher than the values farther down the tube. The last term of Equation [3] $(1.48/(l/d)^{0.10})$ takes care of this averaging and is equal to unity at $l/d = 50$.

It is typical in semiempirical correlations of heat transfer data to find that the heat transfer coefficient is proportional to the eighth-tenths power of the Reynolds number. When the physical properties of the fluid vary moderately with temperature, a correlation can generally be obtained by evaluating the physical properties at some reference temperature. This temperature is usually somewhere between the fluid bulk temperature and the wall temperature, but its relationship to these two temperatures may be influenced by the ratio of the mass flow to the rate of heating of the fluid, and by the upstream history of the fluid (state of development of velocity and temperature distributions, and the rate of change thereof). When the variation of fluid properties is large and nonmonotonic, as for gas in the neighborhood of the critical temperature, the technique of achieving correlation by selecting a suitable reference temperature has questionable justification, but is sometimes used (3).

[3] Numbers in parentheses indicate References at end of paper.

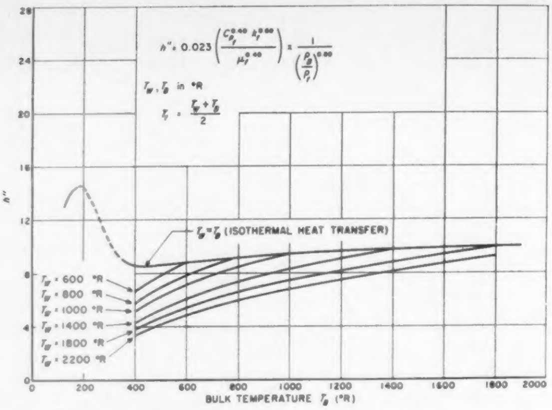

Fig. 3 Computed heat transfer correlation for oxygen at 1000 psia

Equation [3], the correlation equation of (2) for the average heat transfer coefficient, can be put into the form

$$h' = h'' \quad [4]$$

where

$$h' = \frac{q}{(T_W - T_B)}\frac{d^{0.20}}{G^{0.80}};\; h'' = 0.023\,\frac{C_{pf}^{0.40}\,k_f^{0.60}}{\mu_f^{0.40}}\,\frac{1}{(\rho_B/\rho_f)^{0.80}}$$

here h' is the generalized heat transfer coefficient for fully developed heat transfer and it is assumed that the average heat transfer coefficient over the first 50 diameters of tube length is sufficiently close to the fully developed heat transfer coefficient to make further correction unnecessary. Equation [4] should not be presumed valid for conditions where the fluid bulk temperature (air or oxygen) is less than 400 R. Below this temperature, the fluid properties change with temperature in a different manner from that at higher temperatures.

Equation [4], though no longer dimensionless, is convenient because the left-hand side contains only quantities which were measured as part of the experimental program, whereas the right-hand side of the equation is a function of the physical properties of the fluid. It is also possible, by means of this equation, to compare data which were obtained at different mass flow rates of the fluid.

The dimensional values of h' used in this report are computed from the quantities q in (ft lb)/(ft^2 sec), $(T_W - T_B)$ in °R, d in ft, and G in slugs/(ft^2 sec).

The fully developed generalized heat transfer coefficient predicted by the correlation, the quantity h'', was calculated for oxygen at a pressure of 1000 psia and at bulk temperatures greater than 400 R. The results are plotted as a function of the bulk temperature and the wall temperature in Fig. 3. The physical properties of oxygen were collected from the literature, and the values used are shown in Table 1 (4–12).

The effective film temperature recommended in (2), $T_f = (T_W + T_B)/2$, was used for these calculations. The predicted isothermal generalized heat transfer coefficient is shown throughout the bulk temperature range, but between $T_B = 175$ R and $T_B = 350$ R the values are uncertain.

Reference (13) gives theoretical and experimental data on the variation of the point heat transfer coefficient within the region in which the equilibrium velocity and temperature distributions are being developed. The experimental equipment used in the present investigation had a medium-long calming section upstream from the heated section; for a tube of this configuration, the heat transfer coefficient at the upstream end of the heated section may be twice as high as the corresponding fully developed heat transfer coefficient, which

Table 1 Physical properties of oxygen at 1000-psia pressure[1]

$R = 1552 \frac{\text{ft lb}}{\text{slugs °R}}$ $T_{cr} = 278°\text{R}$ $P_{cr} = 730$ psia

T (°R)	C_p $\left(\frac{\text{ft lb}}{\text{slugs °}R}\right)$	k $\left(\frac{\text{ft lb ft}}{\text{ft}^2 \text{ sec °}R}\right)$	μ $\left(\frac{\text{lb sec}}{\text{ft}^2}\right)$	ρ $\left(\frac{\text{lb}}{\text{ft}^3}\right)$	h'' $0.023 \frac{C_p^{0.40} k^{0.60}}{\mu^{0.40}}$	Pr $\frac{C_p \mu}{k}$
125	94.0×10^2	332.0×10^{-4}	760.0×10^{-8}	76.0	12.96	2.15
150	97.0×10^2	275.0×10^{-4}	475.0×10^{-8}	73.0	14.04	1.68
175	101.0×10^2	220.0×10^{-4}	330.0×10^{-8}	69.0	14.45	1.52
200	106.0×10^2	155.0×10^{-4}	260.0×10^{-8}	64.0	13.23	1.78
250	132.0×10^2	63.0×10^{-4}	207.0×10^{-8}	51.3	8.69	4.33
300	250.0×10^2	32.3×10^{-4}	48.0×10^{-8}	23.0	15.30	3.72
350	93.0×10^2	28.5×10^{-4}	45.0×10^{-8}	11.2	9.12	1.47
400	74.0×10^2	29.8×10^{-4}	45.0×10^{-8}	8.60	8.60	1.12
450	67.0×10^2	31.7×10^{-4}	45.5×10^{-8}	7.20	8.48	0.96
500	65.0×10^2	33.7×10^{-4}	46.7×10^{-8}	6.30	8.60	0.90
600	62.0×10^2	37.5×10^{-4}	50.0×10^{-8}	5.30	8.79	0.83
800	60.0×10^2	44.4×10^{-4}	58.1×10^{-8}	3.80	9.12	0.79
1000	60.5×10^2	51.0×10^{-4}	67.0×10^{-8}	3.05	9.39	0.80
1400	63.5×10^2	62.0×10^{-4}	84.0×10^{-8}	2.16	9.75	0.86
1800	65.0×10^2	70.8×10^{-4}	98.0×10^{-8}	1.67	9.94	0.90
2000	67.0×10^2	72.5×10^{-4}	104.0×10^{-8}	1.50	10.06	0.96

[1] The properties at bulk temperatures of 200, 250 and 300 are estimates only.

is closely approached beyond approximately 20 diameters of the heated section.

The experimental data of the present report were reduced to obtain values of the dimensional generalized heat transfer coefficient h', thus implicitly assuming that the heat flux was proportional to the eight-tenths power of the mass flow rate for all of the flow conditions encountered in the tests. This assumption was necessary in order to correlate the data, since the tests were made at a variety of mass flow rates and heat flow rates.

The data were not otherwise corrected for entrance effect, axial wall temperature gradient, pressure or rate of heating, though information on these conditions is tabulated with the data.

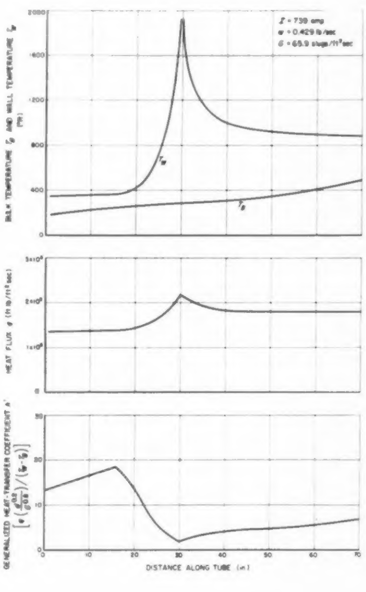

Fig. 4 Plotted data of test 135-C

Correlated Test Data—Oxygen

Tests were made over a wide range of values of fluid flow rate and heat flux, but most of the tests were controlled to give fairly high wall temperatures. Consequently, combinations of high flow rate and low heat flux are almost entirely absent.

Data obtained from a typical test are plotted vs. tube length in Fig. 4.

Table 2 Minimum heat-transfer-coefficient points for oxygen at supercritical pressure

$d = 0.016$ ft

Test No.	P (psia)	I (amp)	G $\left(\frac{\text{slugs}}{\text{ft}^2 \text{ sec}}\right)$	T_W (°R)	T_B (°R)	$T_W - T_{cr}$ (°R)	q $\left(\frac{\text{ft lb}}{\text{ft}^2 \text{ sec}}\right)$	$\frac{q}{G^{0.40}}$	$\frac{q}{T_W - T_{cr}}$ $\left(\frac{\text{ft lb}}{\text{ft}^2 \text{ sec °R}}\right)$	$q\left(\frac{d^{0.20}}{G^{0.80}}\right)$	$\frac{q\left(\frac{d^{0.20}}{G^{0.80}}\right)}{T_W - T_{cr}}$
130A	885	864	86.76	1800	282	1522	2.80×10^5	4.69×10^4	184	3500	2.30
131A	990	607	19.13	2030	...	1752	1.37×10^5	4.21×10^4	78	5670	3.23
131B	980	719	31.69	2050	300	1772	1.95×10^5	4.89×10^4	110	5380	3.03
131C	990	652	33.45	1900	283	1622	1.60×10^5	3.93×10^4	98	4200	2.59
131D	980	655	27.53	1890	...	1612	1.60×10^5	4.24×10^4	99	4950	3.07
133F	950	737	53.99	1800	...	1522	1.83×10^5	3.72×10^4	120	3900	2.56
134C	1062	698	57.30	1900	280	1622	1.89×10^5	3.74×10^4	116	3250	2.00
135C	1040	739	65.87	2050	284	1772	2.16×10^5	4.05×10^4	122	3300	1.86
135D	1000	708	76.06	720	307	442	1.52×10^5	2.69×10^4	344	2060	4.66
144A	900	703	70.89	1720	...	1442	2.03×10^5	3.69×10^4	140	3050	2.11
144B	900	703	61.62	1010	...	732	1.58×10^5	3.04×10^4	216	2340	3.19
144C	890	670	67.50	760	...	482	1.33×10^5	2.46×10^4	276	2000	4.15

When the fluid at supercritical pressure was heated from a temperature below its critical temperature, a pronounced minimum in heat transfer coefficient was observed as the bulk temperature passed through the region of the critical temperature. This can be seen in Fig. 4.

Twelve fairly accurate determinations of minimum generalized heat transfer coefficient were made, corresponding to peak wall temperatures on as many tests. These data are given in Table 2. Correlation in terms of the generalized heat transfer coefficient is given in Fig. 5.

Generalized heat transfer coefficients at three values of wall temperature, 600, 1000 and 1800 R, were obtained by interpolating the data of many tests. The interpolated data are given in Table 3. Each set of data shows a minimum in heat transfer coefficient vs. bulk temperature which is consistent with the values given in Table 2 and Fig. 5. The data for T_W = 600 R and T_W = 1000 R show a decrease from a high initial generalized heat transfer coefficient at low bulk temperature to the minimum at the critical temperature, and all three groups show a portion of a subsequent recovery toward a higher generalized heat transfer coefficient as the bulk temperature increases beyond the critical temperature.

For bulk temperatures between 300 and 600 R, there is considerable scatter in the data, and many points lie above the curves which were sketched in to represent the lower limit of the generalized heat transfer coefficient with bulk temperature in this region. Many of the high values represent measurements made near the inlet to the heat transfer tube and can be discounted on the basis of the ordinary entrance tube and can be discounted on the basis of the ordinary entrance effect. It should be noted also that most of the data in this region were obtained from tests in which the oxygen entered the tube at a temperature higher than the critical temperature; the upstream history of these flows is considerably different from that of the flows which yielded the data in the bulk temperature range of 200 to 300 R. The scatter of the data and the deviation from the curve drawn are much less for T_W = 1800 R than for T_W = 1000 R.

After the data obtained at a value for l/d of less than 20 had been discounted, the few remaining points in the region of high scatter did not show any definite trend with fluid pressure, rate of heating (q/G), or axial temperature gradient in the tube wall.

The faired curves from the constant wall temperature cross plots and the data from the tests such as that shown in Fig. (4) were combined to obtain the summary correlation curve given as Fig. 6, which represents the generalized heat transfer coefficient for oxygen at 1000 psi as a function of bulk temperature and of wall temperature.

At the upper left-hand corner of the summary curve (Fig. 5) there appears a boundary line which slopes steeply up-

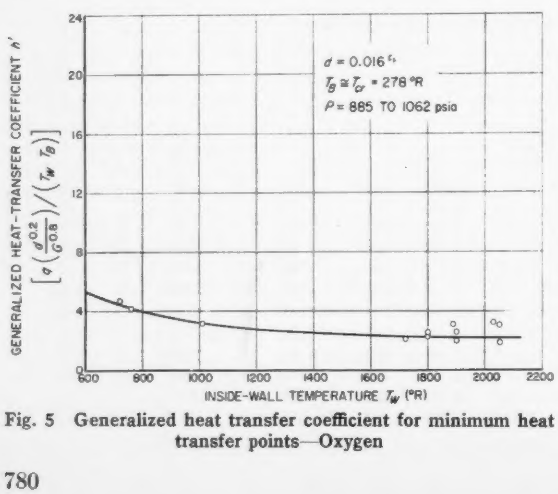

Fig. 5 Generalized heat transfer coefficient for minimum heat transfer points—Oxygen

Table 3 Heat transfer to oxygen—Selected data at various constant wall temperatures

Test No.	$T_{B_{in}}$ (°R)	P_{in} (psia)	G $\left(\frac{\text{slugs}}{\text{ft}^2\text{sec}}\right)$	I (amp)	$\left(\frac{q_1}{G}\right)_{T_W=1000°R}$ $\left[\frac{\text{ft lb/slug}}{4(l/d)}\right]$
96C	180	975	141.4	1363	4296
96D	186	1000	118.4	1255	4350
96E	355	635	37.7	826	5918
96F	409	630	34.8	838	6599
96G	422	625	35.4	778	5591
96H	429	256	13.4	557	7571
96I	445	258	13.4	566	7818
96J	455	255	14.6	437	4277
97A	178	1025	133.5	1349	4457
97B	180	1030	141.1	1368	4337
97C	423	653	35.4	881	7170
97E	450	635	37.0	751	4984
97F	454	254	13.6	619	9213
97I	480	259	14.8	442	4316
99E	500	922	34.1	917	8064
99F	500	448	23.4	756	7987
99G	498	452	23.1	773	8458
99I	498	449	25.1	595	4612
101A	500	838	39.4	646	3554
101D	497	868	34.9	847	6722
101E	498	865	35.9	806	5917
101G	496	388	17.5	494	4560
101H	495	399	15.9	605	7528
101I	496	380	20.0	274	1227
101J	496	388	19.8	360	2140
104A	177	910	164.7	1680	5604
104B	184	898	173.9	1582	4706
106B	184	1060	161.8	1483	4445
106D	326	613	46.7	823	4743
106E	344	524	37.0	792	5544
106F	358	440	28.9	754	6433
109B	179	1004	150.1	1363	4047
109E	333	1057	37.7	785	5345
109F	376	1059	33.3	790	6128
109G	388	1059	32.8	742	5489
109H	404	1035	32.2	655	4357
109K	421	904	26.1	454	2582
110C	185	964	135.9	1320	4192
110G	310	1010	37.6	696	4213
110H	345	1015	35.2	773	5551
110K	404	950	25.3	706	6442
110L	413	904	24.1	631	5402
110M	421	863	23.7	487	3272
111B	179	938	149.8	1454	4615
111D	190	940	146.7	1397	4350
111E	323	994	37.0	696	4281
118B	175	900	138.2	1294	3962
118D	402	600	55.2	1061	6669
118E	438	460	42.6	912	6384
119D	420	640	59.0	1080	6465
119E	432	650	57.8	1092	6746
119F	444	637	59.2	979	5294
119G	460	823	43.7	996	7423
119H	468	790	44.3	898	5952
130A	182	973	86.8	864	2812
131A	215	1007	19.1	607	6308
131C	191	1007	33.5	652	4150
131C	191	1007	33.5	652	4150
131D	199	1009	19.1	655	7345
131D	199	1009	19.1	655	7345
134C	193	1075	57.3	698	2780
134C	193	1075	57.3	698	2780
135C	189	1064	65.9	739	2710
135C	189	1064	65.9	739	2710
135D	195	1068	76.1	708	2154

$d_1 = 0.016$ ft
$d_1^{0.20} = 0.44$ ft$^{1/5}$
$(q_1)_{T_W = 1000°R} \cong 0.327\, I^2_{amp}$ (ft lb)/(ft^{2}sec)

$T_W = 600°R$				$T_W = 1000°R$				$T_W = 1800°R$			
l (in.)	T_B (°R)	$\frac{dT_W}{dl}$ (°R/in.)	$\frac{h'}{q\left(\frac{d^{0.20}}{G^{0.80}}\right)} = \frac{\,}{T_W - T_B}$	l (in.)	T_B (°R)	$\frac{dT_W}{dl}$ (°R/in.)	$\frac{h'}{q\left(\frac{d^{0.20}}{G^{0.80}}\right)} = \frac{\,}{T_W - T_B}$	l (in.)	T_B (°R)	$\frac{dT_W}{dl}$ (°R/in.)	$\frac{h'}{q\left(\frac{d^{0.20}}{G^{0.80}}\right)} = \frac{\,}{T_W - T_B}$
8.6	233	113	12.1	10.1	241	550	6.6	...	...	...	...
9.8	240	300	11.7	10.4	251	850	6.3	...	...	...	...
...	...	...	...	2.0	390	190	8.5	...	...	...	...
...	...	...	...	1.4	440	260	10.2	10.0	630	42	5.8
...	...	...	...	2.6	469	92	9.2	...	...	...	...
...	...	...	...	1.2	458	310	9.5	9.9	665	36	5.3
...	...	...	...	...	...	...	...	7.7	642	55	5.5
...	...	...	...	9.0	583	18	7.2	...	...	...	...
9.9	230	530	11.9	...	...	...	...	...	...	...	...
8.6	242	45	12.1	...	...	...	...	...	...	...	...
...	...	...	...	...	...	...	...	9.9	655	70	6.3
...	...	...	...	7.6	533	29	9.2	...	...	...	...
...	...	...	...	...	...	...	...	3.2	549	100	5.9
...	...	...	...	9.0	610	25	7.7	...	...	...	...
...	...	...	...	...	...	...	...	5.0	628	96	7.0
...	...	...	...	...	...	...	...	5.5	639	75	6.4
...	...	...	...	...	...	...	...	4.0	609	100	6.6
...	...	...	...	5.5	570	35	8.5	...	...	...	...
...	...	...	...	21.4	706	20	10.1	...	...	...	...
...	...	...	...	...	...	...	...	22.4	1019	15	8.6
...	...	...	...	1.9	533	100	10.8	...	...	...	...
...	...	...	...	6.0	585	55	7.9	...	...	...	...
...	...	...	...	...	...	...	...	11.9	800	50	6.2
10.0	535	5	11.5	...	...	...	...	...	...	...	...
1.0	500	25	13.0	...	...	...	...	...	...	...	...
...	...	...	...	2.0	191	310	8.9	...	...	...	...
1.6	193	395	13.1	2.7	200	320	7.5	...	...	...	...
2.9	203	290	12.4	...	...	...	...	...	...	...	...
...	...	...	...	3.2	351	110	6.6	...	...	...	...
...	...	...	...	2.4	370	210	7.6	...	...	...	...
...	...	...	...	1.5	382	280	8.5	...	...	...	...
6.7	228	230	11.7	...	...	...	...	...	...	...	...
...	...	...	...	...	...	...	...	5.7	393	105	3.9
...	...	...	...	...	...	...	...	6.3	480	75	4.6
...	...	...	...	2.1	420	175	8.1	...	...	...	...
...	...	...	...	7.1	490	40	7.2	...	...	...	...
3.0	445	11	11.3	...	...	...	...	...	...	...	...
6.6	225	210	11.6	...	...	...	...	...	...	...	...
2.0	320	75	11.3	...	...	...	...	...	...	...	...
...	...	...	...	1.6	361	295	7.5	7.2	419	65	...
...	...	...	...	1.9	438	168	9.3.	...	...	...	...
...	...	...	...	4.0	468	65	8.1	...	...	...	...
1.3	440	32	13.8	...	...	...	...	...	...	...	...
3.8	207	235	12.7	...	...	...	...	...	...	...	...
4.5	220	280	12.0	...	...	...	...	...	...	...	...
4.5	330	55	11.7	...	...	...	...	...	...	...	...
9.2	233	190	11.1	...	...	...	...	...	...	...	...
...	...	...	...	1.5	452	160	11.9	...	...	...	...
...	...	...	...	1.6	470	130	11.0	...	...	...	...
...	...	...	...	1.3	450	170	11.6	10.1	627	50	6.7
...	...	...	...	...	...	...	...	8.5	620	65	6.7
...	...	...	...	3.4	500	55	10.4	...	...	...	...
...	...	...	...	...	...	...	...	7.5	650	75	7.1
...	...	...	...	2.3	510	100	11.1	...	...	...	...
32	260	70	7.4	35.5	280	160	4.0	...	...	...	...
1.0	225	140	10.9	3.8	262	140	6.4	9.2	330	140	3.8
10.3	260	130	8.9	12.8	277	180	4.8	16.6	280	210	2.7
...	...	...	...	...	...	...	...	19.0	288	−170	2.7
3.8	246	125	10.1	7.0	285	130	5.8	13.3	364	80	3.4
...	...	...	...	...	...	...	...	19.8	445	−32	3.6
17.6	265	62	7.2	21.6	276	170	3.9	...	...	...	...
...	...	...	...	37.0	306	−20	4.0	...	...	...	...
23.5	272	65	7.3	27.4	280	160	4.0	...	...	...	...
...	...	...	...	39.2	305	−22	4.1	...	...	...	...
4.2	295	27	6.5	...	...	...	...	...	...	...	...

wards. This line is clearly defined by data in the range of $T_B = 190$ to 215 R and $T_W = 340$ to 480 R; the curves for the higher wall temperatures seem to approach this boundary at their low bulk temperature ends.

The minimum values of generalized heat transfer coefficient shown in Fig. 6 are consistent with the locus of minimum values given in Fig. 5.

Above bulk temperatures of 400 R, the summary curve is drawn to represent results obtained by heating the fluid through the critical temperature, and is remarkably similar to the calculated values of h'' shown in Fig. 3.

A few tests were made in which oxygen at a pressure somewhat less than its critical pressure was heated through its saturation temperature. The behavior seemed similar to that of the fluid at supercritical pressure, except that the minimum values of generalized heat transfer coefficients are even lower, and the minimum occurs at a slightly lower bulk temperature.

Conclusions

The experimental work described here has resulted in the collection of empirical data on convective heat transfer to oxygen near its critical temperature. These data are presented in the form of plots of generalized heat transfer coefficient vs. fluid bulk temperature. The parameters used in presenting the data are the over-all quantities which would be known for any proposed engineering application, rather than the more general dimensionless quantities involving the physical properties of the fluid which are ordinarily used in the presentation of convective heat transfer data. Thus the data can be used directly for engineering purposes, eliminating the need for an extensive knowledge of the physical properties of the fluid.

The fluid exhibited a minimum in heat transfer coefficient near its critical temperature. This minimum will be the limiting design factor in most applications utilizing these fluids as coolants in heat transfer equipment. It was possible in the case of oxygen to obtain enough data in the region of the minimum heat transfer coefficient to define this minimum for the particular test equipment used. The information available was not sufficient to permit general prediction of this minimum heat-transfer coefficient for other systems.

The modified Humble, Lowdermilk, Desmon correlation (Equation [4]) is in reasonably close agreement with the experimental results when the fluid bulk temperature is above the critical temperature.

APPENDIX

Analysis of Flow of Heat in Electrically Heated Tube

Consider the flow of heat and electricity in a small annular element of a tube. By writing the expressions for conservation of electricity (current) and heat, the following two equations can be obtained

$$\frac{\partial^2 e}{\partial x^2} = 0 \qquad \text{[A-1]}$$

$$\frac{J}{R}\left(\frac{\partial e}{\partial x}\right)^2 + k\frac{\partial^2 T}{\partial r^2} + \frac{k}{r}\frac{\partial T}{\partial r} + \frac{\partial k}{\partial T}\left(\frac{\partial T}{\partial r}\right)^2 = 0 \qquad \text{[A-2]}$$

subject to the assumptions

$$\left.\begin{aligned} \frac{\partial e}{\partial r} &= 0 \qquad \frac{\partial^2 e}{\partial r^2} = 0 \\ \frac{\partial T}{\partial x} &= 0 \qquad \frac{\partial^2 T}{\partial x^2} = 0 \end{aligned}\right\} \qquad \text{[A-3]}$$

These assumptions are reasonable for a long thin-walled tube.

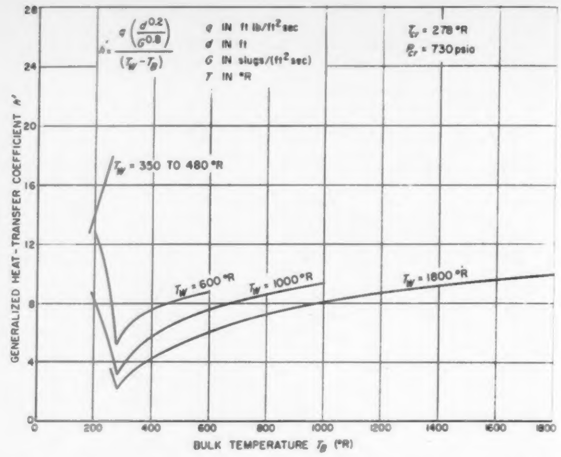

Fig. 6 Summary curve—Generalized heat transfer coefficient for oxygen at 1000 psia

If the outside surface of the tube is adopted as a reference, a position parameter can be defined

$$s = \left(1 - \frac{r}{r^2}\right) \qquad \text{[A-4]}$$

The thermal conductivity and electrical resistivity can be written

$$k = k_2 + \frac{dk}{dT}(T - T_2) \qquad \text{[A-5]}$$

$$R = R_2 + \frac{dR}{dT}(T - T_2) \qquad \text{[A-6]}$$

where it is assumed that these properties vary linearly with temperature.

Equation [A-2] can now be written in the form

$$\frac{R}{R_2}\frac{d}{ds}\left[(1 - s)\frac{k}{k_2}\frac{d(T - T_2)}{ds}\right] + (1 - s)\frac{Jr_2^2(de/dx)^2}{R_2k_2} = 0 \qquad \text{[A-7]}$$

Approximate solutions to this equation, in the form of series, can be obtained in several forms. The solution used, with the voltage gradient expressed in terms of an average resistivity of the tube, is

$$q_1 = \frac{JI^2 R_2}{2\pi r_1 A_{\text{tube wall}}}\left(\frac{R_{\text{avg}}}{R_2}\right) \times \left[1 - \frac{\delta}{\left(s_1 - \dfrac{s_1^2}{2} + \dfrac{Bs_1^3}{6} - \dfrac{B\delta s_1^2}{2} + \dfrac{B\delta s_1^3}{6} + \ldots\right)}\right] \qquad \text{[A-8]}$$

$$T_{W_2} - T_{W_1} = \frac{JI^2 r_2^2 R_2}{k_2 A^2_{\text{tube}}}\left(\frac{R_{\text{avg}}}{R_2}\right)^2 \times \left(\frac{F}{1 + \sqrt{1 - AF}} - \frac{B\delta s_1^3}{6} + \frac{Bs_1^4}{24} - \frac{B\delta s_1^4}{12} + \ldots\right) \qquad \text{[A-9]}$$

where

$$\frac{R_{\text{avg}}}{R_2} = \frac{(s_1 - (s_1^2/2))}{\left(s_1 - \dfrac{s_1^2}{2} + \dfrac{Bs_1^3}{6} - \dfrac{B\delta s_1^2}{2} + \dfrac{B\delta s_1^3}{6} + \ldots\right)} \qquad \text{[A-10]}$$

and

$$\delta = \frac{q_2 A^2_{tube}}{JI^2 r_2} \frac{1}{(R_{avg}/R_2)^2 R_2} \quad \text{[A-11]}$$

$$A = \frac{JI^2 r_2^2 R_2}{A^2_{tube} k_2} \left(\frac{R_{avg}}{R_2}\right)^2 \frac{(dk/dT)}{k_2} \quad \text{[A-12]}$$

$$B = \frac{JI^2 r_2^2 R_2}{A^2_{tube} k_2} \left(\frac{R_{avg}}{R_2}\right)^2 \frac{(dR/dT)}{R_2} \quad \text{[A-13]}$$

$$F = (1 - 2\delta) \log_e \frac{1}{(1 - s_1)} - (s_1 - (s_1^2/2)) \ldots \text{[A-14]}$$

The heat flux at the outside surface, q_2, is computed as a function of tube surface temperature, taking into account both radiation and free convection terms.

References

1 Eckert, E. R. G., "Introduction to the Transfer of Heat and Mass," 1st edit., pp. 128–140, McGraw-Hill, New York, 1950.

2 Humble, L. V., Lowdermilk, W. H., and Desmon, L. G., "Measurements of Average Heat-Transfer and Friction Coefficients for Subsonic Flow of Air in Smooth Tubes at High Surface and Fluid Temperatures," NACA TR 1020, Dec. 31, 1950.

3 Eckert, E. R. G., Hartnett, J. P., and Tobin, H. F., "Heat Transfer," *Industrial and Engineering Chemistry*, vol. 47, no. 3, 1954, p. 647.

4 Lobo, W. E., "Technical Data—Final Report to the National Defense Research Committee—Contract No. OEMsr-365," Library of Congress no. P. B. 8900, The M. W. Kellogg Co., Jersey City, N. J., Aug. 24, 1924.

5 "Density and Pressure of Saturated Oxygen," Technical Publication no. 424. National Bureau of Standards, Washington, D. C.

6 Hammann, Von G., "Warmeleitfahigkeit von flussigem Sauerstoff, flussigem Stickstoff and ihren Gemischen," *Annalen der Physik*, vol. 32, 1938, p. 593.

7 Critchell, W. G., Jones, L. F., and Zeibland, H., "Thermal Conductivity of Liquid Oxygen Between 90°K and 105°K," Report no. 11/R/52, Ministry of Supply, Explosives Research and Development Establishment, London, Nov. 1952.

8 Perry, J. H., "Chemical Engineers' Handbook," 2nd edit. McGraw-Hill, New York, 1941.

9 Sachsel, G. F., Youtz, M. A., and Moore, J. R., "Propellants for Supersonic Vehicles: Liquid Oxygen," RA 15044. Douglas Aircraft Co., Battelle Memorial Institute, Columbus, Ohio, 1948.

10 Tribus, M., and Boelter, L. M. K., "An Investigation of Aircraft Heaters—11. Properties of Gases," ARR (WR W-9), NACA, Oct. 1942.

11 Ellenwood, F. O., Kulik, N., and Gay, N. R., "The Specific Heats of Gases Over Wide Ranges of Pressures and Temperatures," Bulletin no. 30, Cornell University Engineering Experiment Station, Ithaca, N. Y., 1942.

12 "International Critical Tables of Numerical Data: Physics, Chemistry, and Technology," vol. III, McGraw-Hill, New York, 1928.

13 Boelter, L. M. K., Young, G., and Iverson, H. W., "An Investigation of Aircraft Heaters—XXVII. Distribution of Heat-Transfer Rate in the Entrance Section of a Circular Tube," NACA TN 1451, July 1948.

Instrumentation to Measure Gas-Phase Composition

(Continued from page 775)

$$\frac{\int_0^{y_m} \int_0^{\delta'} \delta^3 \left(\frac{dn}{d}\right) d\delta\, dy}{125\, n_0 \frac{V_S}{V_x} x_S (\bar{\delta})^3} = \int_0^{\infty} \left\{ \int_0^{\mathfrak{D}'} \mathfrak{D}^5 e^{-5\mathfrak{D}} d\mathfrak{D} \right\} \times$$

$$\left\{ \frac{1}{\mathfrak{D}'} e^{-1/\bar{R}\mathfrak{D}'^2} + \bar{R}\mathfrak{D}'(e^{-1/\bar{R}\mathfrak{D}'^2} - 1 \right\} d\mathfrak{D}' \ldots \text{[A10b]}$$

where

$$\bar{R} = \frac{\rho_\omega V_x(\bar{\delta})^2}{18\mu_{av} x_S}; \quad \mathfrak{D} = \frac{\delta}{\bar{\delta}}; \quad \mathfrak{D}' = \frac{\delta'}{\bar{\delta}}$$

The limits $\mathfrak{D}' = \infty$ and $\mathfrak{D}' = 0$ correspond to $y = 0$ and $y = y_m$, respectively.

Combination of Equations [A10, A10a, Al0b] yields the expression for error

$$E = \frac{25}{12} \int_0^{\infty} \left\{ e^{-1/\bar{R}\mathfrak{D}^2} \left[\frac{1 + \bar{R}\mathfrak{D}^2}{\mathfrak{D}} \right] - \bar{R}\mathfrak{D} \right\} \times$$
$$\left\{ e^{-5\mathfrak{D}} \left[25\mathfrak{D}^5 + 25\mathfrak{D}^4 + 20\mathfrak{D}^3 + 12\mathfrak{D}^2 + 24\mathfrak{D} + \frac{120}{125} \right] - \frac{120}{125} \right\} d\mathfrak{D} \ldots \text{[A10c]}$$

The authors have not attempted to carry out the integration of Equation [A10c] in other than numerical form. The results of such calculations are

$\bar{R}$	E
10	0.066
100	0.010
1000	0.0018

It is important to note that this approximate analysis which does not include the effects of liquid boundary layer, indicates that the modified Reynolds number $\bar{R}$ is the only parameter upon which the sampling error depends. For large values of $\bar{R}$ (that is, for high velocities, small drops, small probe size, etc.) the error is small. Conversely, as the value of $\bar{R}$ is decreased, the error is made larger. The value of $\bar{R}$ for most of the experimental work described in this paper is estimated to be about 100, and thus the computed error is about 1 per cent. This value compares very well with the measured values of error at the optimum operating conditions.

References

1 Shapiro, A. H., Wadleigh, K. R., Gavril, B. D., and Fowle, A. A., "The Aerothermopressor—A Device for Improving the Performance of a Gas Turbine Power Plant," *Trans. ASME*, vol. 78, no. 3, April 1956.

2 Dussourd, J. L., "A Theoretical and Experimental Investigation of a Deceleration Probe for Measurement of Several Properties of a Droplet-Laden Air Stream," ScD Thesis, MIT, Oct. 1954.

3 Webber, J. H., and Baker, D. F., "The Photometric Measurement of Droplet Size," Naval Engineer Thesis, MIT, 1955.

4 Rona, T. P., "Gas Temperature Measurements by Ultrasonic Pulse Method," ScD Thesis, MIT, 1954.

5 Wadleigh, K. R., "An Experimental Investigation of a Small-Scale Aerothermopressor—A Device for Increasing the Stagnation Pressure of a High Temperature, High Velocity Gas Stream by Evaporative Cooling," ScD Thesis, MIT, 1953.

6 Larson, H. K., "Techniques for Measuring the Specific Humidity of the Gas Phase of a High Temperature, High Velocity, Two Phase Stream of Air and Water," SM Thesis, MIT, 1954.

7 Peterson, D. L., "An Apparatus for the Measurement of the Water Content of High Humidity Water-Air Mixtures," SB Thesis, MIT, 1955.

8 Oman, R. A., "Development of Techniques for the Measurement of Several Properties of Water-Air Two-Phase Flows," SM Thesis, MIT, 1956.

9 Keenan, J. H., "Thermodynamics," John Wiley, New York, 1941.

10 Keenan, J. H., and Keyes, F. G., "Thermodynamic Properties of Steam," John Wiley, New York, 1936.

11 Nukyama, S., and Tanasawa, Y., "An Experiment on the Atomization of Liquid by Means of an Air Stream," *Transactions of the Society of Mechanical Engineers, Japan*, vol. 4, 1938, Reports 1–6.

Gas-Side Wall Temperatures in Rib-Backed Liquid-Cooled Combustion Chambers

J. G. BARTAS[1]

General Electric Co., Lynn, Mass.

A "hot-spot" may form on the wall of a rocket combustion chamber when a thin wall is reinforced by a thick rib. An analytical evaluation of the temperature profile along the axis of symmetry of the rib is carried out. Results are presented in graphical form for convenient computation.

Nomenclature

A, B, C, D = constants
a = $[1 + (g/b)^2]^{-1/2}$
b = one-half rib thickness
g = $t + t'$
h = convective heat transfer coefficient
k = conductivity
T = temperature
t = wall thickness
t' = k/h
u, v = coordinates in the w-plane
x, y = coordinates in the z-plane
ϕ, ψ = coordinates in the ξ-plane

Introduction

IT IS of considerable value to obtain estimates of the temperatures of "hot spots" that may occur on the wall surfaces of rocket combustion chambers. One form of hot spot can occur when a thin wall is reinforced by a thick rib or spacer to satisfy structural requirements. Adding a rib or "fin" is normally desirable from a heat transfer viewpoint since the effective coolant-side surface area is generally increased. However, conditions do exist where a liquid coolant film resistance is very small in comparison with the resistance of the wall material. The rib, if wide enough, can therefore effectively impede the local heat flux to the liquid and raise the gas-side wall temperature several hundred degrees above the temperature of the wall surfaces remote from the rib.

The exact dividing line between a "cooling" fin and an "insulating" fin is rather difficult to establish analytically. If we accept conventional fin efficiency equations as valid, the heat flow from a rectangular plane fin is given by

$$Q_{\text{fin}} = Q_{\text{no fin}} \frac{A_{\text{fin surface}}}{A_{\text{fin base}}} \eta_F$$

where

$$\eta_F = \frac{\tanh ml}{ml} \qquad m = \sqrt{\frac{h}{kb}}$$

Considering the fin to be infinitely long, for heat transfer, the ratio of fin heat flow to no-fin heat flow becomes

$$\frac{Q_{\text{fin}}}{Q_{\text{no fin}}} = \sqrt{\frac{k}{hb}}$$

For a material conductivity of 105 Btu−in/hr−ft²−°F and a liquid-side heat transfer coefficient of 3000 Btu/hr−ft² −°F, a fin of thickness greater than 0.070 in. (b = 0.035) will insulate while a fin of less than 0.070-in. thickness will cool. It is often desirable to carry out a brief "check" similar to the preceding calculation to ascertain if a hot spot formation is probable. Contact resistances between the fin and the wall have been considered negligible.

Analysis

An extensively employed technique suitable for estimating hot spot temperatures consists of setting up an equivalent thermal network and solving the network by either hand or machine methods. Machine methods are especially suitable where maximum hot spot temperature requirements are imposed.

There is, however, an analytical approach which makes possible the calculation of the hot spot temperatures with very little effort. Although the temperature profile is determined only along the axis of symmetry of the rib, this is usually sufficient since the *maximum* wall temperatures fall along this line. Briefly, the approach consists of:

1 Substituting an added "thermal" thickness of metal for the boundary layer. This is equivalent to the network operation of replacing the gas-side heat transfer coefficient by an equivalent resistance.

2 Considering the liquid-side wall temperature to be isothermal. This assumption is usually not valid. However, under the conditions postulated in this analysis (i.e., liquid film resistance is small in relation to the material and gas-side film resistances), the liquid-side wall temperature approaches liquid temperature and experiences relatively little variation along the wall and fin surfaces. The determination of a suitable value of the isothermal liquid-side wall temperature and the error due to this assumption are examined in the following section.

(The two preceding simplifications reduce the problem to one of pure conduction.)

3 Transforming the wall-and-rib geometry to a corresponding slab and relating the linear temperature pattern in the slab to the wall-and-rib geometry temperatures.

It is implicitly assumed in the analysis that each wall-rib region may be considered independently and that the wall and rib are of the same material with temperature-independent conductivity. It is also assumed that folding the outer wall into an extension of the rib is admissible (cf. Figs. 1 and 2).

The transformation of the geometry in Fig. 1 into the geometry as shown in Fig. 2 has idealized the rib into an infinitely long fin. This case is an important one but not the only one encountered in practice. However, a fin may be of finite length and act, for all practical purposes, as an infinitely long fin. A fin that transfers 99, or 98, or 95 per cent of the heat transferred by an infinitely long fin may be considered, thermally speaking, to be infinitely long, depending on its function, the degree of accuracy required, the established criteria, etc. Assuming 99 per cent as the criteria, (tanh

Received Aug. 27, 1956.

[1] Senior Heat Transfer Engineer, Aircraft Accessory Turbine Department.

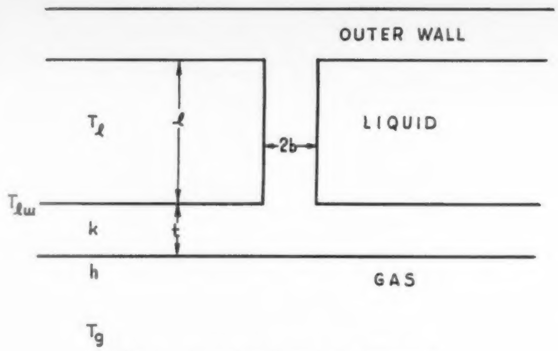

Fig. 1 Actual wall-and-rib geometry

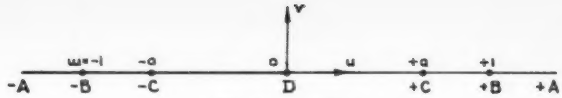

Fig. 3 w**-plane**

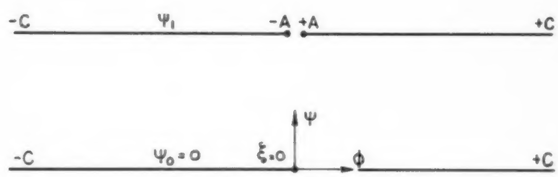

Fig. 4 ξ**-plane**

ml = 0.99) the 0.070-in. fin described need be only 0.093 in. long to be considered infinitely long.

The pertinent equations derived in the Appendix are plotted graphically in Fig. 5. The form of the equations does not permit direct solution for specified temperatures without extensive iteration.

Example

The following example illustrates the ease in solving problems of the type described here with the aid of Fig. 5:

Operating Conditions

Gas temperature: T_g = 4500°F
Liquid-side wall temperature: T_{lw} = 500°F
Gas-side heat transfer coefficient: h = 300 Btu/hr−ft²−°F
Wall and rib thermal conductivity: k = 105 Btu-in/hr−ft²−°F
Wall thickness: t = 0.15 in.

Required Answer

The maximum allowable rib thickness (2b) if the maximum wall temperature is not to exceed 2100 F. (The gas-side wall temperature will be 1700 F if no ribs are present.)

Solution

1. Compute "equivalent" boundary layer thickness: $t' = k/h$ = 0.35 in.
2. Compute total equivalent wall thickness: $g = t + t'$ = 0.5 in.
3. Compute y/g (the point of interest along the y-axis is t'). y/g = 0.7.
4. Compute temperature function: $(T_g - T)/(T_g - T_{lw})$ = 0.6.
5. Enter Fig. 5 with y/g and $(T_g - T)/(T_g - T_{lw})$ values and determine b/g ratio: b/g = 0.5.
6. Maximum allowable rib thickness (2b) is therefore equal to 0.5 in.

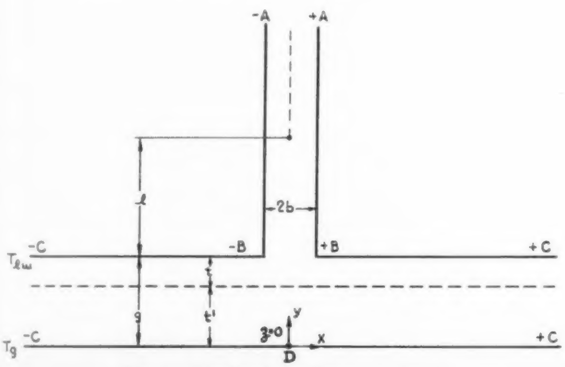

Fig. 2 Idealized geometry—z**-plane**

Discussion of Example

In the example illustrated above, the liquid-side wall temperature has been specified. This temperture is constant along the wall and fin surfaces and is equal to the liquid temperature *only* if the liquid-side heat transfer coefficient is infinite. For the practical case where a large, but finite, liquid-side heat transfer coefficient h_l is present, it is recommended that the "isothermal" liquid-side wall temperature be taken as the liquid-side wall temperature T_{lw}* that is computed if no rib or fin is present. For example, if the liquid temperature is 200 F and h_l has a value of 3000 Btu/hr − ft²−°F, the isothermal wall temperature can be computed to be 481 F for the operating conditions of the example.

The error that is introduced by the use of an isothermal T_{lw}* has not been rigorously established. The use of T_{lw}* has resulted in slightly conservative (high) values for hot-spot temperatures in the few cases that have been analyzed in detail by relaxation methods.

For instance, in the preceding example we may replace the boundary condition of T_{lw} = 500 F by T_l = 220 F, h_l = 3000 Btu/hr − ft²−°F (T_{lw}* = 500 F). A detailed relaxation calculation (40 × 40 mesh per sq in. of wall) with the convective boundary condition results in a maximum hot-spot temperature of 2084 F. This value, 384 F above the no-rib temperature of 1700 F, compares very favorably with the 2100 F obtained using Fig. 5. In the relaxation calculations, it is apparent that the decrease in surface temperature along the fin more than compensates for the higher-than-average surface temperature that exists in the region of the fin-wall junction *when insulating fins are present.* This effect leads to conservative hot-spot temperatures.

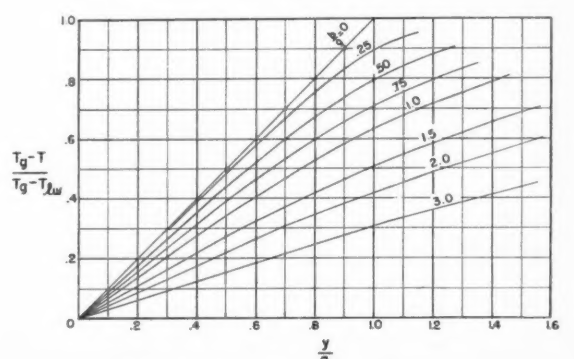

Fig. 5 $(T_g - T)/(T_g - T_{lw})$ **vs.** y/g

Conclusions

Fig. 5 is an extremely convenient aid for estimating the temperature of a possible hot spot which may be induced by a rib or spacer supporting a liquid cooled tube containing a flowing high temperature gas. While the assumptions of a constant wall conductivity and a constant coolant-side wall temperature may deviate from the true situation, the estimate does provide a reasonably accurate measure of the seriousness of the problem.

APPENDIX

The real geometry sketched in Fig. 1 was assumed to be thermally equivalent to the idealized geometry shown in Fig. 2. The boundary layer is replaced by an equivalent thickness of metal (t') where

$$t' = k/h \quad \ldots [1]$$

k is the metal thermal conductivity and h the heat transfer coefficient.

The problem is then reduced to one of pure conduction. It is first necessary to map the shell-and-rib shown in the complex z-plane (Fig. 2) into the upper half of the complex w-plane (Fig. 3) and, subsequently, to map this area of the w-plane into the slab of the complex ξ-plane (Fig. 4).

The transformation mapping the heat conducting region of the z-plane into the upper half of the w-plane is

$$\frac{dz}{dw} = A\,\frac{(1 - w^2)^{1/2}}{w^2 - a^2} \quad \ldots [2]$$

where

$$a^2 = \frac{b^2/g^2}{1 + b^2/g^2} \quad \ldots [3]$$

This transformation may be deduced by the method of Swartz-Christoffel. However, it is conveniently given by Kober.[2] Kober also integrates the equation

$$z = A\left\{\sin^{-1} w + \frac{(1 - a^2)^{1/2}}{2a}\cosh^{-1} \times \left(\frac{w^2 - 2a^2w^2 + a^2}{a^2 - w^2}\right)\right\} + B \quad \ldots [4]$$

One of the many equivalent forms of the integrated equation

$$z = A\left\{\sin^{-1} w + \frac{(1 - a^2)^{1/2}}{a}\tanh^{-1} \times \left(\frac{w^2(1 - a^2)}{a^2(1 - w^2)}\right)^{1/2}\right\} + B \quad \ldots [5]$$

was found more convenient for many phases of this study.

The constants A and B are determined from two convenient boundary points relating the z- and w-planes.

One boundary point (the origin)

$$w = u + iv = 0 + i0 \qquad z = x + iy = 0 + i0$$

leads to the result $B = 0$. Another boundary point

$$w = 1 + i0 \qquad z = b + ig$$

substituted into Equation [4] gives $A = 2b/\pi$.

Therefore

$$z = \frac{2b}{\pi}\left\{\sin^{-1} w + \frac{g}{b}\tanh^{-1}\left(\frac{w^2(1 - a^2)}{a^2(1 - w^2)}\right)^{1/2}\right\} \quad \ldots [6]$$

Along the axis of symmetry

$$w = 0 + iv \qquad z = 0 + iy$$

Solving for y

$$iy = \frac{2b}{\pi}\left\{\sin^{-1} iv + \frac{g}{b}\tanh^{-1}\left[\frac{iv}{a}\left(\frac{1 - a^2}{1 + v^2}\right)^{1/2}\right]\right\}$$

$$y = \frac{2b}{\pi}\left\{\sinh^{-1} v + \frac{g}{b}\tan^{-1}\left(\frac{g}{b}\cdot\frac{v}{(1 + v^2)^{1/2}}\right)\right\} \quad \ldots [7]$$

We next relate the w-plane to the ξ-plane. The required transformation is[3]

$$\frac{d\xi}{dw} = C'\,\frac{1}{w^2 - a^2} \quad \ldots [8]$$

$$\xi = C\ln\frac{w - a}{w + a} + D \quad \ldots [9]$$

The constants are solved for as above. At the origins

$$w = 0 + i0; \qquad \xi = \phi + i\psi = 0 + i0$$

$$C\ln(-1) + D = 0; \qquad D = -i\pi C$$

Another convenient point is

$$w = \infty + i0; \qquad \xi = 0 + i\psi_1$$

$$i\psi_1 = C\ln(1) - i\pi C; \qquad C = -\psi_1/\pi$$

Therefore

$$\xi = -\frac{\psi_1}{\pi}\ln\frac{w - a}{w + a} + i\psi_1 \quad \ldots [10]$$

Along the axis of symmetry

$$w = 0 + iv \qquad \xi = 0 + i\psi$$

and

$$i\psi = -\frac{\psi_1}{\pi}\ln\frac{iv - a}{iv + a} + i\psi_1$$

The expression for the natural logarithm may be converted to a more convenient form by using indentities

$$\ln(-x) \equiv \ln x + i\theta \text{ (here, } \theta = \pi)$$

$$\ln\frac{1 - x}{1 + x} \equiv -2\tanh^{-1} x$$

Therefore

$$i\psi = -\frac{\psi_1}{\pi}\left(\ln\frac{1 - \dfrac{iv}{a}}{1 + \dfrac{iv}{a}} + i\pi\right) + i\psi_1$$

$$i\psi = -\frac{\psi_1}{\pi}\left(-2\tanh^{-1}\frac{iv}{a}\right)$$

$$\psi = \frac{2\psi_1}{\pi}\tan^{-1}\frac{v}{a} \quad \ldots [11]$$

The necessary equation relating the ψ-function in the ξ-plane to the temperature T in the z-plane is

$$\frac{\psi_0 - \psi}{\psi_0 - \psi_1} = \frac{T_g - T}{T_g - T_{lw}} \quad \ldots [12]$$

The working equations, i.e., Equations [7, 11, 12], may be evaluated to determine the temperature along the axis of symmetry in the z-plane. The results are plotted in Fig. 5.

---

[2] Kober, H., "Dictionary of Conformal Representations," Dover, New York, 1952.

[3] Hildebrand, F. B., "Advanced Calculus for Engineers," Prentice-Hall, New York, 1949.

Stability Areas of Missile Control Systems

WALTER HAEUSSERMANN[1]

Army Ballistic Missile Agency, Redstone Arsenal, Huntsville, Ala.

Areas of stability are derived for missile control systems with linear and nonlinear servo components. Methods are shown to adapt signal phase shifting networks to the properties of the missile and a selected servo system. The investigations are extended to missile motions around its center of gravity and about a prescribed line of flight.

Nomenclature

$a_{i=0,1,2}$ = gain coefficients of gyro signals
$b_{i=0,1,2}$ = gain coefficients of angle of attack signals
c_1 = aerodynamic restoring coefficient
c_2 = vane efficiency
d = damping term
$e_{i=0,1,2}$ = gain coefficients of guidance signals
f = frequency
$f_{i=1,2}$ = real function term
G_m, g_m = transfer function of missile moment system
G_n, g_n = transfer function of control network
G_s, g_s = transfer function of servo system
j = $\sqrt{-1}$
k = $\dfrac{57.3 \text{ deg}}{v}$ term in angular relationship, angles measured in degrees
$l_{i=1,2,3}$ = coefficient in lateral force equation
$m_{i=0,1,2}$ = lag coefficients of servo system
n = servo system input
$p_{i=1,2,3}$ = coefficient term in characteristic equation
$q_{i=1,2,3}$ = lag coefficients of control network
r = real component term
s = complex variable
v = velocity vector of missile
w = wind velocity vector
x = radial distance of locus curves at closed loop frequency
z = lateral displacement
α = angle-of-attack
α_w = angle of wind attack
β = angular vane deflection
ϕ = gyro indication
ζ = path angle
ω = $2\pi f$ = circular frequency
$\kappa_{i=1,2}$ = specific gain factors
γ = phase angle

Introduction

THE physical behavior of a missile varies considerably during its flight due to variations of aerodynamic and aeroballistic properties, fuel consumption, etc. The control system of the missile has to be adapted to these variations, which are often not accurately known. Therefore, it is necessary to find means to support the layout and to judge the degree of adaptation of a missile control system. The intention of this report is to present these means in the form of stability areas for varying missile properties and control qualities.

The equations of motions with respect to one control axis (assuming here that each control axis is independent of the other two) of a missile are as follows (Fig. 1 may be used for the additional definition of the symbols used in the following equations):

Lateral force equilibrium results in the linearized lateral force equation

$$\ddot{z} = l_1\alpha + l_2\phi + l_3\beta \qquad [1]$$

in which, after multiplying by the missile mass m, the left term describes the force ($m\ddot{z}$) accelerating the missile in the lateral z direction and is equal to lateral forces due to lift ($ml_1\alpha$), due to axial forces from thrust and aerodynamic drag ($ml_2\phi$), and due to control deflections ($ml_3\beta$).

Moment equilibrium about the center of gravity is described by

$$\ddot{\phi} + d\dot{\phi} + c_1\alpha + c_2\beta = 0 \qquad [2]$$

In Equation [2] after multiplication by the missile moment of inertia I about the center of gravity, the first term exhibits the torque $I\ddot{\phi}$ necessary to impart an angular acceleration $\ddot{\phi}$ to the missile; the second term $Id\dot{\phi}$ stands for the aerodynamic damping due to an angular speed $\dot{\phi}$ of the missile; the third and fourth terms $Ic_1\alpha$ and $Ic_2\beta$ indicate torques due to aerodynamic and control forces.

Fig. 1 gives the angular relationship

$$\alpha - \alpha_w = \phi - \zeta = \phi - k\dot{z} \qquad [3]$$

with $k = 57.3 \text{ deg}/v$.

The behavior of the control and guidance system may be described generally by

$$f_1(\beta) = f_2(\phi, \alpha, z) \qquad [4]$$

This equation expresses that the control angle β is a function of signals from missile attitude ϕ, angle of attack α and guidance information z.

The coefficients of the established equations can be derived from aerodynamic, aeroballistic and physical data of the missile; and for a certain trajectory or range of a missile they can be considered as time functions. The maximum values of the disturbing function α_w with respect to magnitude and gradient can also be derived from additional meteorological observation.

It is well known (1–5)[2] how an ideal and linear control

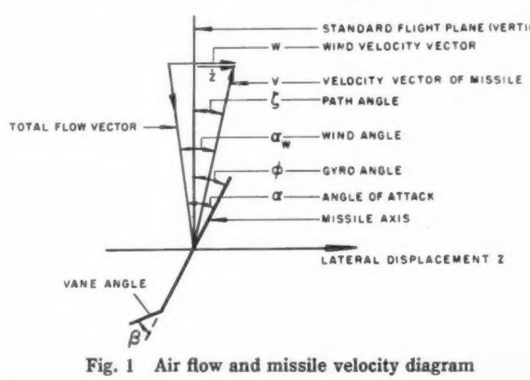

Fig. 1 Air flow and missile velocity diagram

Received Aug. 27, 1956.

[1] Director, Guidance and Control, Development Operations Division. Mem. ARS.

[2] Numbers in parentheses indicate References at end of paper

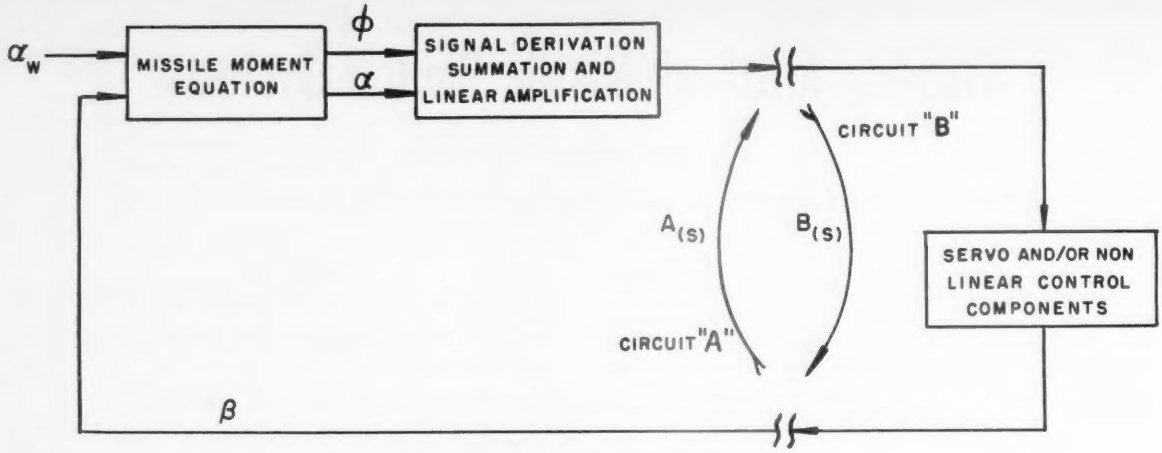

Fig. 2 Principal elements of control loop

Equation [4] can be properly established in order to minimize disturbances and to damp oscillations which will occur due to the differential Equations [1 through 4]. In reality the control and guidance system often cannot be described by a linearized Equation [4], and means have to be found to analyze and investigate the effect of the nonlinearities of the real control system on the motions of the missile.

The oscillations of a missile around its center of gravity show normally a considerably higher frequency than the motions along the flight path. This results in an almost linear behavior of the control system with respect to flight path or guidance oscillations since the nonlinearity of a control system is often attributed to such saturation influences as limited output velocity, amplifier saturation, etc., which will not occur in the lower frequency range. Thus in most cases the stability investigations due to nonlinearities can be limited to pure control problems by omitting Equation [1] and obtaining from Equation [3]

$$\phi = \alpha - \alpha_w \qquad [3a]$$

Equation [3a] substituted in [2] yields

$$\ddot{\phi} + d\dot{\phi} + c_1\phi + c_2\beta = -c_1\alpha_w \qquad [2a]$$

Equation [4] reduces to

$$f_1(\beta) = f_2(\phi, \alpha_w) \qquad [4a]$$

The control Equation [4] can be written explicity[3]

$$\begin{aligned} \ldots + m\ddot{\beta} + m_1\dot{\beta} + m_0\beta + \ldots = \\ \ldots + a_0\phi + a_1\dot{\phi} + \ldots \\ \ldots + b_0\alpha + b_1\dot{\alpha} + \ldots \\ \ldots + e_0 z + e_1\dot{z} + \ldots \end{aligned} \qquad [4b]$$

in which this equation will be normalized for the case of position control systems to $m_0 = 1$ and velocity control systems to $m_1 = 1$.

The signal coefficients of the right side of the normalized Equation [4b] will be referred to as gain coefficients, the coefficients of the left side as lag coefficients.

Nonlinear control systems to be considered later in this report will be of the nonlinear servo type. In this case the m_i coefficients of Equation [4b] before normalization will be nonlinear functions of different variables, for example, frequency and magnitude of input signals, feedback signals within the control system, load of the servo motors, etc.

[3] For practical purposes it is always sufficient and more practical to replace b_1 by an equivalent increase of a_1.

Equation [4b] can be simplified for pure control investigations to

$$\begin{aligned} \ldots + m_2\ddot{\beta} + m_1\dot{\beta} + m_0\beta + \ldots = \\ \ldots (a_0 + b_0)\phi + (a_1 + b_1)\dot{\phi} + \ldots \\ \ldots + b_0\alpha_w + b_1\dot{\alpha}_w + \ldots \end{aligned} \qquad [4c]$$

The angle of wind attack has to be considered as a disturbing function and is, therefore, of no importance (it is assumed here that the signal information is proportional to the true angles) for stability investigations on a linear control system. On nonlinear control systems its magnitude and differential quotients will influence the m_i coefficients if angle-of-attack control will be used.

Equation [4c] shows that, with respect to the attitude signals, the angle-of-attack gain b_i is equivalent to an increase of the corresponding attitude gain a_i. Therefore, some of the following stability investigations have been limited to a_i coefficients or a control equation (normalized to $m_0 = 1$)

$$\ldots + m_2\ddot{\beta} + m_1\dot{\beta} + \beta = a_0\phi + a_1\dot{\phi} + \ldots \qquad [4d]$$

Stability Areas for Varying Coefficients of Moment and Linear Control Equations

The Control Loop

Since it is desirable that the investigations on the linear control system can be extended to a nonlinear servo system, the control loop (Fig. 2) will be split into the partial circuits A and B. Circuit A contains linear elements (except c_1, which is often a nonlinear function of α; in this case it is normally sufficient to investigate the dynamic behavior of the control loop either for the maximum and minimum values or for an average value of c_1) described by the differential Equation [2a] and the right side of [4d]; circuit B contains the eventually nonlinear elements (normalized to gain 1 at $\omega = 0$) on the left side of [4d].

Coefficients (c_1, c_2, etc), which vary slowly during the flight time of the controlled missile, and signal gain values, which have to be adapted to these varying coefficients, are thus combined in the linear circuit A, and simple relationships between the different variables can be expected for the stability behavior of the system. The derivation of such a relationship will be simplified if circuit B is "frozen" to a quasi-steady state, which means in the case of stability-limit investigations that the loop will operate with a constant natural frequency.

The transfer function of circuit A is in agreement with Equations [2a] and [4d]:

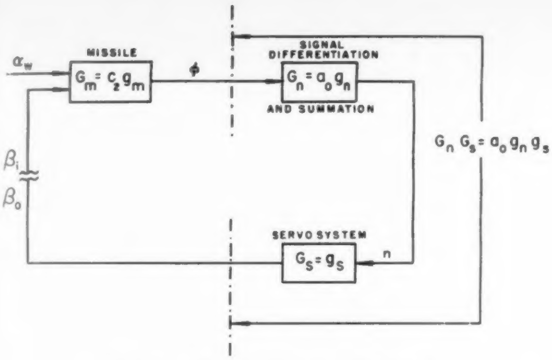

Fig. 3 Block diagram of control loop

$$A(s) = -c_2 \frac{a_0 + a_1 s + a_2 s^2 + \ldots}{c_1 + d_1 s + s^2} \quad \ldots\ldots\ldots\ldots [5]$$

and the transfer function of circuit B according to Equation [4d] is

$$B(s) = \frac{1}{1 + m_1 s + m_2 s^2 + \ldots} \quad \ldots\ldots\ldots\ldots [6]$$

The closed control loop is therefore described by

$$-c_2 \frac{a_0 + a_1 s + a_2 s^2 + \ldots}{c_1 + ds + s^2} = 1 + m_1 s + m_2 s^2 + \ldots\ldots [7]$$

It has been assumed (Fig. 2) that there are no time lags in the signal differentiation and summation block. In reality, phase lag components have to be added (Fig. 3) and the following control equations have to be used

$$\ldots m_2\ddot{\beta} + m_1\dot{\beta} + \beta = n$$
$$\ldots q_2\ddot{n} + q_1\dot{n} + n = a_0\phi + a_1\dot{\phi} + a_2\ddot{\phi} + \ldots\ldots [8]$$

which gives the transfer function

$$g_n g_s = \frac{1 + (a_1/a_0)s + (a_2/a_0)s^2 + \ldots}{1 + q_1 s + q_2 s^2 + \ldots} \times \frac{1}{1 + m_1 s + m_2 s^2 + \ldots}$$

or

$$g_n g_s = \frac{1 + (a_1/a_0)\, s + (a_2/a_0)s^2 + \ldots}{1 + (q_1 + m_1)s + (q_2 + m_2 + q_1 m_1)s^2 + \ldots} \ldots [9]$$

The denominator of Equation [9] is similar to the corresponding expression without q_i lag terms. Therefore the influence of the additional lag terms of the differentiation and summation process can be combined with the m_i terms and further investigations can be based on Equation [7]. However, when signal ratios are considered as variables, the connected variations of the q_i terms will modify the m_i coefficients in Equation [7]. Often an estimate of this variation will result in a negligible effect.

Stability Limits

For the investigation of stability limits the loop frequency will be frozen to $\omega = \omega_0$. Therefore

$$s = j\omega_0 \ldots\ldots\ldots\ldots\ldots\ldots\ldots\ldots [10]$$

will be inserted in Equation [7]

$$-c_2 \frac{a_0 - a_2\omega_0^2 + a_1 j\omega_0}{c_1 - \omega_0^2 + dj\omega_0} = 1 + m_1 j\omega_0 - m_2\omega_0^2 + \ldots$$
$$= \frac{1}{g_s(\omega_0)} \ldots\ldots\ldots\ldots\ldots\ldots\ldots [11]$$

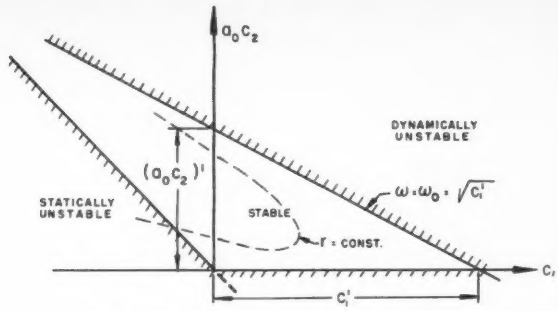

Fig. 4 Stability area in the field of a_0c_2 vs. c_1

Since the right side of Equation [11] contains only constant terms of circuit B and the frozen loop frequency, the left side of the equation gives the relationship among the coefficients of circuit A in Fig. 2 for the closed circuit. The following cases are of interest:

Case a. Linear relationship exists for

1) c_2 vs. c_1 variations if a_0, a_1 and a_2 are constant and $d = 0$.
2) a_0 vs. c_1 variations if c_2, a_1/a_0 and a_2/a_0 are constant and $d = 0$.
3) a_1 vs. c_1 variations if c_2, a_2/a_1 are constant and $a_0 = d = 0$.

Case b. Hyperbolic relationship exists for

1) a_0 vs. c_2 variations if c_1, d, a_1/a_0 and a_2/a_0 are constant.
2) a_1 vs. c_2 variations if c_1, d, a_2/a_1 are constant and $a_0 = 0$.

The different variations shall now be considered somewhat more closely since they can often give conclusions for changes of signal ratios necessary during the flight to maintain stability. It is unimportant that in some cases the aerodynamical damping d has to be neglected, since its contribution to the stability is very small in practical problems or its influence can be estimated and can serve as an additional safety factor with respect to damping.

Case a.1, a.2. The first two variations shall be contracted to one, which allows both to be considered in the same diagram: a_0c_2 vs. c_1 variations if a_1/a_0 and a_2/a_0 are constant and $d = 0$.

Equation [11] can be rewritten as

$$\frac{a_0c_2}{\omega_0^2 - c_1}\,\kappa_1 = 1 \ldots\ldots\ldots\ldots\ldots\ldots [12]$$

where the specific gain factor

$$\kappa_1 = \left(1 + \frac{a_1}{a_0} j\omega_0 - \frac{a_2}{a_0}\omega_0^2\right) g_s(\omega_0) \ldots\ldots\ldots [13]$$

is the gain factor of the control system at $\omega = \omega_0$ divided by the gain factor a_0. Equation [12] gives the stability limit by

$$a_0c_2 + \frac{1}{\kappa_1} c_1 - \frac{1}{\kappa_1}\omega_0^2 = 0 \ldots\ldots\ldots\ldots [14a]$$

or

$$a_0c_2 + \frac{(a_0c_2)'}{c_1'} c_1 - (a_0c_2)' = 0 \ldots\ldots\ldots\ldots [14b]$$

where c_1' and c_2' are defined by the intercepts in Fig. 4

$$c_1' = \omega_0^2$$

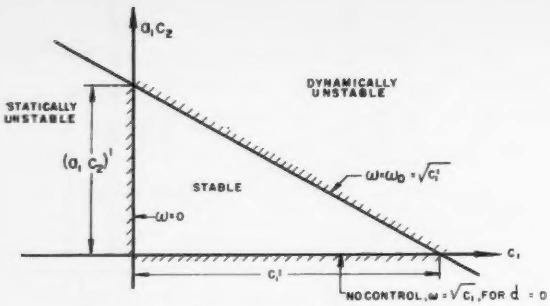

Fig. 5 Stability area in the field of a_1c_2 vs. c_1

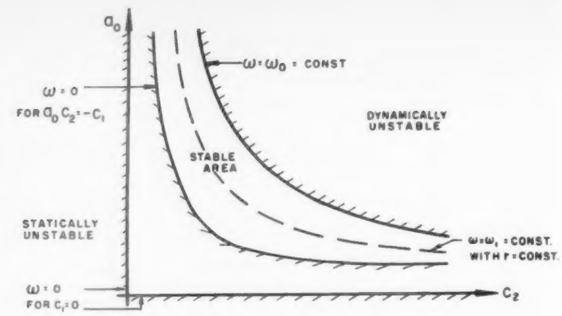

Fig. 6 Stability area in the field of a_0 vs. c_2

and

$$(a_0c_2)' = \frac{\omega_0^2}{\kappa_1} = \frac{c_1'}{\kappa_1} \qquad [14c]$$

In Fig. 4 the static stability limit $a_0c_2 = -c_1$ is plotted as the median in the second quadrant. Negative values of a_0c_2 would also cause instability if the complete equations of motion (Equations [1–4]) were considered.

From Equations [11, 13] the following relationship between the specific gain factor κ_1 and the lag coefficients of the linearized control Equation [4d] can be derived

$$\kappa_1 = \frac{a_1}{a_0m_1} = \frac{1 - (a_2/a_0)\omega_0^2}{1 - m_2\omega_0^2} \qquad [15]$$

and with [14c]

$$m_1 = \frac{c_2'}{c_1'}a_1 = \frac{c_2'}{\omega_0^2}a_1 \qquad [16]$$

and

$$m_2 = \frac{1 - a_0(m_1/a_1)}{\omega_0^2} + a_2\frac{m_1}{a_1} \qquad [17]$$

Case a.3. a_1 vs. c_1 variations if c_2, a_2/a_1 are constant and $a_0 = d = 0$; Equation [11] gives

$$\frac{a_1c_2}{\omega_0^2 - c^1}\kappa_2 = 1 \qquad [18]$$

where the specific gain factor is

$$\kappa_2 = \left(j\omega_0 - \frac{a_2}{a_1}\omega_0^2\right)g_s(\omega_0) \qquad [19]$$

The stability limit is given by Equation [18] or

$$a_1c_2 + \frac{1}{\kappa_2}c_1 - \frac{1}{\kappa_2}\omega_0^2 = 0 \qquad [20a]$$

or

$$a_1c_2 + \frac{(a_1c_2)'}{c_1'}c_1 - (a_1c_2)' = 0 \qquad [20b]$$

where c_1' and $(a_1/c_2)'$ are defined by the intercepts in Fig. 5. Equation [20] reveals that it is practical to consider a_1c_2 vs. c_1 as plotted in Fig. 5.

$$c_1' = \omega_0^2$$

and

$$(a_1c_2)' = \frac{\omega_0^2}{\kappa_2} = \frac{c_1'}{\kappa_2} \qquad [20c]$$

The following relationship can be derived from Equations [11, 19]

$$\kappa_2 = \frac{1}{m_1} = \frac{(a_2/a_1)\omega_0^2}{m_2\omega_0^2 - 1} \qquad [21a]$$

The last term is positive only as required by κ_2 or $1/m_1$ if m_2 is present. The system will be stable if m_2 is missing. Equations [21a, 20c] yield

$$m_1 = \frac{(a_1c_2)'}{c_1'} \qquad [21b]$$

and

$$m_2 = \frac{1}{\omega_0^2} + \frac{a_2}{a_1}m_1 \qquad [21c]$$

Case b.1. a_0 vs. c_2 variations if c_1, d, a_1/a_0 and a_2/a_0 are constant. Equation [11] yields

$$a_0c_2 = (\omega_0^2 - c_1 - dj\omega_0)\frac{1}{1 + (a_1/a_0)j\omega_0 - (a_2a_0)\omega_0^2} \times \frac{1}{g_s(\omega_0)} \qquad [22a]$$

or

$$= (\omega_0^2 - c_1 - dj\omega_0)\frac{1}{\kappa_1} = (a_0c_2)_{\max} \qquad [22b]$$

where κ_1 is defined as in Equation [13]. Due to the presence of d, in this case the specific gain factor κ_1 is complex. Fig. 6 shows a characteristic stability area for this case. The static stability limit is shown for a negative value of c_1. For positive values of c_1 the limits $a_0 = 0$ and $c_2 = 0$ describe the static stability limits of the complete system. The following simple relations can be derived for the lag coefficients and the natural frequency if $d = 0$

$$m_1 = \frac{a_1}{a_0}\frac{(a_0c_2)_{\max}}{\omega_0^2 - c_1} \qquad [23a]$$

and

$$m_2 = \frac{1 - a_0(m_1/a_1)}{\omega_0^2} + a_2\frac{m_1}{a_1} \qquad [23b]$$

$$\omega_s^2 = \frac{1 - (a_0/a_1)m_1}{m_2 - (a_2/a_1)m_1} \qquad [23c]$$

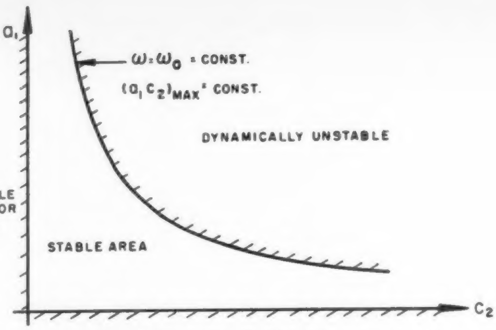

Fig. 7 Stability area in the field of a_1 vs. c_2

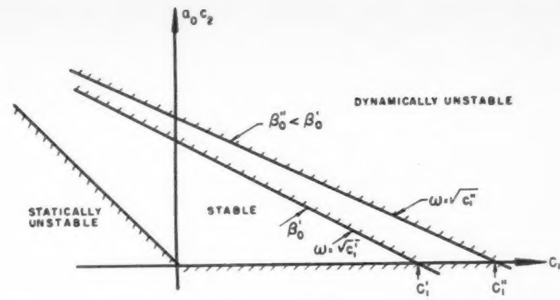

Fig. 8 Stability limits of a control loop with nonlinear servo components in the field of a_0c_2 vs. c_1

Case b. 2. a_1 vs. c_2 variations if c_1, d, a_2/a_1 are constant and $a_0 = 0$. Equation [11] yields

$$a_1c_2 = (\omega_0^2 - c_1 - dj\omega_0)\,\frac{1}{[j\omega_0 - (a_2/a_1)\omega_0^2]g_s(\omega_0)} \ldots [24a]$$

or

$$a_1c_2 = (\omega_0 - c_1 - dj\omega_0)\,\frac{1}{\kappa_2} = (a_1c_2)_{\max} \ldots\ldots\ldots\ldots [24b]$$

with κ_2 being complex as defined in Equation [19]. Fig. 7 shows a characteristic stability area. The low stability limit plotted on this figure is $a_1c_2 = 0$ for $d = 0$.

The following relations can be derived for the lag coefficients and the natural frequency if $d = 0$

$$m_1 = \frac{(a_1c_2)_{\max}}{\omega_0^2 - c_1} \ldots\ldots\ldots\ldots [25a]$$

$$m_2 = \frac{a_2}{a_1}\,m_1 + \frac{1}{\omega_0^2} \ldots\ldots\ldots\ldots [25b]$$

$$\omega_0^2 = \frac{1}{m_2 - (a_2/a_1)m_1} \ldots\ldots\ldots\ldots [25c]$$

Experimental investigation of the stability limit curves derived above can easily be accomplished. Only one stability limit measurement is necessary to determine the complete curve and, if the signal gain ratios are known additionally (in most cases their evaluation can be gained directly from the differential networks), the same measurement allows us to derive the lag terms m_1 and m_2.

Damping Properties

For the investigations of damping properties

$$s = r + j\omega \ldots\ldots\ldots\ldots [26]$$

will be introduced into the transfer function [7]

$$a_0c_2 = \frac{[\omega^2 - c_1 - r^2 - dr - j\omega(d + 2r)]}{1 + \dfrac{a_1}{a_2}\,r + \dfrac{a_2}{a_0}\,(r^2 - \omega^2) + j\omega\left(\dfrac{a_1}{a_0} + \dfrac{2a_2}{a_0}\,r\right)} \times$$
$$[1 + m_1r + m_2(r^2 - \omega^2) + j\omega(m_1 + 2m_2r)] \ldots [27a]$$

It can be seen from this equation that only one simple relationship of the coefficients in circuit A exists for a constant root s: a_0 vs. c_2 variations for a_1/a_0, a_2/a_0, c_1 and d constant.

The product a_0c_2 is equivalent to the over-all gain factor of the control loop as shown in Fig. 2. Therefore, the relationship between a_0 and c_2 with a_0c_2 = const for a constant behavior of the servo loop or a constant root s can easily be understood. In Fig. 6 a hyperbola for the a_0 vs. c_2 relationship is shown within the stable area; ω and r are constant along this curve. If a_0 should be omitted in the control equation, Equation [27a] has to be replaced by the case of a_1 vs. c_2 variations for a_2/a_1, c_1 and d constant

$$a_1c_2 = \frac{[\omega^2 - c_1 - r^2 - dr - j\omega(d + 2r)]}{r + \dfrac{a_2}{a_1}\,(r^2 - \omega^2) + j\omega\left(1 + \dfrac{2a_2}{a_1}\,r\right)} \times$$
$$[1 + m_1r + m_2(r^2 - \omega^2) + j\omega(m_1 + 2m_2r)] \ldots [27b]$$

It is possible to evaluate Equation [27] in a similar way to Equation [11] by assuming values for r, which may be considered as a parameter for curves of constant damping qualities. For this purpose coefficient comparison of the real and imaginary terms of the right side of Equation [27] has to be made. The resulting relationships between s and the coefficients of the transfer function are somewhat more complicated than in the previous case of the stability limit. The evaluation shows that the curves for constant damping qualities will be hyperbolas as indicated in Fig. 4.

In the case of the experimental determination of stability limits, it has been shown that the evaluation of one single measurement is sufficient. It is not possible to derive constant damping quality curves without making several measurements allowing interpolations in the desirable area.

Stability Areas With Nonlinear Servo Components

A control circuit will be considered as shown in Fig. 2 with nonlinear control components as servo elements, control relays, etc., in circuit B. The variation of coefficients for the stability investigations will be restricted again to circuit A and a constant natural frequency ω_0 of the control loop. (In most practical cases control loops with nonlinear elements show a predominant fundamental natural frequency, which will be considered here.) With these limitations, a constant quasi-steady state behavior of the partial circuit B becomes necessary; this can be accomplished if in addition to the frequency ω_0, the output amplitudes β_0 of circuit B are "frozen" too. The closed control loop can now be approximated for the stability limit by

$$c_2\,\frac{a_0 + a_1\omega_0 j - a_2\omega_0^2 + \ldots}{\omega_0^2 - c_1 - d\omega_0 j} = \frac{1}{g_s(\beta_0, \omega_0)} \ldots\ldots [28]$$

In Equation [28] the complex term of the right side is constant so long as β_0 and ω_0 are constant values.

The stability areas described for the nonlinear control system are, as comparison of Equation [28] with Equation [11] shows, similar to the stability areas of linear systems, except that in the nonlinear system the servo output amplitude β_0 will be an additional parameter. Thus the area of stability will vary with the output amplitudes. Usually, larger servo output amplitudes decrease the stability of control loops due to saturation influences, and therefore the stability diagram shows normally smaller stable areas for larger vane deflections (Fig. 8).

The output amplitudes β, which can be expected during flight, can be estimated from wind gusts and other disturbances. The stability diagram of Fig. 8 or similar diagrams (the preceding section) will then serve to determine the range of coefficients which can be used safely.

As in the case of linear control components, the stability limits can be determined by one measurement per limit and it is possible to derive the lag coefficients which would be valid for an equivalent linear system.

The derivation of constant damping quality curves is very difficult since nonlinear effects which are a function of the control output magnitude are of considerable influence. Experimental investigation by simulation of the control loop is here preferable for a complete evaluation of the damping qualities.

Adaptation of Control Network to Missile and Servo System

In the foregoing sections methods have been described which allow the area of stability for a system to be determined, in which the gain factor a_0 or a_1 was the only variable of the control system. In order to reach a good design optimum, adaptation of the control network to the missile requirements and to a usable servo system has to be accomplished. Many applicable methods are well known from common literature; however, they do not allow quick evaluations. The following method proved to be advantageous:

The stability or instability of a closed loop (see Fig. 3) depends on the feedback ratio β_0/β_i measured on the open loop for β_0 and β_i being in phase if an excitation occurs with a sinusoidal input

$$\frac{\beta_0}{\beta_i}\left.\begin{array}{l} > 1 \text{ results in instability} \\ = 1 \text{ is the stability limit} \\ < 1 \text{ results in stability} \end{array}\right\} \qquad [30]$$

Since

$$\frac{\beta_0}{\beta_i} = G_m \times G_n \times G_s \qquad [31]$$

the stability limit also can be expressed by combining [30] and [31]

$$G_m \times G_n \times G_s \gtrless 1$$

If the differentiating network has to be adapted to the other two elements in the control loop, it is more convenient to compare

$$G_n \gtrless \frac{1}{G_m G_s}$$

or with

$$G_n G_s = a_0 g_n g_s$$

and the missile transfer function

$$G_m = c_2 g_m = \frac{c_2}{-s^2 - ds - c_1}$$

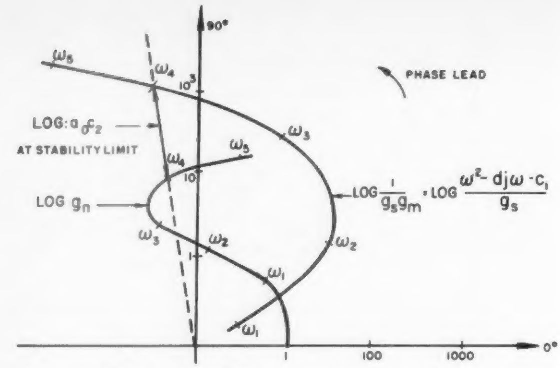

Fig. 9 Stability limit evaluation from the log g_n and log $(1/g_s g_m)$ diagram

The stability limit can be described by

$$a_0 c_2 \gtrless \frac{1}{g_s g_m} \cdot \frac{1}{g_n}$$

or if the curves will be shown in a log-polar coordinate diagram

$$\log a_0 c_2 \gtrless \log \frac{1}{g_s g_m} - \log g_n \qquad [32]$$

or with $s = j\omega$ for sinusoidal input

$$\log a_0 c_2 \gtrless \log \frac{\omega^2 - dj\omega - c_i}{g_s} - \log g_n \qquad [33]$$

Since a_0c_2 is a real gain factor the right side terms of Equation [33] must be in phase. Such a condition is shown in Fig. 9, from which the stability limit can be found as the distance log a_0c_2.

Equation [33] can be applied in Fig. 9 at the frequency ω_4. The logarithm of the gain factor of the total loop for the stability limit can be found as the radial distance of both curves for ω_4, which is also the closed loop frequency at the stability limit.

The curve for log $(1/g_s g_n)$ may be drawn manifold for variations of coefficients of the missile moment equation and for variations characterizing "frozen" conditions of a nonlinear servo system as, for example, its output amplitude.

Similarly, the curve for log g_n may be drawn for desirable types of differentiating networks as exhibited for a normalized single differentiating *RC* configuration in Fig. 10. It is recommended that transparent paper be used for the log g_n diagrams, thus providing a tool to apply easily the method of evaluation described above by means of Fig. 9. This method of comparison of log $(1/g_s g_m)$ and log g_n avoids the multiplication of transfer functions as required in common methods.

By means of diagrams as in Fig. 9, a differentiating network can be selected from the viewpoint of a maximum a_0c_2 value at the stability limit. In addition, it is desirable to get information about the damping properties of the control loop. Since the damping is normally small its influence to the loop frequency can be neglected; therefore the circular loop frequency ω_1 is given by

$$\omega_1 = \sqrt{c_1 + a_0' c_2} \qquad [34]$$

with a_0' defined as the real component of the locus curve $G_N G_S$ (see Fig. 11) at ω_1. The value of a_0' can also be found from the log-polar diagram as shown in Fig. 12, from which it is determined by

$$a_0' \approx a_0(\omega_1^2 - c_1) \cos \gamma \qquad [35]$$

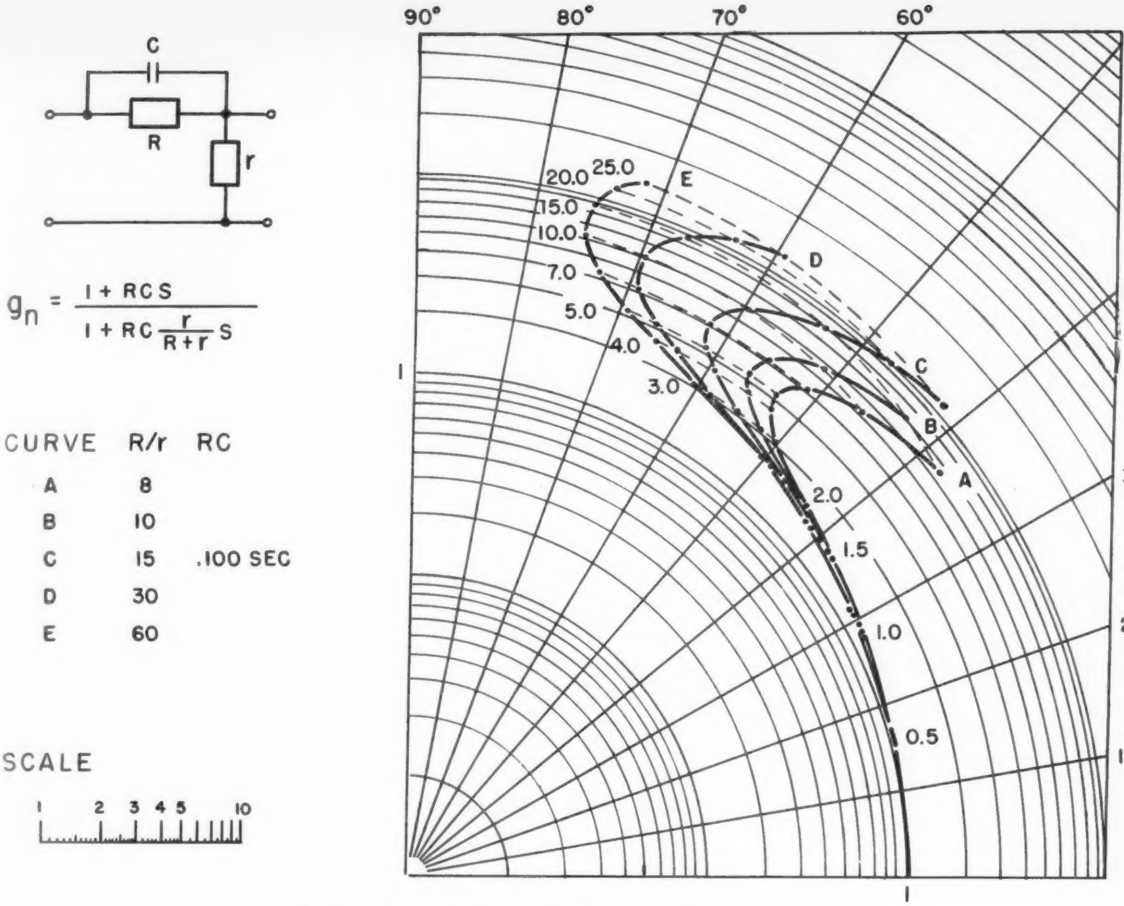

Fig. 10 Normalized locus curve for single differentiating network

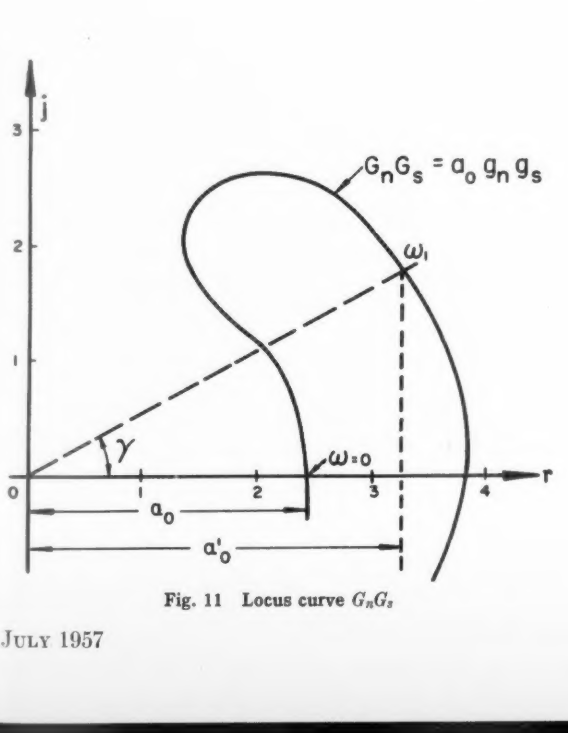

Fig. 11 Locus curve G_nG_s

The influence of aerodynamical damping is here neglected.

Starting with an assumed ω_1 a step-by-step approximation gives a_0', γ and ω_1 which will fulfill Equations [34, 35]; γ, which is the open loop phase lead angle at ω_1, can be used to determine the amplitude decrease ratio per cycle in the closed loop for several parameters of $c_1/a_0'c_2$ and $d = 0$ (see Fig. 13).

Stability Investigations of a Linear Control and Guidance System

It has been mentioned in the Introduction that the oscillations due to guidance of a missile along its prescribed flight path are considerably lower than the missile oscillations around its center of gravity. Therefore, it is normally sufficient to omit the lag coefficients of the control equation and it might even be satisfactory to omit high order terms on the moment equation in order to investigate the stability of missile path motions.

Stability Limits of the Complete System

The complete guidance and control system may be described by Equations [1, 2, 3], and the control equation without lag coefficients by

$$\beta = a_0\phi + a_1\dot{\phi} + b_0\alpha + e_0z + e_1\dot{z} \qquad [4e]$$

The characteristic equation of the system is

$$s^4 + p_3s^3 + p_2s^2 + p_1s + p_0 = 0 \qquad [36]$$

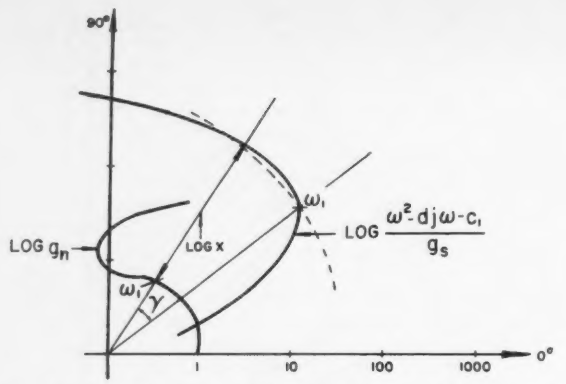

Fig. 12 Damping evaluation from the log g_n and log $(1/g_s g_m)$ diagram

with

$$p_3 = d + a_1c_2 + k(l_1 + l_3b_0) - e_1l_3$$

$$p_2 = c_1 + (a_0 + b_0)c_2 + kd(l_1 + l_3b_0) + a_1k(l_1c_2 - l_3c_1) - e_1dl_3 - e_0l_3$$

$$p_1 = e_1(c_2(l_1 + l_2) - c_1l_3) - e_0dl_3 + a_0k(l_1c_2 - l_3c_1) - kl_2(c_1 + b_0c_2)$$

$$p_0 = e_0(c_2(l_1 + l_2) - c_1l_3)$$

The stability limit for Equation [36] can be derived with $s = j\omega$ and results in

$$\left(\frac{p_1}{p_3}\right)^2 - \frac{p_1p_2}{p_3} + p_0 = 0 \qquad [37a]$$

with

$$\omega^2 = \frac{p_1}{p_3} \qquad [37b]$$

Equations [36, 37] show that a relatively complicated relationship among the coefficients and gain factors exists for the stability limit. Furthermore most of the coefficients (as the k and l_i coefficients) are entangled by aerodynamic and aeroballistic linkages and cannot be selected as mutually independent. Thus the stability investigation will be limited here to the field of the guidance gain factors e_0 and e_1 and the assumption that the coefficients d and l_3 are of negligible influence on the over-all system as it is in practical cases. Equations [36, 37] result in

$$e_0 \approx \frac{p_2}{p_3}\left(e_1 + \frac{p_1''}{p_1'}\right) - \frac{p_1'}{p_3}\left(e_1 + \frac{p_1''}{p_1'}\right)^2 \qquad [38]$$

with

$$p_3 = a_1c_2 + kl_1$$
$$p_2 = c_1 + (a_0 + b_0)c_2 + a_1kl_1c_2$$
$$p_1 = e_1p_1' + p_1'' = e_1c_2(l_1 + l_2) + a_0kl_1c_2 - kl_2(c_1 + b_0c_2)$$
$$p_0 = e_0p_1'$$

The stability limit for usual conditions is shown in Fig. 14.

Stability Limits With Reduced Missile Moment Equation

If the frequencies of the oscillations of the missile around its center of gravity and along its flight path are sufficiently apart, the investigation for the guidance oscillation can be carried out without the derivatives of the gyro angle. Equations [2, 4e] will be replaced by

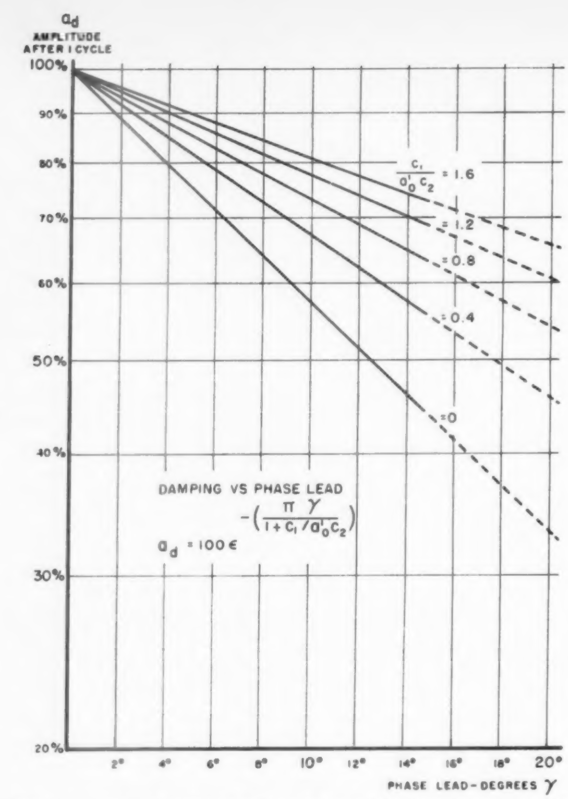

Fig. 13 Amplitude decay per cycle as a function of phase lead

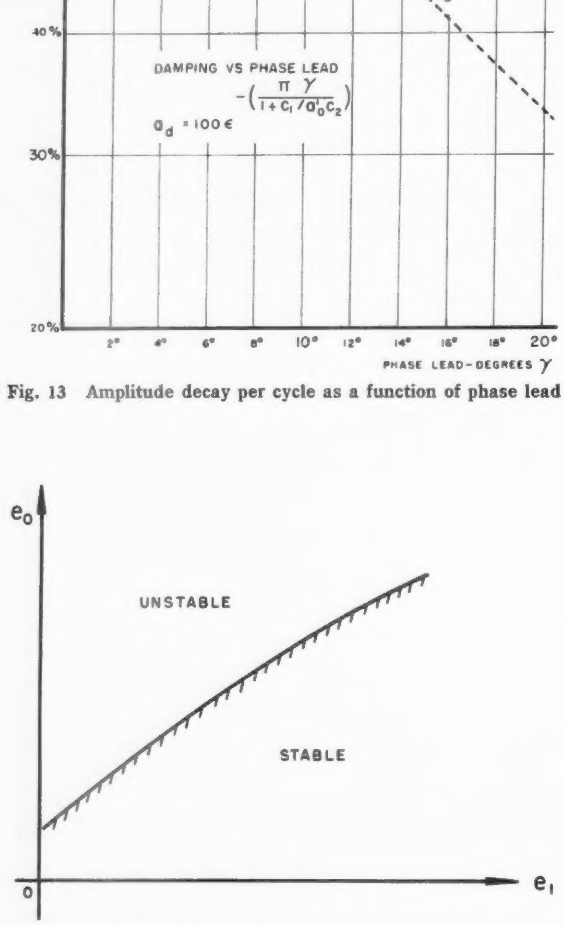

Fig. 14 Stability limit in the field of guidance gain factors e_0 vs. e_1

$$c_1\alpha + c_2\beta = 0 \qquad [2b]$$

and

$$\beta = a_0\phi + b_0\alpha + e_0z + e_1\dot{z} \qquad [4f]$$

The characteristic equation of the system, which includes also Equations [1, 3], is

$$s^2 + \left(\frac{(e_1 + a_0k)[c_2(l_1 + l_2) - c_1l_3]}{c_1 + (a_0 + b_0)c_2} - l_2k\right) s + e_0 \frac{c_2(l_1 + l_2) - c_1l_3}{c_1 + (a_0 + b_0)c_2} = 0 \ldots [39]$$

The system is stable for

$$(e_1 + a_0k)[c_2(l_1 + l_2) - c_1l_3] > l_2k(c_1 + (a_0 + b_0)c_2) \ldots [40]$$

and for negligible damping properties, its highest frequency is reached at

$$\omega_1^2 = e_0 \frac{c_2(l_1 + l_2) - c_1l_3}{c_1 + (a_0 + b_0)c_2} \ldots\ldots\ldots\ldots [41]$$

Undamped oscillations of the missile around its center of gravity show a frequency, derived from Equation [12] of

$$\omega_0^2 = c_1 + \kappa a_0c_2 \ldots\ldots\ldots\ldots [42]$$

Interference of natural frequencies in a network as described by Equations [1–4] are practically negligible if they are approximately 10:1 apart. Thus the reduced moment equation is applicable if $\omega_1^2 < \omega_0^2/100$. If this condition is not fulfilled, Equation [37] should be applied for the stability investigation.

Investigations by Analog Computation

The preceding analytical investigation may be used when the change of coefficients is slow with respect to the response and the time constants of the complete system. If the characteristic coefficients change so rapidly that they can no longer be considered as "frozen" coefficients for a loop response under one disturbing influence, such as a wind gust, the mathematical investigation should be replaced by analog computation, in which components of the guidance and control system should participate in order to comprehend their nonlinearities.

Fig. 15 exhibits a block diagram for the simulation of missile motions in agreement with the basic system of Equations [1–4].

The analog evaluation of the missile behavior is especially valuable in the following cases:

1 During short time periods the mathematical evaluation with constant coefficients would result in poor stability or even instability of the system; analog evaluation will determine whether the over-all performance will be sufficient due to the change of the system coefficients or if a more complicated control system guaranteeing good "frozen coefficient stability" has to be applied.

2 The mathematical evaluation considering constant coefficients gives sufficient stability. However amplitudes will build up due to the continuous change of the system coefficients. This may occur when constraining coefficients as c_1 decrease rapidly.

References

1 Chestnut, Harold, and Mayer, Robert W., "Servomechanisms and Regulating System Design," John Wiley & Sons, New York, 1947.

2 Brown, G. S., and Campbell, D. P., "Principles of Servomechanisms," John Wiley & Sons, New York, 1948.

3 Evans, Walter R., "Control-System Dynamics," McGraw-Hill, New York, 1954.

4 Truxal, John G., "Control System Synthesis," McGraw-Hill, New York, 1955.

5 Chu, Yaohan, "Synthesis of Feedback Control System by Phase-Angle Loci," *Trans. AIEE*, vol. 71, 1952, pp. 330–339.

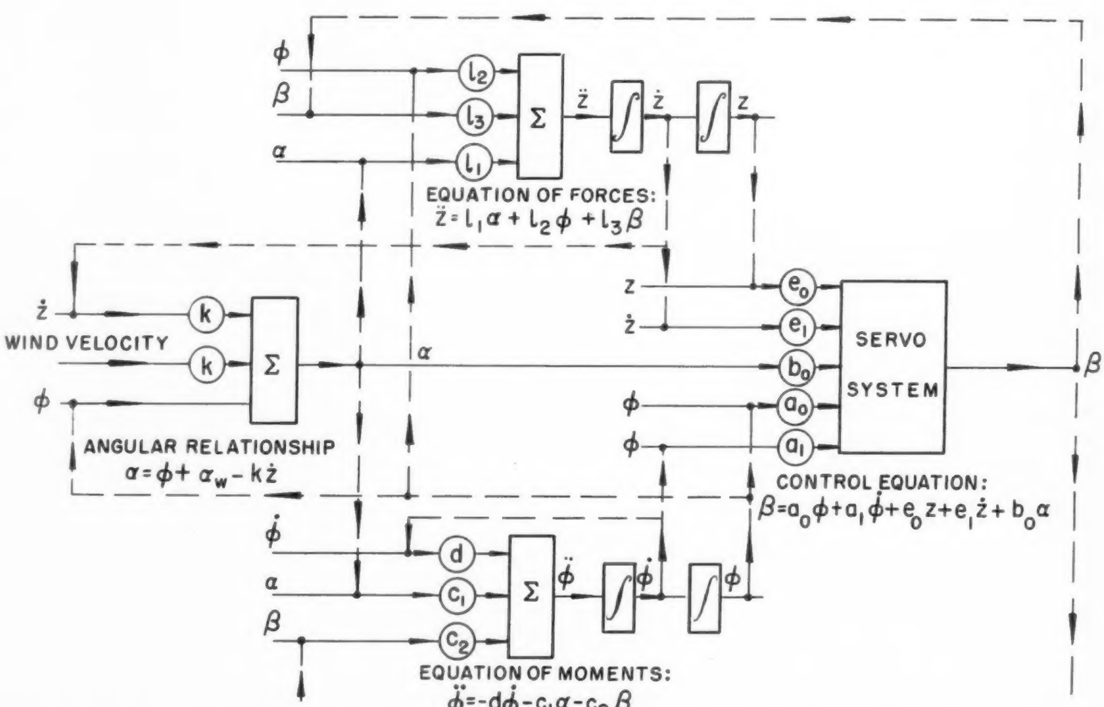

Fig. 15 Simulation of missile motions with guidance and control loops

Technical Notes

Development of an Apparatus for Warming Hydrogen Peroxide by Its Own Controlled Decomposition

JOHANN G. TSCHINKEL[1] and ARLIN E. GRAVES[2]

Army Ballistic Missile Agency, Huntsville Ala.

An apparatus was developed for safely warming aqueous hydrogen peroxide solution (76 per cent) by its own controlled decomposition.

Introduction

THE objective was to develop an apparatus for warming hydrogen peroxide solution of 76 weight per cent to a desired temperature prior to use. For a field unit it was desirable that it require no external source of power. The hydrogen peroxide was to be used as the heat source. The apparatus had to be simple and safe to operate and versatile enough to maintain the hydrogen peroxide at any selected temperature above ambient temperature.

The principle of heating by controlled decomposition[3] is the basis for this development. Heating is accomplished by decomposing a portion of hydrogen peroxide in a submerged catalyst chamber with thermostatically controlled feeding. The heat of decomposition is transferred to the surrounding liquid, thus warming it.

Requirements

A drum of 72 gal net volume of 76 per cent hydrogen peroxide was to be maintained at some selected temperature above freezing (−22 F) up to about 80 F. The temperature differential was to be limited to 50 F above ambient. The drum was to be exposed to a 20-mph wind without insulation.

Heat loss from the drum (50 in. high × 24 in. diam) was estimated by common heat transfer correlations. The cases considered are listed in Table 1.

Table 1 Heat loss rates

Case	Convection	Wind velocity, mph	Temp. diff., F	Heat loss rate, Btu/hr
1	natural	...	20	380
2	natural	...	50	1320
3	forced	20	20	3250
4	forced	20	50	8150

Selecting the extreme condition (case 4), the necessary capacity of the heater at equilibrium becomes 8150 Btu/hr and the heat required for warm-up is found to be 27,670 Btu.

Received Jan. 4, 1957.

[1] Chief, Combustion and Fuel Laboratory. Mem. ARS.
[2] Chemist, Combustion and Fuel Laboratory.
[3] U. S. Patent No. 2,627,454, J. G. Tschinkel, Feb. 3, 1953.

With a heat of decomposition of 76 per cent hydrogen peroxide at 77 F and 1 atm of 928 Btu/lb (liquid H_2O), the consumption during 1 hr warm-up would be 34.2 lb/hr. The hourly consumption thereafter would be 8.8 lb/hr. Obviously, the heater capacity is mainly determined by the chosen warm-up rate.

In order to reduce the required capacity, a warm-up time of 3 hr over the 50 F differential; that is, 0.06 hr/°F, was selected, thus yielding a capacity of about 11.4 lb/hr.

Description of Apparatus

The unit developed consists of five major components, cover, thermal expansion valve, check valve, heat exchanger and a catalyst chamber (see Fig. 1), and weighs 18 lb. The catalyst chamber is charged with a granular catalyst for decomposition of hydrogen peroxide. The thermal expansion valve uses fluorolube oil, grade FS, as a medium. The check valve is flapper-type. The heat exchanger is a helical tube. A component weight breakdown is given in Table 2.

Table 2 Components weight breakdown

Component	Weight, lb	Per cent of total weight	Description
Catalyst chamber assembly	5.6	31.1	comprises concentric cylinders with a helical tube heat exchanger in annular space plus catalyst and catalyst retainers
Fluorolube	4.6	25.5	as expansion medium and heat exchanger medium
Thermal expansion valve	4.4	24.3	consists of connector tube, check valve assembly, bellows, flow control plunger, sensing bulb, valve body
Cover	2.7	14.7	contains support ring and guide
Heat exchanger tube	0.8	4.4	Helical tube
TOTALS	18	100	

The heater is constructed of stainless steel throughout, except for a teflon gasket and packing. Aluminum gave difficulties in fabrication and corrosion.

Function of Heater

Flow through the heater is maintained by the excess of hydrostatic head of the peroxide outside the heater over the head of the discharging products (liquid water slugs and oxygen gas) inside the heater.

The flow can be interrupted by closing the thermal expansion valve or the exit of the discharge tube. The catalyst chamber cannot be flooded with water, since the evolving gas will drive out the water collecting in the heat exchanger, at least as long as the tube diameter is not excessively large so that water can flow downward while gas flows upward.

The flow pattern in the heater may be traced in Fig. 2.

EDITOR'S NOTE: This section of JET PROPULSION is open to short manuscripts describing new developments or offering comments on papers previously published. Such manuscripts are published without editorial review, usually within two months of the date of receipt. Requirements as to style are the same as for regular contributions (see masthead page of this issue).

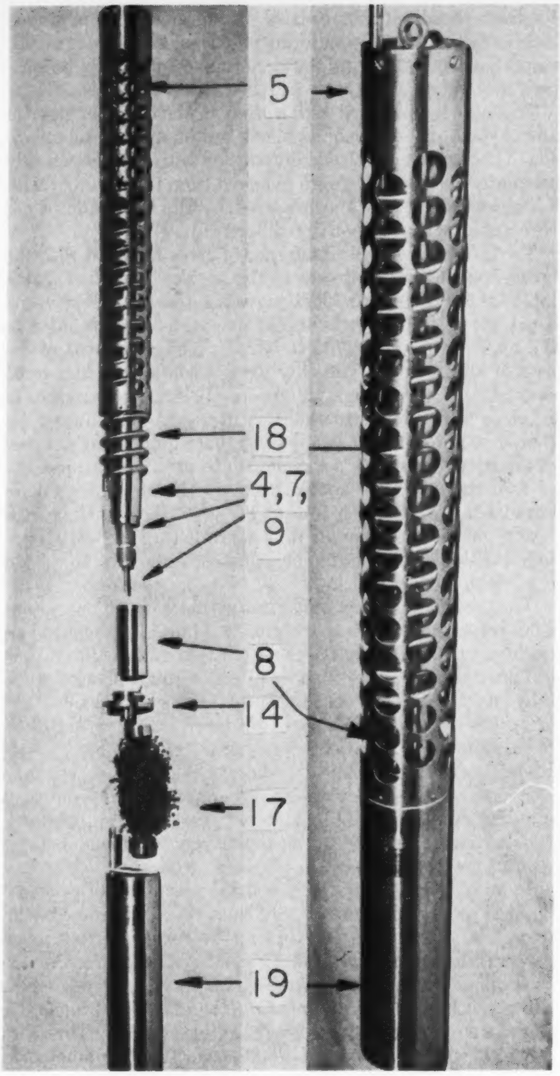

Fig. 1 Views of apparatus (see Fig. 2 for explanation of numbers)

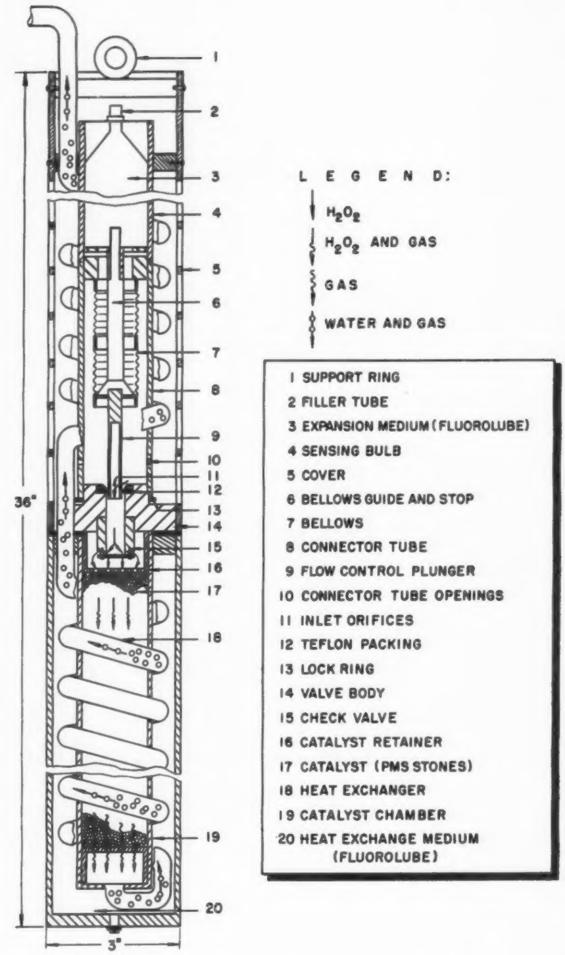

Fig. 2 Catalytic heater (chamber type) Model 3-B

The convection currents within the vessel maintain the liquid at a selected and nearly uniform temperature.

The desired temperature may be obtained by rotating the threaded connector tube, clockwise or counterclockwise, on the boss of the valve body. The operating range for this heater lies within 60 F.

Testing

An aluminum shipping drum, containing 72 gal of 76 per cent hydrogen peroxide, was placed inside a portable refrigerator (5 ft × 5 ft × 5 ft inside dimensions). Three thermocouples (T_1, T_2 and T_3) were positioned at different levels in the peroxide vessel. A fourth thermocouple (T_4) was outside the vessel indicating ambient temperature.

Temperatures and hydrogen peroxide consumption (from weight of water collected) were recorded on five strip chart recorders.

The peroxide was cooled to 35–40 F before the heater was placed in the liquid. Then the heater was observed relative to the function of the valve and discharge of the condensate. Warm-up and sustaining cycles were studied along with operational sensitivity of the thermal expansion valve. Temperature gradients within the liquid were also observed.

A selected temperature level was maintained with a deviation of only ± 2 F of the average temperature of all three thermocouples. The temperature gradient was only 3 F from top to bottom of drum.

The heater has accumulated a total run time of 675 hr. There is no apparent change in the effectiveness of the catalyst bed and the unit operates smoothly and consistently.

Fig. 3 shows a record of typical full-scale run, including warm-up and sustaining cycles. Temperature differentials and peroxide consumption rates are noted also.

At the chosen low temperature, the refrigerator and fan circulating the air inside were running continuously. Thus, the experiment simulates exposure to cold wind. Unfortunately, the effective wind velocity could not be accounted for.

The 76 per cent hydrogen peroxide solution consumed per hour and degree F at equilibrium as related to the quantity heated and the temperature differential was 0.01 per cent solution per hour per degree F.

The coefficient of heat transfer to surroundings of the 72-gal drum at equilibrium was found in this experiment to be about 2.4 (Btu)(hr)(ft^2)(°F).

It is concluded that the heater is suitable for its intended application.

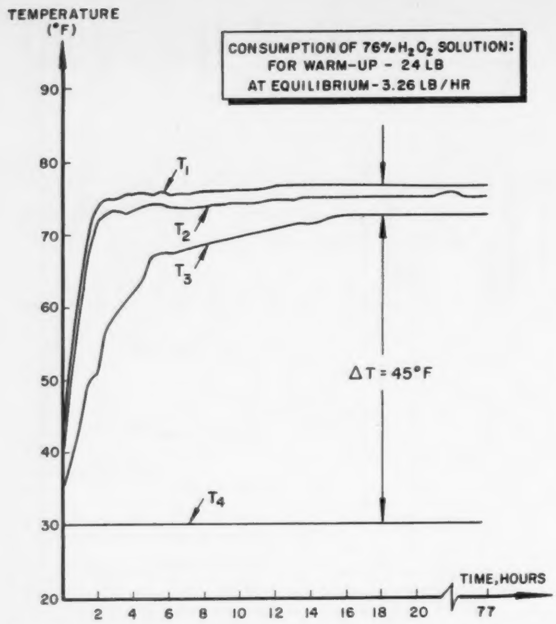

Fig. 3 Temperature of H_2O_2 solution vs. operating time of heater

Acknowledgment

The valuable assistance in design and precise shop work rendered by the instrument design and maker unit of Test Laboratory, ABMA, is gratefully acknowledged.

Ethylene Oxide as a Monopropellant

STANLEY A. GREENE[1] and LEONARD J. GORDON[2]

Aerojet-General Corp., Azusa, Calif.

THE calculated decomposition products of ethylene oxide have been reported by other investigators. Products were postulated and the composition of the products at the chamber conditions were calculated from equilibrium constants. Robison (1)[3] postulated decomposition to yield CO and CH_4, or CO, $C_{(s)}$ and H_2. Glassman and Scott (2) assumed decomposition to CO, CH_4, CO_2, O_2, H_2, C_2H_4 and H_2O at 1860 to 1900 F. Equilibrium calculations yielded appreciable quantities of only CO, CH_4, H_2 and C_2H_4. Meehan and Eldridge (3) postulated the same products as Glassman and Scott, including solid carbon, and found the equilibrium products to contain $C_{(s)}$, CO, H_2, CO_2, CH_4 and H_2O in the temperature range 1677 to 1820 F.

For propellant systems which yield low flame temperatures (ca. 2000 F), the chemical-reaction kinetics of the systems are no doubt such that reactions do not proceed to yield the most probable products as predicted by equilibrium constants. Being thermodynamic functions, equilibrium constants predict the correct products of a system after an infinite length of time. The possibility of observing these products at any time depends on the temperature and activation energy of the system; thermodynamics tells us which products to expect and their concentrations, whereas kinetics tells us how long we must wait in order to observe the predictions made by thermodynamics.

To illustrate, equilibrium calculations at 1740 F and 1 atm pressure predict that methane will be 98 per cent decomposed to carbon and hydrogen, while at this temperature the half-life of methane is approximately 100 sec. Such a time is at least 10^4 times the dwell time usually encountered in monopropellant motors. Thus, equilibrium-type calculations must be suspect when calculating the performance of low flame temperature systems.

This note is concerned with a study of the chamber gases of an ethylene oxide monopropellant motor and the comparison of the experimental gas composition with the theoretically calculated ones. Gases were removed from the chamber with a water-cooled probe and analyzed by the technique of gas chromatography (carbon by difference) (4).

Table 1 shows a typical analysis of gases removed with the probe located just upstream of the nozzle. Included in the table are the results of a kinetic investigation by Heckert and Mack (5) on the products of ethylene oxide decomposition in the temperature range 706 to 832 F. The agreement of the data is remarkable. The only oxygen-containing compound ever isolated was carbon monoxide. In some runs, traces of ethylene were noted, but the concentrations were always less than 0.10 per cent. It is apparent that equilibrium in terms of the water-gas reaction was never attained. Utilizing heats of formation and enthalpies from the National Bureau of Standards Circular No. 461 and −18.29 kcal/mole as the heat of formation of liquid ethylene oxide (6, 7) at 298 K, it is found that the chamber temperature corresponding to the gas composition of Table 1 is 1960 F.

The products that are listed in the tables are the ones that would be expected from the thermal decomposition of ethylene oxide as predicted from the theory of free radicals (8). Most puzzling, though, is the absence of any significant amount of ethylene, the primary decomposition product of ethane. The latter has a half-life (8) of 0.01 to 0.04 sec, which is the order of magnitude of the dwell time of gases in the motor, and it would be expected that the concentrations of ethane and ethylene would be comparable. At out chamber conditions ethylene would be expected to polymerize to resinous materials, but the excellence of the oxygen-hydrogen balance seems to preclude this.

In an effort to qualitatively test the possibility of pressure-induced polymerization of ethylene at our chamber temperatures, slugs of gaseous ethylene oxide were swept through a quartz tube (heated to 1600 F) at atmospheric pressure and at dwell times of approximately 0.1 sec. Analyses of these gases yielded concentrations of ethane of 1.5 to 2 per cent, whereas ethylene was five to six times this amount. Thus with other things being equal, it would seem that the amount of ethylene derived from the decomposition of ethylene oxide depends markedly on the pressure.

From the experimentally determined gas composition and the calculated chamber temperature, a theoretical C^* can be computed. C^* was computed from the relation

$$C^* = \frac{\sqrt{g\bar{\gamma}RT_c/\bar{M}}}{\left(\frac{2\bar{\gamma}}{\bar{\gamma}+1}\right)^{(\bar{\gamma}+1)/2(\bar{\gamma}-1)}} \qquad [1]$$

with the parameters having their usual meaning. To take into account the effect of solid carbon on $\bar{M}$, carbon was assumed to have mass but no volume. Carbon was also assumed not to lag and to be in thermal equilibrium with frozen gas flow through the nozzle; $\bar{\gamma}$ was then calculated from the expression

$$\bar{\gamma} = \frac{\bar{C}_p}{\bar{C}_p - n_g R} \qquad [2]$$

where

$\bar{\gamma}$ = average specific heat ratio of mixture
$\bar{C}_p$ = average molar specific heat of gas and solid mixture
n_g = moles of gas in mixture
R = gas constant

Received March 18, 1957.
[1] Chemist, Research Department, Project 107-A.
[2] Chemical Engineer, Solid Engine and Chemical Department.
[3] Numbers in parentheses indicate References at end of paper.

C^* calculated for the analysis of Table 1 yielded 3680 fps; C^* calculated from propellant mass flow rate, throat area and chamber pressure (750 ± 50 psia) at 1000–2000 L^* was averaged for 14 runs and found to be 3474 fps, which is 94 per cent of our theoretical C^*.

Table 1 Ethylene oxide decomposition products

Product	% Volume This work	% Volume Heckert and Mack
H_2	9.1	7
CO	46.6	50
CH_4	38.4	36
C_2H_6	2.0	7
Carbon	3.9	...

References

1 Robison, W. C., "Ethylene Oxide as a Monopropellant," Jet Propulsion, vol. 24, March-April 1954, pp. 111–112.

2 Glassman, I., and Scott, J. E., Jr., "Performance of Ethylene Oxide as a Monopropellant," Jet Propulsion, vol. 24, Nov.-Dec. 1954, p. 386.

3 Meehan, D. M., and Eldridge, S., "Equilibrium Performance Calculation for Ethylene Oxide," Jet Propulsion, vol. 25, Oct. 1955, pp. 544–545.

4 Greene, S. A., "Separation of Gases by Gas Adsorption Chromatography," *Analytical Chemistry*, vol. 28, Aug. 1956, pp. 1369–1370.

5 Heckert, W. H., and Mack, E. M., "Thermal Decomposition of Ethylene Oxide," *Journal of the American Chemical Society*, vol. 51, Nov. 1929, pp. 2706–2717.

6 "Selected Values of Chemical Thermodynamic Properties," Circular no. 500, National Bureau of Standards, Feb. 1, 1952.

7 "Selected Values of Chemical Thermodynamic Properties," Series III, National Bureau of Standards, March 1954.

8 Steacie, E. W. R., "Atomic and Free Radical Reactions," Reinhold Publishing, New York, 1946, pp. 90–97.

Estimation of Optimum Mixture Ratio for Fuming Nitric Acid Propellants

JOHN S. GORDON[1]

Reaction Motors, Inc., Denville, N. J.

DURING extensive use of Johnston's "JPL Short Method" of performance estimation,[2] it was noted that peak I_{sp} was given with very good accuracy but that optimum mixture ratio for peak I_{sp} was almost always higher than actually found by rigorous calculations. Upon examining about thirty WFNA and RFNA systems, good results were obtained by the equation

$$r = \frac{X}{M} = \frac{12.6(2.92{\cdot}C + 0.83{\cdot}H - 2{\cdot}0)}{M}$$

where nomenclature follows Johnston.[2] For the systems studied, optimum mixture ratio r by this equation was within 4 per cent of the value given by rigorous frozen-equilibrium calculations. No significant difference was noted in optimum mixture ratio between anhydrous HNO_3 and RFNA (type 3A). More stable fuels containing hydrogen give optimum O/F ratios slightly closer to stoichiometric (to CO_2 and H_2O) than unstable (endothermic) fuels, in line with the resultant flame temperatures. However, this equation does not reflect any variation in fuel heat of formation.

A short method is currently being developed for various fuels with 90 per cent H_2O_2.

Received March 18, 1957.

[1] Propellants Liaison Engineer, Chemistry Department.

[2] S. A. Johnston, JPL Progress Report 20-202, 1953.

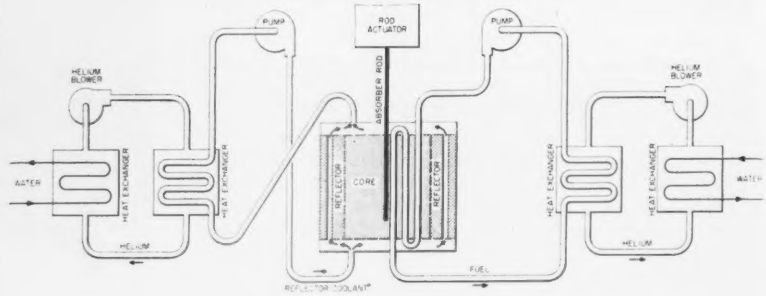

Oak Ridge aircraft reactor flow diagram

Closed Loop Nuclear Aircraft System

NUCLEAR propulsion for aircraft has been studied fairly intensively for a number of years, according to all indications. Only recently, however, have some official details of a possible aircraft reactor been revealed and weight figures aired.

Loads of between 25,000 and 100,000 lb for the reactor-shielding assembly will burden the nuclear plane, according to a newly declassified paper from the Lockheed Aircraft Corp. Translated, these weights mean densities of 100 to 200 lb/cu ft vs. 20 to 25 for a conventional turbojet and about 50 lb/cu ft for chemically fueled planes.

Emphasizing this staggering weight problem even further was the recent budget-hearing disclosure by the Air Force that it wants to spend only $213 million on developing a propulsion system, rather than $600 million originally asked for fiscal year 1958, because of "more and more unfavorable" weight and efficiency estimates. (In fiscal 1957, $237 million was spent.)

Most of the cuts are in airframe development, with effort shifting strongly toward making the reactor lighter. Present plans call for a "more conservative approach," presumably meaning that progress in other phases of the project, notably a weapons system, will be shelved until the outsized weight handicap is solved.

First public description of a reactor propulsion system, and one that has perhaps been discarded, was given at a symposium on the peaceful uses of the atom by Alvin M. Weinberg, director of the Oak Ridge National Laboratories. Because of past joint efforts by Oak Ridge and Pratt & Whitney Aircraft, this high temperature system was considered by some observers to approximate one under study at P&W.

Basically a closed loop system, because reactor heats must be transferred to the discharge gas through an intermediate, closed heat exchanger, the unit employed liquid fuel composed of mixtures of molten fluoride salts containing UF_4. The circulating fuel became critical only in the core, which was bound by a beryllium oxide neutron reflector.

Built and operated (for four days in 1954) at Oak Ridge, the reactor system generated a peak power of 2500 kw although it was designed for 1500 kw. Continuous operating temperatures of 1500 F were recorded, according to Dr. Weinberg, with fuel entering the core at 1200 F.

The active region was a right circular cylinder, 33.3 in. in diameter and 35.8 in. high. The reflector was 7.4 in. thick. Critical mass was 14.9 kg of U^{235}, and total mass of the U^{235} in the whole system (core plus exterior piping) was about 66 kg. Flow velocity of the fuel was 1 m/sec; Reynolds number was 10,000.

The reflector was cooled by liquid sodium, while the core was cooled by the circulating fuel. Each dumped its heat in helium heat exchangers which, in turn, transferred the energy to what would have been the working fluid (see flow diagram).

Because of the intermediate step in the heat transfer, this closed loop system is believed to be much heavier than an open circuit unit. In an open circuit system, discharge air is piped directly through the reactor to pick up the heat. Perhaps weight is the reason Dr. Weinberg advanced the unit for ground power generating uses.

Before being dismantled, the Oak Ridge reactor developed small gas leaks in the fuel pumps caused by the hot fluorides. P&W was reported to be having high temperature problems with its unit.

Jet Propulsion News

MISSILES

• Atomic clocks will be used in plotting the course of long-range missiles, according to Air Force officials. The device detects variation of frequency of time measuring signals, automatically correcting fluctuation. Cost of the devices is $45,000 each.

• Boeing's Bomarc missile will replace manned interceptor planes in some of the "area defense" of the country. Area defense involves the idea of locating defense units to intercept enemy attacks remote from, and with no reference to, individual vital installations, industrial complexes or centers of population. The recently announced production order for the Bomarc points up the trend toward replacing manned aircraft by missiles.

• Referring to the military experts who are devising defenses against intercontinental ballistic missiles, Gen. James Gavin, Army research and development chief, said: "We are confident of getting a missile to defeat the missiles." Deputy Defense Secretary Donald A. Quarles, former AF Secretary, said he doubted that countermeasures could be devised as early as the ICBM itself.

• Buildings and test installations costing $9 million are under construction at AEC's Los Alamos Scientific Laboratory. At a new technical area adjacent to the nuclear weapons test site in Nevada, ground tests will be conducted as part of the nuclear rocket studies.

• Army Secretary Wilber M. Brucker in a speech at Philadelphia said: "The Lacrosse guided missile will replace heavy artillery in strikes against strong points delaying the advance of ground troops. Because of its light weight and the ease with which it can be moved, it is particularly suitable for airborne operations."

Lacrosse is under production at The Martin Co.'s Orlando, Fla., facility, and is under the administration of the Philadelphia Ordnance District.

• Production of components for the Titan ICBM program will be transferred by American Bosch Arma Corp. from an Air Force plant in Chicago to its facilities at Hicksville and Mineola, Long Island.

• Thiokol received a $790,758 contract from Air Materiel Command for rocket boosters for the Martin TM 61B Matador guided missile. Production of the engines is assigned to Thiokol's division at Brigham City, Utah.

• At Mare Island Naval Shipyard, the keel was laid for a nuclear-powered submarine, the Halibut, first of its class to be constructed for launching guided missiles.

The Navy also announced contracts with four shipbuilding companies for eight guided missile destroyers. They will be equipped to launch the Tartar surface-to-air missile.

• The Army announced a new missile system for use against low-flying attackers. Previous missiles were ineffective against such targets because radar scopes give uncertain or misleading images when merged with ground-level objects. The new system to combat this difficulty employs the 16-ft Hawk surface-to-air guided missile which can carry a warhead capable of destroying an enemy plane at tree-top level. The Army is acquiring sites in the New York and Washington areas for launching the Hawk, each battery requiring about 40 acres.

• The Atlas missile, designed for a 5000-mile range at speeds up to 20,000 miles per hour, was unofficially reported to have been tested at the Cape Canaveral launching site, and exploded while in flight. No one was injured. Air Force officials said valuable information was gained as a result of the test.

AIRCRAFT

• Rising and descending on a column of exhaust gases, the Ryan-built USAF Vertijet X-13 (photo) depends solely upon thrust from its jet engine for both direct lift and level flight. At Edwards

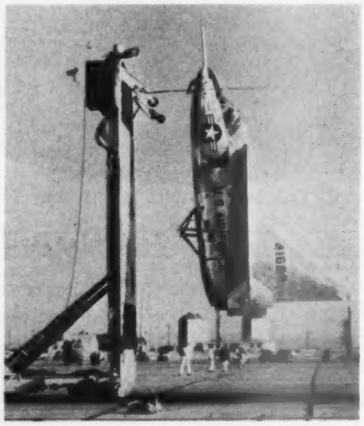

AFB the X-13 made a vertical take-off, transitioned to level flight, returned to vertical position, and again hooked onto its ground service trailer.

• Westinghouse publicly displayed its new J54 turbojet aircraft engine at the jet engine flight test center, Olathe Naval Air Station, Kan. The 6000-lb-thrust class engine has subsonic and supersonic versions. The original version (Navy J54-WE-2) is 10 ft long and 35 in. in diam.

The J54 was the first turbojet specifically designed to take advantage of the high strength and lightweight characteristics of titanium. The engine met its performance specification on the initial test run, and further testing was conducted in an altitude chamber at the Naval Air Turbine Test Center, Trenton, N. J.

• Unretouched photo shows the newest supersonic fighter-bomber of USAF, the Republic F-105B Thunderchief. The plane is powered by a P&W J-75 turbojet engine in the 15,000-lb-thrust class.

• In Washington, General Electric made the first public display of its J79 military jet engine which is claimed to produce more thrust per pound of weight than any other large engine in production. It is in the 10,000-lb-thrust class, has a diameter less than 3 ft, and is 17 ft long. The first six stages of the 17-stage compressor are variable to permit maximum compressor efficiency under all flight conditions.

The J79 powers the Lockheed F-104A, Convair B-58 and Grumman F 11F-1F.

• Curtiss-Wright's new commercial jet engine, the TJ38 was shown at Quehanna, Pa. This powerplant was developed in cooperation with the Bristol Aeroplane Co., from the Olympus engine. Weighing 3600 lb, its thrust is 12,500 lb. C-W will produce a package pod having a noise suppressor and clam shell thrust reverser. The TJ38 passed its 150-hour test, and is scheduled for delivery next summer.

• The Department of Defense and Pratt & Whitney aircraft revealed details of the J-75 turbojet engine now in production. In the 15,000-lb-thrust class, its power is augmented by use of an afterburner. It was tested at the Willgoos Turbine Laboratory, P & W's development facility. Extensive flight tests were made with the J-75 installed in a bomb bay pod of a North American B-45 jet bomber.

The J-75 powers the Republic F-105 Air Force fighter, the Navy's Martin P6M water-based bomber, and is sched-

uled to power versions of the Boeing 707 and Douglas DC-8 commercial airliners.

• In preparation for the launching of the earth satellite, Naval Research Laboratory recently conducted the

second in a projected series of test firings at the Air Force Missile Test Center, Cape Canaveral, Fla. (photo).

COMPANIES

• Harvey Aluminum is in full production on a 4000-ton forging press at its Torrance, Calif., plant. The unit is part of the company's battery of hydraulic and mechanical forging presses which range up to 8000 tons' capacity.

• Oregon Metallurgical Corp., Albany, Ore., is operating a 100-lb-capacity consumable electrode furnace for producing castings of titanium and zirconium.

• Receipt of a $1,600,000 Air Force contract for high power UHF transmitting equipment was announced by Mack Electronics Div., Plainfield, N. J.

• An additional quantity of Ryan KDA-1 Firebee jet target drones was ordered by the Navy in a contract exceeding $4 million. Ryan recently acquired an assembly plant and a 27-acre industrial site in the Los Angeles Harbor area, adjacent to the Torrance Municipal Airport.

• Republic Aviation Corp. was awarded an Air Force contract for the study and design of a 1000 F hydraulic system. The company will also study and develop high temperature hydraulic fluids for the system.

• Eldon Fiberglass Mfg. Co., Aircraft Div., added 40,000 sq ft of plant facilities at Los Angeles. They concentrate heavily on research, development and application of plastics, with special emphasis on polyester, phenolic, epoxy and silicone resins.

• Representing an investment of $200,000, the new experimental shop of Ford Motor Co.'s Glendale subsidiary, Aeronutronic Systems, Inc., leased from the Grand Central Industrial Center, represents the latest expansion pending construction of a permanent office, laboratory and manufacturing complex.

• Construction started on a new plant on a 200-acre site at Lawrence, Kan., for Callery Chemical Co. It will cost between $3 and $4 million.

• International Business Machines will move the headquarters of its Data Processing Div., the company's largest, from New York City to Westchester County.

• Production is now in progress at Douglas Aircraft Co.'s $20-million DC-8 jetliner manufacturing plant at Santa Monica. Floor space is approximately 1 million sq ft.

• Air Force contracts by the Air Materiel Command include: Curtiss-Wright Corp., $7,850,000 for improvement of the J-65 turbojet engine; G.E., $3 million for facilities for producing T-58 turboprop engines; Utica Bend Corp., $1 million for production facilities for J-57 jet engine components; General Cable Corp., $1,215,000 for insulated electrical wire; and Bendix Aviation Corp., $1,110,075 for an unspecified project.

• Tally Register Corp., Seattle, builder of specialized electronic and mechanical machines, was awarded a $90,000 Navy contract to build a high speed data reduction system.

• To facilitate the research and development of magnetic amplifier products, American Electronics, Inc., has established a new magnetic amplifier laboratory at its Electrical Machinery and Equipment Div., El Monte, Calif. The laboratory began full operations May 1.

INSTITUTIONS

• The University of Michigan will dedicate two modern laboratories for research and instruction in aeronautical and automotive engineering on Oct. 15. On the following Sunday, the public will tour the new units and five other laboratories on the campus. The aeronautical engineering laboratory is composed of units for work in aerodynamics and aircraft propulsion. It has a low speed, low turbulence wind tunnel, fixed-block and variable Mach test sections of a supersonic tunnel, and provisions for a hypersonic tunnel.

• First National Conference on Heat Transfer will be held Aug. 12–15 at Pennsylvania State University, University Park, Pa. This conference, jointly sponsored by the ASME and AIChE, marks the first time the two groups have cooperatively sponsored an independent technical program. The program includes 35 technical papers and inspection trips to the nuclear reactor and Naval Ordnance Laboratory at the University.

• A separate classification and pay schedule for engineers employed by the Federal Government has been recommended to a State subcommittee in testimony by the National Society of Professional Engineers. The testimony emphasized that an adjustment of the salaries of engineers and scientists in the federal service is in order and is required if the government is not to fall further behind in its effort to obtain and retain competent engineering staffs.

• American industry will consume over 1 million lb of lithium metal annually by 1970, according to the American Lithium Institute. Lithium chemicals find use in such fields as catalysis and organic chemistry, and in the preparation of new chemical fuels for aircraft and missiles.

• Scientists at Armour Research Foundation of Illinois Institute of Technology have developed a way to make titanium compound at a temperature much lower than required in the present method, with higher purity and at less cost. The compound is titanium tetrachloride, used in the manufacture of titanium for jet aircraft, rockets and missile parts.

FOREIGN

Canada: Ryan KDA-1 Firebee target drone missiles similar to those used by the U. S. Navy will be used by the Royal Canadian Air Force. Canada is the first foreign country to adopt the air-launched Firebee for antiaircraft training.

England: A new organization in the Air Ministry under Air Vice-Marshal D. G. Morris will integrate the introduction of defense guided missiles into the RAF fighter defense systems. First missile station is under construction at North Coates.

• The English Electric Co.'s missile, about which brief information was given by the Minister of Supply, is officially reported to be named "Thunderbird." It will be used by the Army for defending overseas bases and ground forces.

Germany: At Cuxhaven this summer, sounding rockets with a ceiling of 100,000 ft will be tested. Near Stuttgart, antiaircraft guided missiles are under design and a surface-to-surface missile is under development.

Switzerland: The Swiss government purchased 20 de Havilland Vampire trainers powered with Goblin jet engines. The Swiss have been licensed to manufacture Vampire and Venom fighters, and Ghost engines.

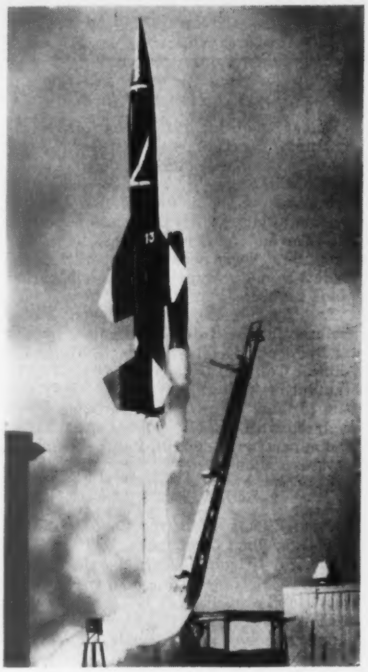

Vertical launcher falls away from Bomarc IM-99 in test firing.

Bomarc Goes Into Production

An initial "quantity" production contract for the Bomarc IM-99 interceptor missile has been awarded the Boeing Airplane Co. by the Air Force. The contract, for $7,109,195, followed successful firings of the weapon against drone aircraft over the Atlantic Ocean.

A twin-ramjet missile boosted to ram speeds by a liquid rocket motor, the weapon was designed to operate at "extreme" altitudes and supersonic speeds (figures not released). It features long-range capabilities necessary for area defense, for which it carries a high explosive warhead.

Physical measurements of the Bomarc, revealed for the first time by the company, include: Length, 47 ft (10 ft longer than the F-86 Sabrejet fighter); wingspan, 8 ft 2 in.; weight, 15,000 lb.

Bomarc design and development benefited from information acquired by Boeing in its ground-to-air pilotless aircraft program of the late 1940's. A total of 112 such aircraft were fired. They ranged to 16 ft in length, reached speeds of 1500 mph at altitudes from 6000 to 80,000 ft, the company stated.

Helping Boeing in the early stages of the Bomarc was the University of Michigan's Aeronautical Research Center (the "marc" of Bomarc).

More than 70 per cent of the Bomarc will be subcontracted, including work to Aerojet-General for the rocket engines and Marquardt Aircraft for the ramjets.

ARS News

700 Attend ARS San Francisco Meeting

A TOTAL registration of almost 700 engineers and scientists heard 34 papers read during eight technical sessions at the ARS Semi-Annual Meeting June 10–13 in San Francisco.

At a luncheon meeting, Dan A. Kimball, president of Aerojet-General Corp., said that his company expected to be producing 300 to 400 mph underwater rockets in the foreseeable future.

The banquet speaker, Adm. William F. Raborn, USN, Director of Special Projects for the Navy Bureau of Ordnance, gave an account of the progress being made in development of the Polaris IRBM program.

About 150 people took the opportunity to go on a field trip to Ames Aeronautical Laboratory, where inspection tours of a low speed tunnel, a supersonic tunnel, and a hypersonic free-flight tunnel were made.

The 34 papers, along with short abstracts, follow:

INSTRUMENTATION AND GUIDANCE

Elements of Inertial Navigation, by W. T. Russell, Ramo-Wooldridge Corp., Los Angeles, Calif. (431-57). Paper not available at press time.

Elements and Applications of Radio Guidance, by C. R. Gates, Jet Propulsion Laboratory, CalTech, Pasadena, Calif. (432-57). Paper not available at press time.

The Bomarc Flight Vibration and Its Development Into an Equipment Specification, by G. G. Setterlund, Boeing Airplane Co., Seattle, Wash. (433–57). Present vibration testing is discussed with light and loaded beam analogies. Vibrations and evolved specifications are presented. Emphasis is placed on problems of reasonable substitute single-frequency test.

Instrumentation for Rocket Engine Controls Research Testing, by J. D. Gillett, Rocketdyne, Canoga Park, Calif. (434-57). The measurement problems that arise from requirements for testing a fully controlled model engine to obtain frequency response data about the over-all system, major component frequency responses, and control loop interactions are discussed and solutions developed are described.

Recent Advances in Dynamic Pressure Measurement Techniques, by F. F. Liu and T. W. Berwin, Rocketdyne, Canoga Park, Calif. (435-57). A critical survey of theoretical and experimental aspects of pressure transducers and dynamic pressure measurement systems are presented with discussion of problems involved in their design. Several new high speed techniques and systems developed by the authors are described.

LIQUID ROCKETS

Design of Cooled Jet Deflector Plates, by Paul J. Petrozzi, Aerojet-General Corp., Sacramento, Calif. (436-57). General design method is described, with characteristics of deflected and free jets correlated. Spread of the deflected jet is calculated and other considerations listed.

Exhaust Nozzle Contour for Optimum Thrust, by G. V. R. Rao, Marquadt Aircraft Co., Van Nuys, Calif. (437-57). A method of designing the wall contour of nozzle is established. Governing conditions are enumerated. Assuming isentropic flow, the variational integral is formulated.

A Liquid Propellant Rocket for Group Training, by John W. Salter, George S. James and Daniel Starrett, Aerojet-General Corp., Sacramento, Calif. (438-57). Design, construction and testing of a small, unclassified, liquid propellant thrust chamber and propulsion system are described. Called Spark I, the rocket was developed by 20 members of the local ARS Section in their spare time.

Development of the CML-4N Rocket Engine, by R. C. Truax, Western Development Division, ARDC, Inglewood, Calif. (440-57). Paper not available at press time.

Analysis of Regenerative Cooling in Rocket Thrust Chambers, by Leo E. Dean and Lucian A. Shurley, Aerojet-General Corp., Sacramento, Calif. (460-57). This paper discusses the experimentally determined heat transfer data obtained on JP-4 and RFNA under conditions simulating those occurring during thrust chamber operation. Heat flux and temperature distribution are obtained.

Automatic Heat Transfer and Data Machine, by Robert W. Ellison, Reaction Motors, Inc., Denville, N. J. (461-57). Design and construction of a laboratory apparatus for heat transfer studies is described. In studying heat transfer problems of rockets, the semiautomatic machine computes the derived parameters of interest from measured values and plots complete families of curves during the course of a single continuous test.

Spreading of Supersonic Jets from Axially Symmetric Nozzles, by C. J. Wang and J. P. Peterson, Ramo-Wooldridge Corp., Los Angeles, Calif. (462-57). This paper contains a formulation of the method of characteristics for computing the flow field in a supersonic jet. The method is programmed on an 1103 computer. Twenty-two cases are reported for jets from two types of nozzles at various Mach numbers.

The Application of High-Speed Motion Pictures in Fuel Injection Studies, by Carl H. Builder and Gilbert S. Bahn, Marquardt Aircraft Co., Van Nuys, Calif. (463-57). Instantaneous patterns in the fuel spray were studied and the role of turbulence was analyzed with respect to flame stabilization. The apparatus is described and examples of pictures are included.

SOLID ROCKETS

Some Effects of Charge Configuration in Solid-Propellant Combustion, by Leon Green Jr., Aerojet-General Corp., Azusa, Calif. (441-57). Static tests of a high energy, composite solid propellant at 170 F in four types of charge are considered, and comparisons of various phenomena with predicted behavior are made.

Development of ASP Rocket, by Robert Greene, Grand Central Rocket Co., Redlands, Calif. (442-57). The design and development program of the high performance solid-rocket engine is detailed and trials and triumphs encountered are illustrated.

Solid Propellant Gas Generators for Auxiliary Power, by P. G. Butts and H. E. Perkins, Olin Mathieson Chemical Corp., East Alton, Ill. (443-57). The design and types of propellant used in generators and the advantages of such devices are outlined.

Production Problems in Solid Propellants, by J. A. McBride, Phillips Petroleum Co., Bartlesville, Okla. (444-57). Paper not available at press time.

At Columbus Section's Annual Banquet

John W. Townsend Jr. of NRL (seated left), featured speaker at the annual banquet of the Columbus Section, is shown with officers and directors of the Section at the banquet.

Others in the picture are Abbott A. Putnam, Section president (seated), and (l to r) M. W. Jack Bell, Loren Bollinger, Rudolph Edse, directors, and James L. Harp, recording secretary.

A Practical Mathematical Approach to Grain Design, by Max W. Stone, Rohm and Haas Co., Huntsville, Ala. (445-57). Equations were developed relating solid propellant grain geometry to the important ballistic parameters of cross-sectional loading density, sliver or tail-off fraction, progressivity ratio, initial surface and web. The equations were solved and the results graphed. Illustrations for use of the graphs are given.

COMBUSTION

Influence of Pressure on the Combustion of Liquid Spheres, by George A. Agoston, Bernard J. Wood and Henry Wise, Stanford Research Institute, Menlo Park, Calif. (446-57). An experimental study of the influence of pressure on burning rates of liquid fuels coating the surface of porous Alundum spheres of various diameters was made. Data observed and other information were correlated to reveal quantitatively the influence of free convection.

Flame Stabilization in the Boundary Layer of Heated Plates, by Richard W. Ziemer, Armour Research Foudation, Chicago, and Ali Bulent Cambel, Northwestern University, Evanston, Ill. (447-57). A graphical analysis of boundary layer flame stabilization is proposed and verified by an experimental investigation of propane-air flames.

A Theory of Spray Combustion, by C. C. Miesse, Armour Research Foundation, Chicago, Ill. (448-57). The performance characteristics of a liquid propellant combustor are determined as a function of droplet lifetime and the relative burning rate of its vapors. Various effects on performance characteristics are presented graphically and conditions necessary for optimum performance are determined analytically.

Theory of Maximum Rates of Heat Release in Inhomogeneous Combustion, by H. N. Powell, General Electric Co., Cincinnati, Ohio (449-57). This paper is a mathematical implementation of the Wolfard-Parker conclusion for the combustion of initially unmixed gaseous fuels and oxidants. Attempt is made to establish a basic mathematical methodology for describing the limiting or ideal performance of such combustion processes.

RAMJETS

Ramjet Test Facility Planning, by Robert O. Dietz Jr., and Arthur H. Hinners, ARO, Inc., Tullahoma, Tenn. (450-57). A method of planning adequate test facilities to meet future ramjet test requirements is discussed.

Techniques of Flight Simulation for Ramjet Engines, by Raymond Greenberg, Curtiss-Wright Corp., Wood-Ridge, N. J. (451-57). Ground testing of ramjets with Curtiss-Wright's blowdown-type facility is described.

Testing Air Breathing Supersonic Powerplants, by G. A. Sears and J. J. Bajek Marquardt Aircraft Co., Van Nuys, Calif. (452-57). Basic information concerning the free jet method of supersonic engine development testing is presented. Parameters are discussed and performance levels of various diffuser types are shown.

Techniques, Facilities and Instrumentation for Experimental Determination of Ramjet Dynamic Characteristics, by Carl B. Wentworth and George Vasu, Lewis Flight Propulsion Laboratory, NACA, Cleveland. (453-57). Specialized test equipment, instrumentation and experimental procedures used to determine ramjet dead times and time constants are presented and discussed.

HYPERVELOCITY FLIGHT

Recent Developments in Hypersonic Flow, by Lester Lees, California Institute of Technology, Pasadena, Calif. (455-57). The paper reviews progress of the last two years in the field, specifically concerning blunt-body aerodynamics and heat transfer; aero-

dynamics of blunt-nosed slender bodies, including viscous interactions; and real gas effects.

Performance of Long Range Hypervelocity Vehicles, by A. J. Eggers Jr., Ames Aeronautical Laboratory, NACA, Moffett Field, Calif. (456-57). Flight over the surface of the earth is discussed in terms of vehicle motion in powered flight and motion and heating in unpowered flight. Skip, glide and ballistic trajectories are analyzed for unmanned craft; observations on manned glide vehicles are made. Re-entry and recovery of ballistic satellites are considered. (See Jet Propulsion, June 1957, p. 710.)

A Survey of Heat Transfer Problems Encountered by Hypersonic Aircraft, by Jackson R. Stalder, Ames Aeronautical Laboratory, NACA, Moffett Field, Calif. (457-57). Aerodynamic heating appears to be the determining factor in speed, flight path and configuration of vehicles. Major problems encountered in the design of such craft because of heating are broadly outlined.

Some Characteristics of the Upper Atmosphere Pertaining to Hypervelocity Flight, by C. Frederick Hansen, Ames Aeronautical Laboratory, NACA, Moffett Field, Calif. (458-57). Chemical processes occurring in the air are discussed and reactions responsible for most of the solar energy absorption are outlined. Other factors are considered. The author concludes that manned flight through the upper atmosphere will soon become feasible.

Structural Problems in Hypersonic Flight, by Samuel A. Batdorf, Lockheed Aircraft Corp., Burbank, Calif. (459-57). Stress-strain relationships become obsolete in high-speed flight, with a stress-strain-time-temperature expected to replace it. No such relation has been found yet. Problems encountered are mentioned.

SPACE FLIGHT

Ground Simulation of Meteoritic Dust Impact on High Flying Vehicles, by Donald H. Robey, Convair-Astronautics, San Diego, Calif. (465-57). General discussion of dust is presented and deductions concerning properties and speeds are given. A proposal for accelerating dust particles to 30 km/sec is given.

Effect of Air Drag on Elliptic Satellite Orbits, by Robert E. Roberson, Autonetics Div., North American Aviation, Inc., Downey, Calif. (466-57). Such effects are difficult to analyze, so the author presents an approximate analytic solution that is easy to apply to provide fair estimates of true behavior.

Cislunar Operations, by Krafft Ehricke, Convair-Astronautics, San Diego, Calif. (467-57). Paper not available at press time.

Sections

Cleveland-Akron: New officers of the Cleveland-Akron Section are Luis R. Lazo, Thompson Products, president; Paul M. Ordin, NACA Lewis Lab., vice-president (Cleveland); Wayne E. Wiant, Goodyear Aircraft, vice-president (Akron); and Edward G. Rapp, Thompson, secretary-treasurer. Directors are Pierce T. Angell, Thompson Products; A. O. Tischler, NACA Lewis Lab.; and J. C. Feldscher, Goodyear.

Columbus: John W. Townsend Jr., head, Rocket Sonde Branch, Atmosphere and Astrophysics Div., Naval Research Laboratory, and assistant science program coordinator, Project

Vanguard, was the guest speaker at the annual banquet of the Columbus Section, attended by 115 members and guests, and held at the Port Columbus Naval Air Station.

Mr. Townsend disclosed a number of interesting facts concerning the earth satellite program, discussing the proposed orbit, the three-stage vehicle designed to place the satellite in orbit, and the telemetering system to be used for relaying data to earth. He also pointed out the dangers to the satellite from micrometeorites.

Northern California: Joseph Kaplan of UCLA, chairman of the U. S. National Committee for the IGY, gave the AMERICAN ROCKET SOCIETY a pat on the back at a recent joint meeting of the Northern California Section, the IAS and the ASME in San Francisco. In opening his address on the IGY program, Dr. Kaplan noted that he had seen ARS develop into a top-notch professional society in the past few years, and commented that "the Society will certainly give the IAS a run for its money in the future."

Princeton: The annual Honors Night banquet of the Princeton Group was attended by some 50 members and guests. The guest speaker for the occasion, Rear Adm. W. A. Schoech, was unable to attend; in his stead, Capt. F. E. Hilliard, USMC (ret.), spoke in commemoration of Armed Forces Day and brief addresses were delivered by James J. Harford, ARS executive secretary, and J. P. Layton, chief engineer, Jet Propulsion Research Program, Princeton University.

Section officers for 1957–1958, all from Forrestal Research Center, are: John B. Fenn, director, Project SQUID, chairman; Kimball P. Hall, research associate, vice-chairman; and Marshall Fisher, librarian, re-elected for a third term as secretary-treasurer.

Sacramento: Over 60 persons recently attended a confidential meeting of the Sacramento Section. A special report on "Rocket Powerplants from the Gound Up" was delivered at the meeting by R. C. Stiff, manager, Engineering and Research Div., and G. W. Lothrop, missile rocket projects department, Aerojet-General Corp.

San Diego: The May meeting of the San Diego Section was attended by a dinner audience of some 80 members and guests, who heard Clifford E. Smith, professor of astronomy at San Diego State College and nationally known astronomer, discuss the planet Mars. Dr. Smith noted that most observers disagree as to what they have seen on this planet, an example being

(Continued on page 815)

People in the News

APPOINTMENTS

• **Albert E. Schwerin,** manager of flight test engineering, Missile and Ordnance Systems Dept., General Electric Co., has been assigned to the Air Force Missile Test Center, Patrick AFB. He will head the department's test activities on Air Force strategic ballistic missiles.

• **Roy L. Queen,** assistant manager, Test and Field Service Div., has been named Aerobee-IGY coordinator for Aerojet-General Corp. Other Aerojet promotions include those of **James C. Sampson** to head infrared projects department, Avionics Div.; **Richard E. Minnick** to head material operations department; and **Thomas E. Johnston** to general purchasing agent, Material Div.

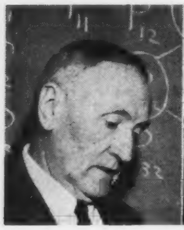

Zwicky

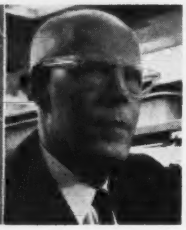

Law

• **Fritz Zwicky,** professor of astrophysics, California Institute of Technology, has been appointed to the Scientific Advisory Board of Hycon Mfg. Co. Dr. Zwicky has been a member of the Air Force Scientific Advisory Board and director of research for Aerojet.

• Lockheed Missile Systems Div. has named **John P. Nash** manager of its Information Processing Div. and added **Joseph F. Quilter** to its Product Planning Branch. Dr. Nash has been research professor of applied mathematics at the University of Illinois since 1950, while Rear Adm. Quilter has been chief of staff of the Naval Air Materiel Center, Philadelphia.

• **Walker L. Cisler,** president, Detroit Edison Co.; **Clifford C. Furnas,** chancellor, University of Buffalo; and **Arthur H. Peterson,** controller, Cornell University, have been elected to the board of directors of Cornell Aeronautical Laboratory, Inc.

• **Milton E. Mohr,** director of Control Systems Div., Ramo-Wooldridge Corp., has been named a group director in charge of the Control Systems and Boston Divs. Mr. Mohr will retain his position as division director, as will **George E. James,** director of the Boston Div. **Donald B. Jacobs** has joined Ramo-Wooldridge's Guided Missile Research Div.

• **George S. Schairer** has been appointed director of research at Boeing Airplane Co. He was formerly assistant chief engineer of its Seattle Div.

• Grand Central Rocket Co. has reorganized its project management setup. **Willem Schaafsma,** formerly director of engineering, has been promoted to director of projects and **Stanley Waxman,** former director of research and development, has been named director of engineering and research.

• **Igor Sikorsky,** who developed and flew the first successful helicopter in the Western Hemisphere in 1939, will retire from active duty as engineering manager of Sikorsky Aircraft Div., United Aircraft Corp. He will serve as a consultant to the company.

• **Russell R. Law,** former director of research and development for CBS-Hytron Div., Columbia Broadcasting Inc., has joined Hughes Aircraft Co. as director of new product development, Hughes Products Group.

• Guided Missiles Div., Fairchild Engine and Airplane Corp., has established a new development planning staff, to be headed by **Harry Iddings,** formerly at Cornell Aeronautical Laboratory.

• **Nelson Kling,** formerly chief engineer, Arkwin Industries, has been appointed chief design engineer of Eastern Aircraft Products Corp. **Bernard Wasdyke** and **Marvin Rosenfeld** have been named project engineers for Eastern.

White

Tabors

• **Perry A. White,** general controller of Baldwin-Lima-Hamilton Corp., has been appointed vice-president and general manager of the Eddystone Div. and **Robert G. Tabors,** vice-president and general manager of the Hamilton Div., has been named vice-president and general manager of the Electronics and Instrumentation Div.

• **Paul Meeks,** general manager, Automatic Controls Div., Clary Corp., has been elected to the board of directors and made a vice-president of the corporation. Mr. Meeks was at one time on the Guided Missile Committee of the National Research and Development Board and the U. S.-Canadian Mission to London on explosives, rocket propellants and fuels.

• **Frederick I. Ordway III** has been transferred to the Huntsville Field Office of General Astronautics Corp. as project director.

• **Charles R. Strang** has been named chief engineer and **Anthony G. Puglisi** assistant chief engineer of Tulsa Div., Douglas Aircraft Co.

• Systems Laboratories Corp. has appointed **James A. Marsh** president, **Richard H. DeLano** executive vice-president, **Wilbert Lloyd** treasurer and **A. J. F. Clement** secretary.

• The Daven Co. has appointed **Frederick A. Schamer** chief engineer. He was previously manager, receiver engineering, Research and Development Div., Air Associates, Inc.

• **B. A. Martin,** former division chief pilot, has been named weapons systems 125A manager, Georgia Div., Lockheed Aircraft Corp., and **R. R. Kearton** has moved up to head missile systems sales branch, Van Nuys, Calif.

HONORS

• **Lawrence A. Hyland,** vice-president and general manager of Hughes Aircraft Co., has received the 1957 Pioneer Award from the Institute of Radio Engineers' professional group on aeronautical and navigational electronics. Mr. Hyland was honored for his demonstration in radar work, in the early 1930's, that radio waves reflect from objects.

• **Maj. Gen. Frederick R. Dent Jr.,** USAF, recipient of over a dozen military decorations, was awarded the Distinguished Service Medal upon his retirement from the U. S. Air Force. Gen. Dent has been commander of the Mobile Air Materiel Area since 1953 and was commander of Wright Air Development Center in 1951. The general will become a vice-president of Electronic Corp. of America.

DEATHS

Dr. Harold M. Hipsh, faculty advisor to the University Park Section of the American Rocket Society and head of the Aeronautical Engineering Dept. at Pennsylvania State University, passed away on May 23.


WHY DOUGLAS ENGINEERS AND SCIENTISTS GO FURTHER...
At DOUGLAS
...your
missiles assignment
can be as big as
your talents
Now in its 16th year, the Douglas missiles program is projected far into the future by such exciting new projects as THOR
Out of such veteran projects as Nike and Honest John are coming fantastic new missile systems to challenge the finest engineering talents in the land.
Since early in World War II, Douglas has been engaged in missile projects of prime importance. New engineering teams are constantly being formed for research, design, development and production. Engineers advance rapidly as Douglas expands its leadership in this challenging field.
You are stimulated to accelerate your career by the importance of each assignment ...by the help of your associates who are recognized experts in missile work...by the vastness of opportunity for engineers in this company that is run by engineers.
There is no more promising future than that which awaits you in the Douglas Missiles Divisions.
THOR—an intermediate range ballistics missile now under development—has top priority in our country's program for national defense.
For complete information, write:
E. C. KALIHER,
MISSILES ENGINEERING
PERSONNEL MANAGER,
DOUGLAS AIRCRAFT COMPANY,
BOX J-620,
SANTA MONICA, CALIFORNIA
GO FURTHER
WITH
DOUGLAS
FIRST IN AVIATION

Space Flight Notes

JOHN GUSTAVSON, Convair-Astronautics, Contributor

Stations in Space

SOMETIME within the next year, man will launch an artificial satellite and bring a payload to orbital velocity for the first time. The IGY satellites will eventually be followed by larger ones; ultimately, a manned space station will be considered.

The cost of such a space station will be great. The technological problems of establishing and maintaining it will be the most challenging ever to be undertaken. But within ten years we may see the first crude space laboratories in orbit around the earth, and occupied by scientists who will descend in escape capsules after their work is done.

Orbits

The earth is assumed to be a perfect homogeneous sphere with radius equal to 6.375×10^6 meters and gravitational acceleration equal to 9.80665 m/sec^2. Table 1 presents some equatorial orbits calculated on this basis with corresponding number of revolutions per day, n; time of revolution, T; altitude, h; and velocity, v.

The three fundamental requirements for a space station orbit are:

- The orbit must lie above the earth's atmosphere.
- For certain research purposes, as well as for economic reasons, the orbit must be fixed at a minimum altitude above the earth's surface.
- The orbit must be stable or the perturbances known and compensated for.

Selection of a particular orbit will, of course, depend upon the applications.

Pseudo-Gravity

Living areas in the station must simulate earth conditions to provide for prolonged occupancy by observers and scientists. Besides a continuous air and food supply, including facilities for purification and renovation, the living quarters must provide a pseudo-gravitational acceleration which will give the inhabitants a sense of weight.

Fig. 1 Wernher von Braun's space station project

There can be very little doubt that prolonged exposure to the weightless state will promote unfavorable physical and emotional reactions. One means of combatting this problem is to create a fictive force field by rotating the space vehicle. These enormous flywheel-type space stations (Fig. 1[1]) are perhaps more popular than any other design.

But the "flywheel" station also has its limitations. Among other things, a fast-spinning station will create a sensation of rotation in an individual on the station since the difference in centrifugal force acting upon his head and feet, resulting from the fact that his feet are further away from the center of the station than his head, will cause nausea and even total blackout. Obviously, this effect becomes more pronounced with increased rotation of the station. It is most severe for small stations, where the ratio of the distance from center to the height of the person is small.

At the same time any object moved toward or away from the center will undergo Corioli acceleration perpendicular to the direction of motion and proportional to the velocity. This effect can cause discomfort to the crew, as any moving object or person will be subject to the additional force component, disturbing or upsetting the sensations which normally enable the individual to determine what is "up" and "down."

[1] Ryan, Cornelius, Edit., "Conquest of The Moon," Viking Press, New York, 1953, p. 11.

Historical

As early as 1928, the rotating space station was proposed by Germany's Hermann Noordung.[2] His design included a wheel-shaped station which made one revolution in 8 sec. The radial distance was 50 ft, and the centrifugal acceleration corresponded to 1 g. Noordung designed his space station to orbit at 22,000 miles altitude. One revolution around the earth takes 24 hours, during which period the earth rotates one complete turn around its axis.

Noordung's space station had air locks at the hub of the wheel, and also featured a huge parabolic reflector for collection of sunlight. The energy was concentrated on boiler tubes, and a heating cycle including condenser coils on the shady side was established. This method of providing accessory power for the space station is still regarded as promising.

Recent Types

A proposal made by members of the British Interplanetary Society appears in Fig. 2. Based on sensible estimates, this huge collector and the living quarters behind it can be brought up to orbit by special ferry rockets with expendable

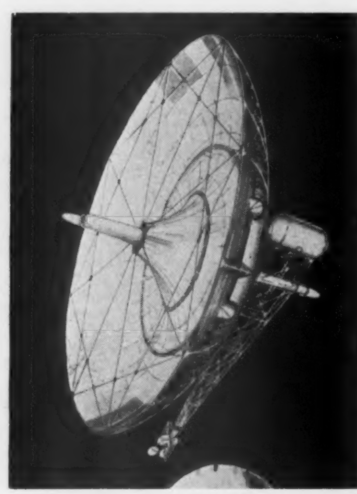

Fig. 2 BIS space station proposal

[2] Noordung, Hermann, "Das Problem Der Befahrung Des Weltraums," R. C. Schmidt, Publisher, Berlin, 1928.

Table 1 Equatorial space station orbits

n	T solar secs	h km	h miles	v m/sec	v fps
15	5,760	570	355	7,576	23,107
$13\frac{1}{3}$	6,480	1,137	709	7,284	22,216
$12\frac{1}{2}$	6,912	1,467	915	7,129	21,743
12	7,200	1,684	1,050	7,033	21,451
1	86,400	35,000	22,000	3,000	9,100

Fig. 3 Krafft Ehricke's manned satellite

propellant tanks and engines. The station will be constructed in space, piece by piece, and will furnish a platform for astronomical and terrestrial observations.

Another model appears in Fig. 3. Designed by Krafft Ehricke, this manned satellite combines the advantages of a rotating space station with centralized mass, a feature which secures stable rotation. The station would be set in rotation by tangential rockets, and the crew would live in the facilities at each end of the structure. The principal building elements of this design are propellant tanks from the ferry rockets.[3]

Applications

The major applications of a space station can be divided roughly as follows: (1) Refueling and interchange for interplanetary flight; (2) military purposes; (3) meteorological observation of the earth; (4) astronomical observations; and (5) research in extraterrestrial environments.

The first of these had already been thoroughly analyzed as early as 1928 by the Austrian Guido von Pirquet, who was the first to realize that escape velocity was not necessary in order to accomplish space flight, but that orbital velocity was sufficient for a rocket ship to enter a stable orbit outside the atmosphere of the earth. After refueling, the rocket can easily attain escape velocity and travel to other celestial bodies.

When advanced propulsion systems eventually become available for space flight, space stations will play an important role as interchange stations. The high impulse systems, such as the ion rocket, the solar-powered thermodynamic rocket, and the arc-heated rocket, all have low thrust-to-weight ratios and will not be capable of ascent or descent maneuvers. But these vehicles could be constructed in space station orbits and perform their duties in interplanetary space. Passengers, freight and crews would transfer to chemical descent vehicles at the stations.

Wernher von Braun has pointed out many of the military advantages of a space station. Equipped with powerful telescopes, it will be able to keep the earth under constant surveillance and

Fig. 4 Hermann Oberth's space observatory

[3] Ehricke, Krafft A., "Analysis of Orbital Systems," Proceedings of the Fifth International Astronautical Congress, Innsbruck, 1954, Springer-Verlag, Vienna, p. 35.

serve as an ultimate method of aerial reconnaissance. A guided missile launched from a station can be tracked and controlled during its entire flight, even under the particularly difficult re-entry phase.

The space station is, of course, best designed for peaceful purposes, such as meteorological observation of the earth. Severe storms can be tracked and weather predictions made more accurate.

Another purpose of a space station might be as an aid to astronomers who are limited in their work by the blanketing effect of the atmosphere and the disadvantage of weighty, bulky telescopic instruments. Both of these limiting factors disappear for the observer in the space station. Lack of atmosphere is an advantage which will open new windows in the electromagnetic spectrum.

The space station laboratory will be capable of duplicating any experiment conducted here on earth, but it will also furnish some important and unique conditions, such as the weightless state and the vacuum of space. The former will prove important in biological studies, while the latter will facilitate electronic and experimental physics where today's imperfect vacuum techniques set the limiting barrier.

In his first book (1923), Hermann Oberth pointed out the many fields which would benefit from such a space laboratory. Fig. 4 shows a recent proposal of his,[4] a space station devoted to the exploration of the universe around us—the universe we will shortly enter.

[4] Oberth, Hermann, "Menschen in Weltraum," Econ-Verlag, Duesseldorf, 1954, p. 112.

(Continued from page 809)

the much discussed "canals." He concluded that many of the mysteries of Mars may be solved by observation posts in space which would eliminate interference with visual observation and spectrum analysis.

The dinner was followed by a short directors' meeting at which the nominating committee submitted the slate of officers from which Section members will select officers for the coming year.

ARS Meetings Calendar

Aug. 25–28: ARS-Northwestern Technological Institute Gas Dynamics Symposium, Northwestern University, Evanston, Ill.
Oct. 7–12: International Astronautical Federation 8th Annual Conference, Barcelona, Spain.
Dec. 2–6: ARS Twelfth Annual Meeting, Hotel Statler, New York.
Dec. 6–7: ARS Eastern Regional Student Conference (under the auspices of Polytechnic Institute of Brooklyn Student Chapter), Hotel Statler, New York.

New Equipment and Processes

Equipment

Electrical, Electronic

Miniaturized Gyro. Model 55,000 Floated Rate Gyro was designed to meet the rugged environmental conditions encountered in missiles. Damping ratio, maintained without a heater, can be established to suit customer requirements and maintained within 0.1 over the temperature range of −55 to +85 C. Norden-Ketay Corp., Commerce Rd., Stamford, Conn.

Transistorized Power Supplies. Power supplies for filament, transistor and plate voltage applications are available for use in computers, guided missiles and aircraft electronic equipment. The units are as low cost and small as transformers alone, and as lightweight as 1 oz per watt. UAC Electronics Div. of Universal Transistor Products Corp., 143 E. 49 St., New York 17, N. Y.

Mechanical

Pneumatic Check Valve. Designed to check rapidly reversing high temperature, high pressure air surges. Barber-Colman check valves are used on many jet airliners now under construction. The valve allows high temperature airflow into a wing thermal anti-icing manifold from an engine compressor bleed port, and prevents reverse flow when pressure downstream from the valve exceeds that upstream. It has an inside diameter of 3 in. and weighs 3.1 lb. Barber-Colman Co., Rockford, Ill.

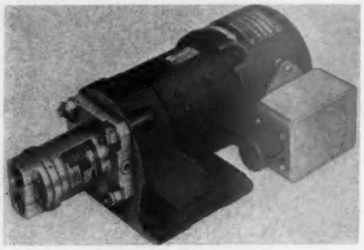

Piston-Type Motorpump. Model AA-19054 miniaturized motorpump for missile applications delivers 84 gpm at 7400 rpm and 1000 psi. The hydraulic pump weighs 1 lb and the electric motor 7 lb. Vickers Inc., Detroit 32, Mich.

Materials—Fabricated Parts

Pressure-Filled O-Rings. Principal uses of pressure-filled metal O-rings are for missiles, rockets, aircraft gas turbines and other applications where operating temperatures exceed 1000 F. Standard 0.010 stainless steel O-rings are filled with gas at various pressures ranging from 500 to 3000 psi at room temperature. The gas pressure offsets the inherent loss of the metal's strength at elevated temperatures. The Advanced Products Co., 59 Broadway North Haven, Conn.

Materials

Polyester Molding Compound. Atlac Thermaflow 800, a glass fiber reinforced polyester molding compound, meets Mil. Specs. for alkyd high impact compounds. The material is suitable for producing lightweight complex shapes and parts requiring deep draw. Atlas Powder Co., Wilmington 99, Del.

Nylon Fiber Batting. A self-supporting batting made of nylon fibers is useful for thermal insulation, liquid and gaseous filtration, vibration and shock absorption in guided missiles. It is available in weights from 2 to 8 oz/sq yd in widths up to 55 in. Star Woolen Co., Cohoes, N. Y.

Processes

Tough Metal Softener. A new furnace, pioneered in titanium melting, is being made available in the metals industry. The furnace, called a consumable electrode vacuum remelting furnace, also melts zirconium, high alloy steels or other nonferrous alloys which are free from impurities and possess improved qualities such as used in jet aircraft and engines, missiles and atomic reactors. Allegheny Ludlum Steel Corp., Pittsburgh 22, Pa.

Vacuum Brazing. For experimental and limited-scale production vacuum brazing of aircraft components, The Martin Co. is using two horizontal retort vacuum furnaces with a movable work-

LAVELLE...Wherever Precision Fabrication is Required

FAIRINGS
BAFFLES
COWLINGS
SHROUDS
ENGINE MOUNTS

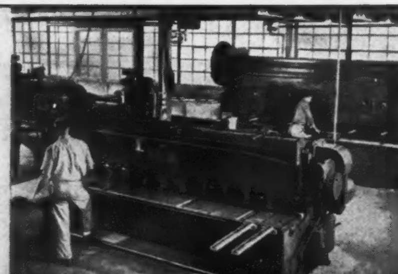

PRECISION WELDED AND MACHINED SHEET METAL PARTS AND ASSEMBLIES

ENGINE DUCTS
SHIELDS
COMBUSTION CHAMBERS
BURNER SUPPORTS
COMBUSTION LINERS

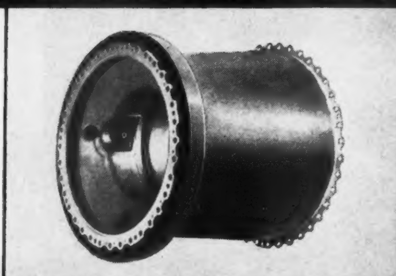

JET ENGINE, MISSILE, ROCKET, AIRFRAME AND ELECTRONIC COMPONENTS

EXHAUST NOZZLES
TAIL PIPES
FLAME HOLDERS
SEALS
ENGINE CASINGS

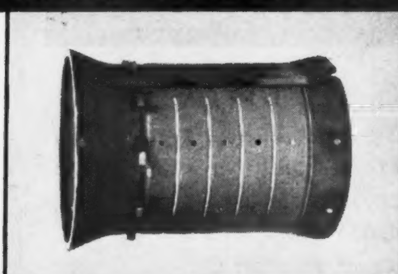

FABRICATED OF STAINLESS STEEL, TITANIUM, NICKEL AND ALUMINUM ALLOYS

SHELTERS
HOUSINGS
REFLECTORS
CONSOLES
NACELLES

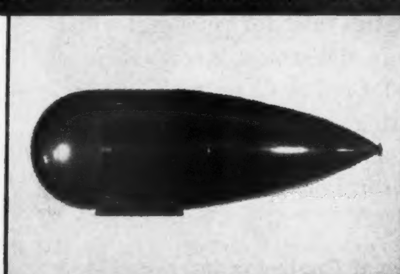

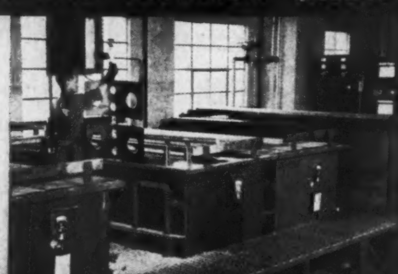

TO GOVERNMENT SPECIFICATIONS BY CERTIFIED MEN, METHODS AND MACHINES

Lavelle's services include engineering production planning, tool making, machine shop and sheet metal facilities . . . inert gas, resistance and metallic arc welding, inspected by X-Ray, Zyglo or Magnaflux, painting, anodizing and quality control.

Lavelle

Lavelle Aircraft Corporation • Newtown, Bucks County, Pa.
Between Philadelphia, Pa., and Trenton, N.J.

Write for this illustrated brochure describing Lavelle's specialized fabricating services in detail.

holding boat. The furnaces can also be used for vacuum de-gassing, annealing and other heat-treating operations. Temperatures as high as 2150 F can be obtained and maintained uniformly throughout the processing cycle. F. J. Stokes Corp., 5500 Tabor Rd., Philadelphia 20, Pa.

Test

Vibration Tester. Model 305 portable vibration amplitude meter is used to set up programs of seeking out vibration and establishing acceptable tolerances in production, inspection and maintenance. It weighs 24 oz. International Research & Development Corp., 595 E. Broad, Columbus 15, Ohio.

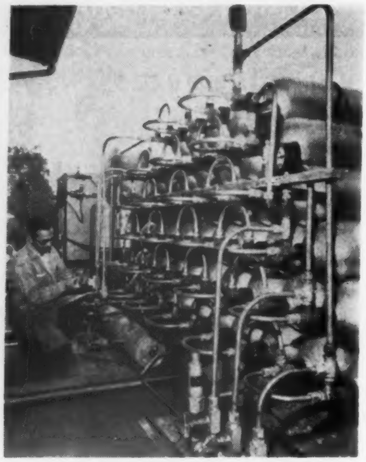

Helium Test Facility. A new facility has been placed in operation for simulating internal environmental conditions encountered by aircraft and missiles employing helium, nitrogen, oxygen or other gases as propellants or pressurization agents. It consists of five 2 cu ft cylinders manifolded together and capable of storage pressures up to 6000 psig, fifty 8½ cu ft cylinders for storage up to 2400 psig, and two 1000 cu ft low pressure receiver tanks used to collect helium expended during testing. Aeronautical Div., Robertshaw-Fulton Controls Co., 401 Manchester, Anaheim, Calif.

Product Literature

Joints and Couplings. Rubber, neoprene and Teflon-lined expansion joints and flexible couplings, their characteristics and limitations, are explained in bulletin AD-137. Garlock Packing Co., 408 Main St., Palmyra, N. Y.

Low Temperature Containers. Sturdy containers for use in the low-temperature field are described in a 16-page "Low Temperature Apparatus" catalog. The containers have a double wall separated by a high vacuum, and highly polished internal surfaces for reduction of radiant heat losses. The outer steel casing withstands rough handling. Hofman Laboratories, Inc., 219–221 Emmet St., Newark, N. J.

Missiles Machinery. Contour machining of metals is described in a folder illustrating a variety of turning, boring and milling operations used in producing missiles. Parts currently produced include nozzles, rings, cones, pressure vessels, radomes, bulkheads, midsections and adapters. Diversey Engineering Co., 10257 Franklin Ave., Franklin Park, Ill.

When the problem of sealing is a part of *design thinking* the whole design is bound to be better. This is especially true of *no-leakage* sealing. When your designs require sealing ... from −400° to +1000° ... why not call in one of our field men. One of the "O-seal" family*, may be the answer to save you time, money and effort.

FRANKLIN C. WOLFE CO.

A DIVISION OF PARKER APPLIANCE COMPANY

"sealing design specialist"

Culver City, California

New Patents

George F. McLaughlin, *Contributor*

Propellant powder and method of producing same (2,787,533). John J. Oneill Jr. and Thomas F. McDonnell, Collinsville, Ill., assignors to Olin Mathieson Chemical Corp.

Particles of powder base lacquer are agitated in a nonsolvent medium. Solvents are removed from the particles by heating while maintaining the suspension in the medium.

Aircraft auxiliary power device using compound gas turbo-compressor units (2,787,886). Homer J. Wood, Sherman Oaks, Calif., assignor to The Garrett Corp.

A main unit derives a connected load at constant speed, and a free-floating secondary unit. The units, under combined operation, develop full rated power at a predetermined high altitude. Excess pressurized air is bled from the compressor of the secondary unit for pneumatic power purposes during low altitude operation.

System for cooling a turbine bearing of a gas turbine power plant (2,789,416). Rio N. Mirza, Northport, N. Y., assignor to Fairchild Engine and Airplane Co.

An exhaust gas deflector on the outer end of a tail cone has a flared outer surface forming a venturi throat. Exhaust gases flowing around the deflector create a reduced pressure in the cone. A duct connects the cone interior to a source of cooling air for circulation around the turbine wheel bearing.

Tailpipe or afterburning control for turbojet engines (2,789,417). Frank W. Kuzimitz, South Bend, Ind., assignor to Bendix Aviation Corp.

Fuel supply system having a combustion chamber after the turbine for thrust augmentation. Means responsive to the speed of the aircraft controls the flow of fuel to the afterburner.

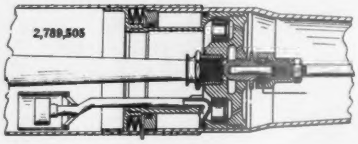

Liquid propellant rocket (2,789,505). James M. Cumming, George P. Sutton, Vernon R. Vorwerk and Darell B. Harmon, Los Angeles, Calif., assignors to North American Aviation, Inc.

A propellant tank with flexible walls within a main fuel tank with rigid walls. Pressure in the main tank pressurizes the inner tank, forcing propellants into the rocket motor.

Fuze for rocket projectiles (2,789,507.) Robert Apotheloz, Wallisellan, Switzerland, assignor to Machine Tool Works Oerlikon.

Rotor mounted in a fuze body, rotatable between a safe position and an operative position. A primer cap detonates on impact of the fuze when the rotor is moved rearwardly to its operative position by acceleration forces during flight of the projectile.

Valve and system for the protection of aircraft occupants (2,789,556). David M. Clark, Waldo J. Guild and Ernest E. Martin, Dayton, Ohio.

System for preventing an unnatural blood distribution within a human body subjected to forces set up when the body is accelerated in space. Inflatable elements loosely engage different parts of the body: when inflated, they affect a control automatically operated in response to abnormal positive or negative g effects, supplying fluid under pressure to inflate the elements, and affecting a pressure against the blood-carrying vessels.

Jet engine fuel and nozzle area control apparatus (2,790,303). Robert J. Kutzler, Minneapolis, Minn., assignor to Minneapolis-Honeywell Regulator Co.

Temperature responsive means controls fuel delivery to the engine. An override

Editors Note: Patents listed above were selected from the Official Gazette of the U. S. Patent Office. Printed copies of Patents may be obtained from the Commissioner of Patents, Washington 25, D. C., at a cost of 25 cents each; design patents, 10 cents.

means reduces fuel flow when engine speed exceeds a predetermined value.

Variable-area constrictor for ramjet diffuser (2,790,304). Carl W. Besserer Jr., Silver Spring, Md., assignor to the U. S. Navy.

Aerial missile of the ramjet type. Means for regulating the air flow through an unobstructed central duct including a flexible sleeve forming a part of the duct throat. Adjustment of the pressure in a Bourdon tube surrounding the sleeve controls the cross-sectional area of the throat.

2,790,352

Spin stabilized rocket wing launcher (2,790,352). John L. Jewett and Clem G. Trimbach, Erie County, N. Y., assignors to the U. S. Navy.

An open-ended tubular rocket launcher in an aircraft wing, covered by a pair of doors at the forward end, flush with the wing leading edge. The doors are withdrawn from the forward aperture and swung open to expose the tube, upon rocket movement through the tube.

Mass accelerator (2,790,354). Yusuf A. Yoler and James D. Cobine, Rexford, N. Y., assignors to General Electric Co.

A nonconducting hollow tube with one end sealed and the other end open to air, includes a material responsive to the heating action of electrical arc discharges. The discharges in the vicinity of the sealed

end heat and ionize the air, setting it in motion down the length of the member, releasing lightweight gases from the material. Generation of a sequential series of arcs down the length of the member maintains the energy behind the ionized gas to propel a mass at a uniformly high level.

Multiple finger dovetail attachment for turbine bucket (2,790,620). Andrew W. Rankin, Schenectady, N. Y., assignor to General Electric Co.

Blades secured by parallel dowel pins to a base having deep grooves extending circumferentially of the rotor. Pins for each bucket pass through the middle of the middle finger, while the end of the pins are disposed in semicircular recesses formed half in one side finger of the leading bucket base and half in the abutting finger of the adjacent following blade base.

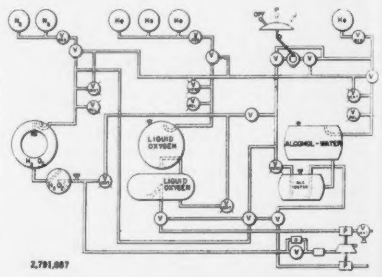

Liquid propellant transfer system (2,791,-087). John A. Gorgenson and Milton V. Clauser, Palos Verdes Estates, Calif., assignors to the U. S. Navy.

System for the control of rocket engines in which pumps and valves operate to control the flow from two pressurized containers of propellants.

Power plant cooling and thrust balancing systems (2,791,091). John B. Wheatley, Otakar F. Prachar, Arthur W. Gaubatz and Donald G. Zimmerman, Indianapolis, Ind., assignors to General Motors Corp.

A double-walled frame between the burners and the shaft has an inlet adjacent to the compressor and an exit adjacent to the turbine. An outlet from a fan connected to the exit has a passage through the shaft to cool the shaft, and another outlet has a passage around the burners and turbine housing to cool the turbine.

Auxiliary trajectory recording means for cameras (2,791,165). Donald A. Hoyt, Levittown, Pa.

To record the trajectory of an airborne object, the shutter is manually controlled for cyclic operation. The shutter is continuously coordinated with the displacement of a sight which is rotatably mounted on the camera body.

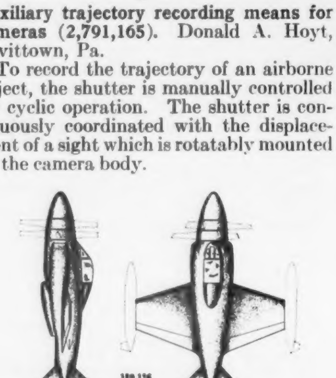

Airplane [design] (180,136). Philip A. Colman, Eugene C. Prost and Arthur E. Flock, Sherman Oaks, Calif., assignors to Lockheed Aircraft Corp.

This design is the VTOL aircraft for the U. S. Navy designated XFV-1, powered by an Allison turboprop engine driving six-bladed contra-rotating propellers.

Stratos' experience with airborne air conditioning systems has been applied to a new, lightweight air conditioner designed for use with gas turbine compressors such as the MA-1A and MA-2 types. Meeting Type MB-1 requirements, the unit is Stratos' Model GEA120-1.

Composed of aircraft quality components, the system is packaged as a compact unit measuring only 48" x 50" x 30". The controls—connected to the package solely by an electrical cable—can be remotely located and, where desired, taken directly into the aircraft.

For additional data on Stratos' line of air conditioning systems, write to:

STRATOS

A DIVISION OF FAIRCHILD ENGINE & AIRPLANE CORPORATION

Main Plant: Bay Shore, L. I., N. Y.

Western Branch: 1800 Rosecrans Ave. Manhattan Beach, Calif.

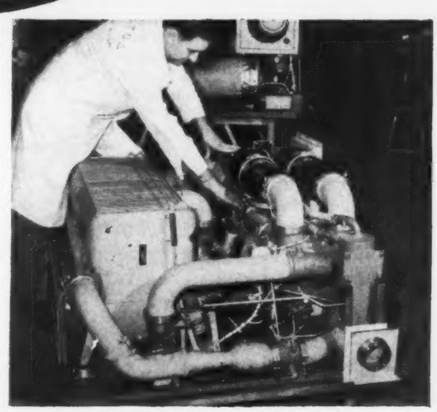

Stratos' Model GEA120-1 air conditioning system being prepared for production test.

Book Reviews

Ali Bulent Cambel, Northwestern University, *Associate Editor*

Laplace Transforms for Electrical Engineers, by B. J. Starkey, Philosophical Library, New York, 1955, 279 pp. $10.

Reviewed by Robert E. Beam
Northwestern University

This book is based on a series of lectures which the author gave to his colleagues at the Signals Research and Development Establishment. The author considers the mathematical language used by mathematicians for presenting the theory of the Laplace transformation to be difficult for engineers; therefore, he attempts to use a physical vocabulary rather than a purely mathematical one. It is assumed that the reader has knowledge of differential and integral calculus and the vector algebra of complex numbers. The treatment is intended to provide general information on the subject for electrical engineers; hence, the examples given are electric circuit ones. Even though this be the case, the book is not one on circuit theory; it should not be considered of interest and value to electrical engineers alone.

In the first chapter the author reviews very briefly the symbolic method of handling the steady state solution of linear differential equations by the use of the vector algebra of complex quantities. This is followed by a very brief statement of Fourier series and Fourier integral transformations. The first chapter, consisting of 14 pages, ends with the application of the Fourier transform method to an idealized filter of the low-pass type.

Chapter 2 deals with the concepts of generalized impedance and cisoidal oscillations. In Chapter 3 the Laplace transform of a function $F(t)$ and its inverse transform $G(p)$ are defined. Then some elemental properties of transforms are considered.

Chapter 4 is devoted to the application of Laplace transform methods to analysis and synthesis problems of electric circuit theory. Included is a discussion of the types of problems for which the Laplace transform theory is applicable utilizing the circuit of an idealized transformer with a suddenly applied sinusoidal voltage as a medium for discussion. The similarity of the Laplace transformation procedure and the procedure of the symbolic method of treating the steady state sinusoidal behavior is outlined in considerable detail. Bridge circuits and electron-tube circuits receive the greatest measure of attention in this chapter. Some emphasis is given to the physical interpretation of Laplace transform solutions and to the significance of the roots of the "characteristic equation" of the Laplace transform solution and to stability criteria.

Chapters 5, 6, 7 and 8 are essentially outlines of complex function theory. The chapter titles indicate this fact: "Functions of a Complex Variable" (Chapter 5); "Integration in the Complex Plane (Chapter 6); "Classification of Functions of a Complex Variable" (Chapter 7); and "Further Analysis of Contour Integration" (Chapter 8). These mathematical chapters consider those aspects of complex function theory which are particularly pertinent for the application of Laplace transform methods.

Chapter 9 uses the mathematical material of the preceding four chapters as a base on which to build a more formal mathematical development of the theory of Laplace transformation. The chapter ends with a discussion of the resemblance of the Laplace transform and Fourier integral.

Most of the important theorems of Laplace transform theory are given in Chapter 10. The Laplace transform is a complex function of frequency and not directly suited for interpretation in terms of measurable quantities. As a result of the fact that electrical engineers make extensive use of the symbolic method of treating steady state circuit problems, the amplitude and phase representations of a Laplace transform possess a clear meaning to them. The inverse Laplace transform represents the solution of a problem directly in real function form as a function of time as one eventually must know it. Chapter 11 deals in considerable detail with inverse Laplace transformations. The last chapter of the book, Chapter 12, is concerned with a generalization of the Laplace transform theory to functions for which the poles of their Laplace transforms are not situated to the left of the contour $(C - j^{\infty}, C + j^{\infty})$ for finite values of c. The book ends with appendices on "Analytic Functions," "Higher Mathematical Functions" and a "Table of Inverse Laplace Transforms" with 166 entries.

It is the reviewer's opinion that the author has done a very creditable job of presenting elementary Laplace transformation methods, but that he did not adequately utilize a "physical vocabulary rather than a purely mathematical" as was his stated intention.

Wing Theory, by A. Robinson and J. A. Laurmann, Cambridge University Press, 1956, 579 pp. $13.50.

Reviewed by D. C. Hazen
Princeton University

Robinson and Laurmann have produced in "Wing Theory," the second volume in the Cambridge Aeronautical Series, a book that covers the subject quite completely and in a rigorous mathematical manner. As the authors state in their preface, mathematical wing theory is of great practical importance and at the same time of considerable theoretical depth and interest. Their book is a major work in the field.

The first chapter contains a development of the basic elements of hydrodynamics that are required for the study of wing theory, ending in a discussion of viscous flow in general and of the boundary layer and fluid turbulence in particular.

The next two chapters treat the classical case of the airfoil and wing in steady incompressible flow. The two-dimensional airfoil development covers methods involving conformal mapping, including discussions of the Joukowski airfoil, Theodorsen's method of computing pressure distributions for arbitrary shapes and Lighthill's method of handling the converse problem of designing an airfoil for a specific pressure distribution. Thin airfoil theory and cascade flow are also presented. The three-dimensional wing chapter includes developments of lifting line and lifting surface theory ending in a consideration of methods suitable for the treatment of very low aspect ratio wings.

The second half of the book deals primarily with the effects of compressible flow, starting with the linearized theory of subsonic flow and proceeding through higher order theories into the problems of supersonic flows. The supersonic treatment includes two-dimensional linear and higher order theories as well as various methods of handling wings in straight or yawed flight.

The final chapter presents the theories of unsteady flows starting with a generalized development of the unsteady incompressible case and continuing with an examination of both oscillating airfoils with a constant forward velocity and motions with nonuniform average velocities. The final portions of the chapter deal with compressibility and three-dimensional effects ending with a discussion of unsteady supersonic flow.

Since it is impossible to deal with all aspects of a field as broad as wing theory within the confines of a single book of reasonable dimensions, the authors have been forced to make selections of the material to be presented. They have elected to start their treatment of an advanced mathematical level assuming a thorough knowledge of the calculus and functions of the complex variable, thereby permitting the rapid development of elegant techniques of solution. They have done a thorough job and their book contains a compilation of the major developments in the field along with extensive references for those desiring to make a more detailed study of a particular aspect of the subject. It is a fine reference book or text for an advanced course.

Book Notices

Frontier to Space, by Eric Burgess, MacMillan and Company, New York, 1956, xvi + 174 pp. $4.50. This book for the layman describes the applications of modern rocketry in obtaining data and information concerning high altitudes.

Freedom or Secrecy, by James Russell Wiggins, Oxford University Press, New York, 1956, v + 242 pp. $4. The author discusses constituent elements of the right to know based on historical facts and cases.

High Speed Flight, E. Ower and J. L. Nayler, New York Philosophical Library, 1957, 227 pp. $10. This book explains the numerous technical problems of high speed flight in simple terms. It should be of interest to laymen or persons related to aviation on a nontechnical basis.

Technical Literature Digest

M. H. Smith, *Associate Editor*, and **M. H. Fisher**, *Contributor*
The James Forrestal Research Center, Princeton University

Heat Transfer and Fluid Flow

Force and Mass Balances of the Incompressible, Isothermal, Planar Laminar Jet Issuing from a Finite Source, by Arthur L. Thomas, *Princeton Univ., Chem. Kinetics Project, Tech. Note* 31, (*AF OSR-TN*-57-21; *ASTIA AD* 115055), Dec. 1956, 41 pp.

Effects of Diffuser and Center-Body Length on Performance of Annular Diffusers with Constant-Diameter Outer Walls and With Vortex-Generator Flow Controls, by Charles C. Wood and James T. Higginbotham, *NACA RM* L54G21, Sept. 1954, 39 pp. (Declassified from Confidential by authority of *NACA Res. Abstracts* 111, p. 17, Jan. 28, 1957.)

Determining Drop Size Distribution of a Nozzle Spray, by W. E. Ranz and Clarence Hofelt, Jr., *Indust. Engng. Chem.*, vol. 49, Feb. 1957, pp. 288–293.

Some Experiments on an Effusion Cooled Turbine Nozzle Blade, by S. J. Andrews, H. Ogden and J. Marshall, *Gt. Brit., Aeron. Res. Council, Curr. Pap.* 267, (Formerly *ARC Tech. Rep.* 17890; *Nat. Gas Turbine Estab. Note NT*. 132), 1956, 22 pp., 14 fig.

A Note on the Correlation of Data in Nucleate, Pool Boiling from a Horizontal Surface, by N. Zuber, *Univ. California, Dept. Engng.*, July 1956, 6 pp.

Foundations of Thermodynamics, by P. T. Landsberg, *Rev. Modern Phys.*, vol. 28, Oct. 1956, pp. 363–392.

On the Noise from Supersonic Jets, by E. J. Richards, *J. Roy. Aeron. Soc.*, vol. 61, Jan. 1957, p. 43–45.

Some Evaporation Measurements on Liquid Sprays, by W. Bergwerk, *J. Roy. Aeron. Soc.*, vol. 61, Jan. 1957, p. 47–49.

Preliminary Measurements of Nonsteady Velocities in a Single Stage Axial Flow Compressor, by Hsuan Yeh, Harry M. Croner and Douglas E. Andrews, *Wright Air Dev. Center, Tech. Rep.* 55-249, June 1956, 41 pp.

Analytical and Experimental Investigations of Incompressible and Compressible Mixing of Streams and Jets, by T. P. Torda and H. S. Stillwell, *Wright Air Dev. Center, Tech. Rep.* 55-347, March 1956, 250 pp.

Jets—Review of Literature, by M. Z. Krzywoblocki, *Project Squid, Tech. Rep.* PR-68-P, Nov. 1956 (reprint from JET PROPULSION, vol. 26, no. 9, Sept. 1956, pp. 760–779).

Pressure Losses of Titania and Magnesium Slurries in Pipes and Pipeline Transitions, by Ruth N. Weltmann and Thomas A. Keller, *NACA TN* 3889, Jan. 1957, 22 pp.

The Efficiency of Supersonic Nozzles for Rockets and Some Unusual Designs, by R. P. Fraser, P. N. Rowe and M. O. Coulter, *Chartered Mech. Engr.*, vol. 4, Feb. 1957, pp. 69–71.

Liquid Atomization and the Drop Size of Sprays, by R. P. Fraser and Paul Eisenklam, *Trans., Instn. Chem. Engrs.*, vol. 34, no. 4, 1956, pp. 294–319.

Conference on Bubble Dynamics and Boiling Heat Transfer Held at the Jet Propulsion Laboratory, June 14 and 15, 1956, Summary of, edited by S. G. Bankoff, W. J. Colahan, Jr., and D. R. Bartz, *California Inst. Tech., Guggenheim Aeron. Lab., CIT. GAL. Memo.* 20–137, Dec. 10, 1956, 42 pp.

A Cascade Impactor for Determining the Drop Size Distribution of Fuel Mists, by J. L. Harp and J. M. Pilcher, *Wright Air Dev. Center, Tech. Rep.* 55-428, (*ASTIA AD* 110484), Nov. 1955, 28 pp.

Effect of Chord Size on Weight and Cooling Characteristics of Air-Cooled Turbine Blades, by Jack B. Esgar, Eugene F. Schum and Arthur N. Curren, *NACA TN* 3923, Jan. 1957, 37 pp.

Effect of Blade Cooling on Performance of a Gas Turbine Power Plant, by Bernard L. Buteau, *Mass. Inst. Techn., Div. Indust. Cooperation, Contract No. N5-ori-7862, Tech. Rep.* 7, June 1955, 35 pp., 14 fig.

Effects of Turbine Cooling with Compressor Air Bleed on Gas-Turbine Engine Performance, by Jack B. Esgar and Robert R. Ziemer, *NACA RM* E54L20, March 1955, 45 pp. (Declassified from Confidential by authority of *NACA Res. Abstracts* 111, p. 12, Jan. 28, 1957.)

Effect of Properties of Primary Fluid on Performance of Cylindrical Shroud Ejectors, by Fred D. Kochendorfer, *NACA RM* E53124a, March 1954, 32 pp. (Declassified from Confidential by authority of *NACA Res. Abstracts* 111, p. 12, Jan. 28, 1957.)

Bubble Growth Rates in Boiling, by Peter Griffith, *Mass. Inst. Tech., Div. Indust. Cooperation, Contract No. N5-ori-07827, Tech. Rep.* 8, June 1956, 20 pp., 16 fig.

The Thermodynamics of Bubbles, by John A. Clark, *Mass. Inst. Techn., Div. Indust. Cooperation, Contract No. N5-ori-07827, Tech. Rep.* 7, Jan. 1956, 33 pp., 7 fig.

The Influence of Vortex Generators on the Performance of a Short 1.9:1 Straight-Wall Annular Diffuser with a Whirling Inlet Flow, by Charles C. Wood and James T. Higginbotham, *NACA RM* L52L01a, Feb. 1953, 38 pp. (Declassified from Confidential by authority of *NACS Res. Abstracts* 111, p. 15, Jan. 28, 1957.)

Performance Characteristics of a 24° Straight-Outer-Wall Annular-Diffuser-Tail-pipe Combination Utilizing Rectangular Vortex Generators for Flow Control, by Charles C. Wood and James T. Higginbotham, *NACA RM* L53H17a, Oct. 1953, 33 pp. (Declassified from Confidential by authority of *NACA Res. Abstracts* 111, p. 16, Jan. 28, 1957.)

A Mathematical Treatment of Turbulent Diffusion, II: Diffusion of Particle Pairs, by R. W. Davies and R. J. Diamond, *Amer. Inst. Aerological Res., Tech. Rep.* 235, Dec. 1954, 49 pp.

Summary of Conference on Bubble Dynamics and Boiling Heat Transfer Held at the Jet Propulsion Laboratory, June 14 and 15, 1956, *Calif. Inst. Tech., Jet Propulsion Lab., Mem.* 20-137, Dec. 1956, 41 pp.

Thermal Conductivity Measurements, by J. M. Davidson, *Atomic Energy Comm.*, HW-47063, Dec. 1956, 18 pp.

Methods of Measuring the Thermal Conductivity of Solids; a Bibliography, by

How to be a magnetic tape recording expert

Introducing a useful new brochure on tape in instrumentation

Tape is the stuff of which memories are made – the versatile data memories for a jet propelled age of electronic miracles. If you are one who keeps up with times and techniques, it is a field well worth knowing. This new brochure gives a wide-angle view of the whole subject.

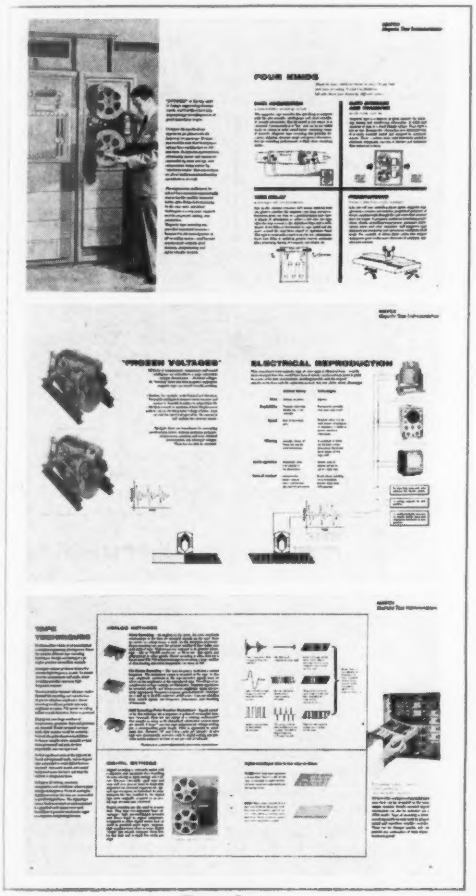

Typical pages

What kinds of applications do you think of when magnetic tape recording is mentioned? Sound recording, of course, and telemetering, if you are in that business. But what about simulating a rough road to test truck axles, controlling a milling machine to cut an aircraft wing section out of a solid billet, monitoring for a sudden occurrence that may happen only once in a year or two, recording data that can be reduced to graphs and tabulations without ever being touched by human hands? These and many more are described.

How significant is the fact that magnetic tape recording reproduces data in the same electrical form in which it was recorded? Enormously important, when you realize all the things the reproduced data can do that couldn't be done with the original signals or with the common forms of visual recording. For example the data can be slowed down to look at fast transients. It can be speeded up for wave analysis. It can be read out in any form. A tabular comparison between original signals and taped signals gives the full story. And a step-by-step pictorial demonstration of magnetic tape recording and reproduction puts the electrical-data idea into tangible, easily visualized form.

What does the data on magnetic tape look like? You can't see it, but the brochure will give you an idea of what it would be like if you could. And incidentally this may help to clarify the differences between various magnetic-tape-recording techniques.

Do you talk in tape's language? When is a tape recorder not a recorder? What is the difference between a channel and a track? What is a servo speed control? A much needed glossary gives the consensus of our views on terms.

For whom did we write this booklet . . . the expert, or the man for whom the whole subject is new? Both. It is written and illustrated so that any engineer or technically trained person can readily grasp the concepts and gain a broad understanding of the subject. If you are one of those who has already worked extensively with tape, you will find some new twists in the way the subject is explained, and perhaps ideas on new areas you hadn't explored. And incidentally, a copy of this brochure in some handy file will give you a good start in indoctrinating that new man in the department.

For your copy, write us today on your company's letterhead. Address your request to Department A 5

INSTRUMENTATION DIVISION

AMPEX
CORPORATION

FIRST IN MAGNETIC TAPE INSTRUMENTATION

934 CHARTER STREET · REDWOOD CITY, CALIFORNIA

District offices serving all areas of the United States and Canada; Foreign Representatives in countries around the world.

MAGNETIC TAPE APPLICATIONS BY AMPEX

5

Series FR-100

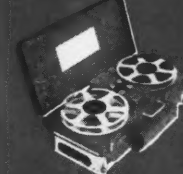

Series 800 Mobile and Airborne

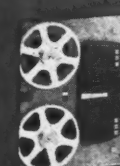

Model FR-200 Digital

Series FL-100 Loop Recorders

Series FR-1100

G. L. Cooper, *Gt. Brit. Atomic Energy Res. Estab. Inf./Bibliog.* 104, 1956, 10 pp.

Analog Computers Calculate Heat Transfer, by Robert S. Schechter, *Petroleum Refiner*, vol. 36, Feb. 1957, pp. 112–114.

Combustion

Photographic Studies of Turbulent Flame Structure, by Joseph Grumer, Joseph M. Singer, J. Kenneth Richmond and James R. Oxendine, *Indust. Engng. Chem.*, vol. 49, Feb. 1957, pp. 305–312.

Numerical and Physical Calculations, Application to Thermokinetics, by Pierre Vernotte, *France, Ministère de l'Air, Pub. Sci. Tech.* no. 319, 1956, 344 pp. (in French).

Investigation of Flame Stability and Drag Losses for Flame Holders in a Free Stream, by Gustave G. Kutzko, *Wright Air Dev. Center, Tech. Rep.* 55-429, (ASTIA AD 110495), Nov. 1955, 51 pp.

Effect of Particle Size on Combustion of Uniform Suspensions, by J. A. Browning, T. L. Tyler and W. G. Krall, *Indust. Engng. Chem.*, vol. 49, Jan. 1957, pp. 142–147.

On the Existence of Steady-State Detonations Supported by a Single Chemical Reaction, by W. W. Wood and J. G. Kirkwood, *J. Chem. Phys.*, vol. 25, Dec. 1956, pp. 1276–1277.

Stability and Burning Velocities of Laminar Carbon Monoxide-Air Flames at Pressures up to 93 Atmospheres, by Rudolph Edse and William A. Strauss, *J. Chem. Phys.*, vol. 25, Dec. 1956, pp. 1241–1245.

Application of Probability Theory to Explosive-Ignition Phenomena, by Ransom B. Parlin and J. Calvin Giddings, *J. Chem. Phys.*, vol. 25, Dec. 1956, pp. 1161–1166.

The Slow Combustion of Methyl Alcohol, a General Investigation, by K. M. Bell and C. F. H. Tipper, *Proc. Royal Soc.*, vol. A238, no. 1213, Dec. 1956, pp. 256–268.

Ignition of Solid Propellants by Forced Convection, by S. W. Churchill, R. W. Kruggel and J. C. Brier, *A. I. Ch. E. J.*, vol. 2, Dec. 1956, pp. 586–589.

Study of Combustion and Heat Transfer Fundamentals in Small Diameter Tubes, by Forrest G. Hammaker, Jr., and Thomas E. Hampel, *Amer. Gas Assoc. Labs., Res. Rept.*, 1225, Aug. 1956.

On the Limit of Stable Flame Propagation in Gases at Variable Pressure, by D. I. Abugov, *Akad. Nauk USSR, Doklady*, vol. 112, no. 1, 1957, pp. 86–89 (in Russian).

A Contribution to Flame Theory, by G. Klein, *Roy. Soc., Phil. Trans.*, vol. 249, Feb. 21, 1957, pp. 389–415.

On the Solution of the Equation of Internal Ballistics with a Cubic Form Function, by N. S. Venkatesan, *Proc. Nat. Inst. Sci. India*, vol. 22, May 26, 1956, pp. 129–136.

Fuels, Propellants and Materials

Valence in the Boron Hydrides, by William N. Lipscomb, *J. Phys. Chem.*, vol. 61, Jan. 1957, pp. 23–27.

The Character of Bonding of Radicals to Aromatic and Olefinic Compounds, by M. Szwarc, *J. Phys. Chem.*, vol. 61, Jan. 1957, pp. 40–45.

Theoretical Combustion Performance of Ramjet Fuels: Hydrogen, by Waldo T. Reimich, *Johns Hopkins Univ., Appl. Phys. Lab.*, CF-2601, Dec. 1956, 4 pp., 5 fig.

Fluorine Propellant Study, Quarterly Progress Report for Period Ending 30 November 1956, *North American Aviation Inc., Rocketdyne Div., Rep.* R-334-2, Dec. 1956, 11 pp.

Kinetics of Gaseous Reactions in the Range 1000° to 1800° C; Study at High Temperatures of the Reactions Between Nitrogen and Metals, Particularly Magnesium and Aluminum, by Farrington Daniels, *Wright Air Dev. Center, Tech. Rep.* 56-536, (*ASTIA AD* 110498), July 1956, 27 pp.

Electronic Spectrum of Trapped Ethanol Radicals, by M. C. R. Symons and M. Townsend, *J. Chem. Phys.*, vol. 25, Dec. 1956, pp. 1299–1303.

Study of the Thermal Decomposition of Methane, by F. William Cagle, Jr., *J. Chem. Phys.*, vol. 25, Dec. 1956, pp. 1300–1301.

Protecting Molybdenum at High Temperatures, by J. J. Harwood, *Materials and Methods*, vol. 44, Dec. 1956, pp. 84–89.

Case for Jelly Propellants, *Missiles and Rockets*, vol. 2, Feb. 1957, p. 84.

Approach to Solid Propellants, *Missiles and Rockets*, vol. 2, Feb. 1957, p. 92.

Plastic Properties at High Temperature of Oneral M47 Cast Refractory Alloy, by H. Bibring and J. Poulignier, *La Recherche Aéronautique*, no. 54, Nov.-Dec. 1956, pp. 49–54 (in French).

The Energy of Interaction between Two Excited Hydrogen Atoms, by Bruno Linder and Joseph O. Hirschfelder, *Univ. Wisconsin, Naval Res. Lab., Rep.* WIS-AEC-8, Nov. 1956, 89 pp.

The Repulsive Interaction of Atoms in S States, by R. A. Buckingham, *University of Wisconsin, Naval Res. Lab., Rep.* WIS-AEC-9, Dec. 1956, 11 pp.

Tables of Chemical Kinetics; Homogeneous Reactions, *Nat. Bur. Stand., Circ.* 510, *Suppl.* 1, Nov. 1956, 472 pp.

Instrumentation and Experimental Techniques

Preliminary Investigation of the Effect of Surface Treatment on the Strength of a Titanium Carbide–30 Percent Nickel Base Cermet, by Leonard Robins and Edward M. Grala, *NACA TN* 3927, Feb. 1957.

Needed: Breakthrough on 1,800°F Alloys, by William Beller, *American Aviation*, vol. 20, Feb. 25, 1957, p. 43.

Design of an Air Supply System and Test Section for Research on Scavenging Systems for Propulsion Wind Tunnels, by John G. Wilder, Kenneth Hindersinn and Roger Weatherston, *Wright Air Dev. Center, Tech. Rep.* 56-6, May 1956, 56 pp.

A Bonded Strain Gage Differential Pressure Transducer, Its Design and Properties, by A. W. Kolb and E. J. Szczepanik, *Wright Air Dev. Center, Tech. Note* 56-284, (*ASTIA AD* 97231), June 1956, 9 pp.

Summary Report on the Development of a Hot Wire Turbulence Sensing Element for Use in Water, by R. G. Stevens, A. Borden and P. E. Strausser, *David W. Taylor Model Basin, Rep.* 953, Dec. 1956, 18 pp.

Theory and Design of a Pneumatic Temperature Probe and Experimental Results Obtained in a High-Temperature Gas Stream, by Frederick S. Simmons and

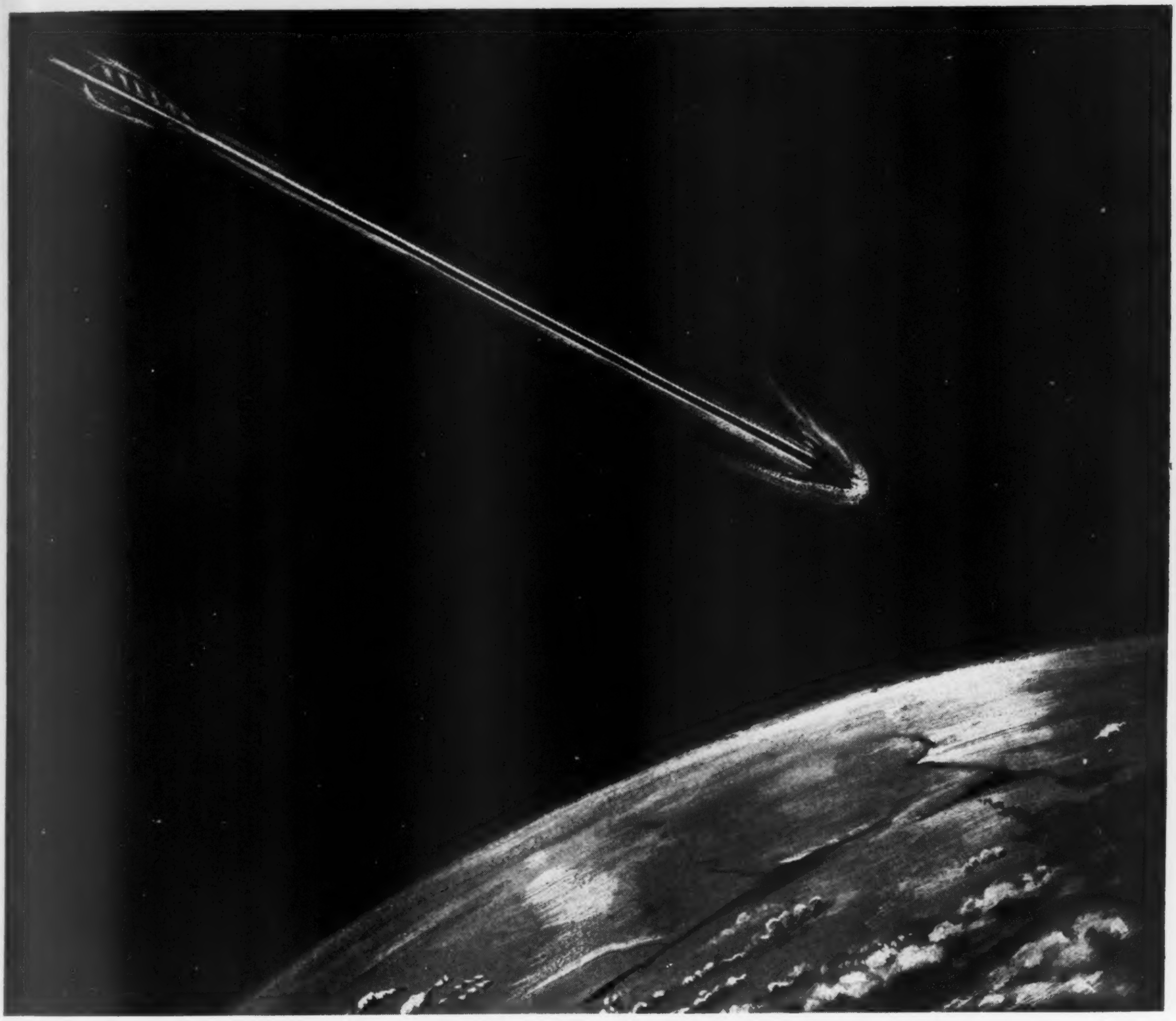

When the tip sublimes!

Away up where it's cold, black and lonely at 500,000 ft., the thermal attack on a missile or "airplane" isn't very meaningful. The air molecules at that height are barely nodding neighbors, rather than crammed together in a fluid mass. But, escape and re-entry into the earth's dense envelope of atmosphere generate thermal attacks of frightening ferocity. Nose and leading-edge temperatures may rise to 3000°F.

Even titanium won't stand such temperatures for more than a few minutes. For all those areas requiring long-time service life up to 1000°F, however, titanium's light weight, great strength and corrosion resistance offer outstanding design advantages.

Production quantities of very high strength heat-treated sheet, to close gage and flatness tolerances, are being engineered into advanced aircraft and missiles. For non-military applications, all types of mill products are obtainable at constantly lower price levels.

T.M.C.A. is again adding to its production facilities to properly service an ever-expanding market. T.M.C.A. engineering service and technical literature are readily available to all those industries challenged by weight, strength and corrosion problems.

. . . FIRST IN *Titanium* . . . .

TITANIUM METALS CORPORATION OF AMERICA, 233 Broadway, New York 7, N.Y.

George E. Glawe, *NACA TN* 3893, Jan. 1957, 41 pp.

The Hot Wire Anemometer for Turbulence Measurements, Part III, by B. Wise and D. L. Schultz, *Gt. Brit., Aeron. Res. Council, Curr. Pap.* 275 (formerly *ARC Tech. Rep.* 16679; *Oxford Univ. Engng. Lab., Rep.* 69), 1956, 35 pp., 80 fig.

Optical Aspect System for Rockets, by James E. Kupperian, Jr., and Robert W. Kreplin, *Rev. Sci. Instr.*, vol. 28, Jan. 1957, pp. 14–19.

Rocket Test Facilities, *Redstone Arsenal, Rocket Dev. Labs., Brochure* No. 1, Jan. 1957, 11 pp.

Method for Improving Sensitivity and Stability of an On-Off Temperature Control, by A. Michels and D. Ritzke, *Applied Sci. Res.*, Sect. B., vol. 6, no. 3, 1956, pp. 137–143.

High Framing Rate, Argon Flash Field Photography, by Robert G. S. Sewell, Lawrence N. Cosner, Henry W. Wedaa and Rolland Gallop, *NAVORD Rep.* 5298 (*NOTS* 1528), Oct. 1956, 21 pp.

A Precision Calorimeter for the Measurement of Heats of Combustion, by Charles E. Holley, Jr., and Elmer J. Huber, Jr., *Atomic Energy Comm.*, LA-2084, Nov. 1955. 18 pp.

Terrestrial Flight, Aerophysics

U.S. Military Aircraft; U.S Missiles; U.S.S.R. Aircraft; Foreign Aircraft. *Aviation Week*, vol. 66, Feb. 25, 1957, 24th Annual Inventory of Air Power, pp. 223–224, 225–226, 227, 238–241.

The Surface-to-Surface Missile, Today and Yesterday (III), by F. I. Ordway, *Interavia*, vol. 12, Feb. 1957, pp. 134–137.

On the Motion of a Projectile in the Atmosphere, by V.-Ch. Liu, *ZAMM*, vol. 8, no. 1, Jan. 25, 1957, p. 76–82(in English).

Prediction of the Motion of Missiles Acted on by Non-Linear Forces and Moments, by Charles H. Murphy, *Aberdeen Proving Ground, Ballistic Res. Lab., BRL Rep.* 995, Oct. 1956, 79 pp.

Jettisonable Cart Speeds Regulus Launching, *Aviation Age*, vol. 27, March 1957, pp. 48–59.

A Note on Missile Launching, by Telford W. Oswald, *J. Aeron. Sci.*, vol. 24, Jan. 1957, pp. 74–76.

Navy Missiles, Roles and Missions, by Rear Adm. James S. Russell, *Missiles and Rockets*, vol. 2, Jan. 1957, pp. 38–41.

Navy Missile Arsenal, *Missiles and Rockets*, vol. 2, Jan. 1957, p. 42.

Polaris: Navy's New Entry in Missile Race, by Henry T. Simmons, *American Aviation*, vol. 20, Jan. 14, 1957, pp. 25–26.

Convection from the Earth's Surface, by C. H. B. Priestley, *Proc. Royal Soc.*, vol. A238, Jan. 8, 1957, pp. 287–304.

Russia's Guided Missile Program, *Missiles and Rockets*, vol. 2, Feb. 1957, pp. 33–41.

What the Russians Tell . . . and Don't Tell, by Professor Albert Parry, *Missiles and Rockets*, vol. 2, Feb. 1957, pp. 70–72.

Aeroballistic Forecasting at Redstone, *Missiles and Rockets*, vol. 2, Feb. 1957, p. 86.

Soviet Missile Science Profile, *Missiles and Rockets*, vol. 2, Feb. 1957, pp. 61–63, 65–67.

Space Flight, Astrophysics

Ion, Proton Power Space Travel Hope, by Irving Stone and Richard Sweeney,


MEASURE MOVING WEIGHT
WEIGH TANKS, BINS, HOPPERS
WEIGH BY CRANE OR HOIST
MEASURE THRUST

Report on the Astronautics Symposium in San Diego, sponsored by the Air Force Office of Scientific Research and Convair, *Aviation Week*, vol. 66, March 4, 1957, pp. 103–113.

Legal Problems of Upper Space, by John Cobb Cooper, *J. British Interplan. Soc.*, vol. 15, Nov.-Dec. 1956, pp. 305–307.

The Descent of an Earth-Satellite through the Upper Atmosphere, *J. British Interplan. Soc.*, vol. 15, Nov.-Dec. 1956, pp. 314–323.

Orientation in Space, by M. Vertregt, *J. British Interplan. Soc.*, vol. 15, Nov.-Dec. 1956, pp. 324–338.

Need for Space Flight Know-how, by Cdr. George W. Hoover, *Missiles and Rockets*, vol. 2, Jan. 1957, pp. 47–48.

European Rocket Engineers in Argentine Astronautics, by F. C. Durant III, *Missiles and Rockets*, vol. 2, Jan. 1957, pp. 82, 84, 86.

The Vanguard Satellite, by Clifford C. Furnas, *Ordnance*, vol. 41, Jan.–Feb. 1957, pp. 596–599.

Atomic Energy

Power from Thermonuclear Reactions, by J. G. Linhart, *Nuclear Engng.*, vol. 2, Feb. 1957, pp. 60–65.

Materials in a Nuclear Environment, by A. J. Mione, *Inst. Aeron. Sciences, Preprint*, Jan. 28–31, 1957, 8 pp.

Nuclear Power for Aircraft, by W. H. L. Porter, *Atomics*, vol. 8, Jan. 1957, pp. 7–14.

Selecting Key Instruments for Nuclear Reactors, by C. C. Scott and T. A. DeBacker, *Control Engng.*, vol. 4, March 1957, pp. 92–97.

How Soon Will We Get Fusion Power?—A Progress Report, by Andrew W. Kramer, *Power Engng.*, vol. 61, Feb. 1957, pp. 75–78.

Bibliography on the Atomic Rocket and Nuclear Propulsion, by Maurice H. Smith, *Princeton Univ., James Forrestal Res. Center, Lit. Search* 11, Feb. 1957, 33 pp.

A Nuclear-Electric Propulsion System, by R. W. Bussard, *J. British Interplan. Soc.*, vol. 15, Nov.-Dec. 1956, pp. 297–304.

Liquid Metals and Nuclear Power, Part I, by C. D. Boadle, *Atomics*, vol. 8, Feb. 1957, pp. 41–45.

Select Best High-Temperature Coolant, by W. E. Parkins, *Chem. Engng.*, vol. 64, March 1957, pp. 253–256.

Some Aspects of Atomic Power Development in the USSR, by I. V. Kurchatov, *J. Nuclear Energy*, vol. 4, Jan. 1957, pp. 59–66.

Boron Carbide Looks Promising for Nuclear Uses, by C. W. Henson, *Materials and Methods*, vol. 44, Dec. 1956, pp. 96–98.

How Radiation Changes Materials, by Michael Ference, Jr., *SAE J.*, vol. 65, Feb. 1957, pp. 49–50.

Nuclear Heat Powerplants for Vehicles, by F. L. Schwartz and H. A. Ohlgren *SAE J.*, vol. 65, Feb. 1957, pp. 56–60.

Nuclear-Powered Aircraft, by Lee A. Ohlinger, *SAE J.*, vol. 65, Feb. 1957, pp. 61–64.

Effects of Radiation on Materials, by Michael Ference, Jr., *SAE, Prepr.* 3, Jan. 1957, 10 pp., 7 fig.

The Atom and SAE: Report of the Nuclear Advisory Committee, by C. R. Lewis, *SAE, Prepr.* 2, Jan. 1957, 5 pp.

on guard . . .
the NIKE HERCULES
To guard our cities and other vital areas the Army's new Nike is more powerful than ever before.
Designated Nike Hercules, the ground-to-air missile maneuvers with pin-point accuracy at extremely high altitudes to intercept today's most advanced aircraft.
The range and other details of the Nike Hercules are secret. But to propel the lethal new Nike at supersonic speed to its target, Army Ordnance and Douglas Aircraft Co. chose an entirely new power plant for the missile proper—a solid propellant rocket system developed by Thiokol Chemical Corporation, one of the leaders in solid propellant engines.
Thiokol®
CHEMICAL CORPORATION
TRENTON, N. J. • ELKTON, MD. • HUNTSVILLE, ALA.
MOSS POINT, MISS. • MARSHALL, TEXAS • BRIGHAM CITY, UTAH
® Registered trademark of the Thiokol Chemical Corporation for its liquid polymers, rocket propellants, plasticizers and other chemical products.
U.S. ARMY

Rocket Logic in Retrospect

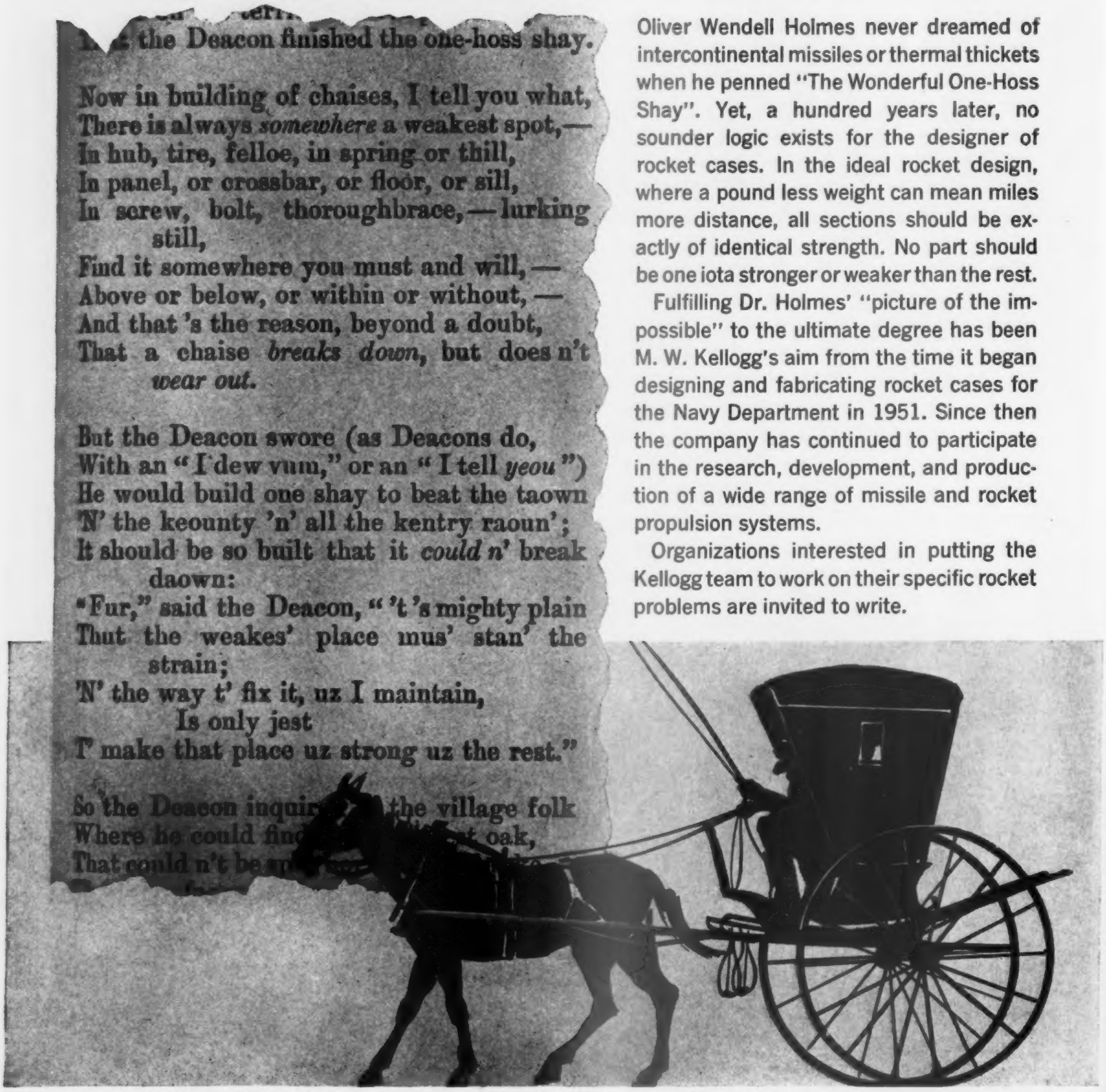

the Deacon finished the one-hoss shay.

Now in building of chaises, I tell you what,
There is always *somewhere* a weakest spot,—
In hub, tire, felloe, in spring or thill,
In panel, or crossbar, or floor, or sill,
In screw, bolt, thoroughbrace,—lurking
still,
Find it somewhere you must and will,—
Above or below, or within or without,—
And that 's the reason, beyond a doubt,
That a chaise *breaks down*, but does n't
wear out.

But the Deacon swore (as Deacons do,
With an "I dew vum," or an "I tell *yeou*")
He would build one shay to beat the taown
'N' the keounty 'n' all the kentry raoun';
It should be so built that it *could n'* break
daown:
"Fur," said the Deacon, "'t 's mighty plain
Thut the weakes' place mus' stan' the
strain;
'N' the way t' fix it, uz I maintain,
Is only jest
T' make that place uz strong uz the rest."

So the Deacon inquir the village folk
Where he could fin oak,
That could n't be sp

Oliver Wendell Holmes never dreamed of intercontinental missiles or thermal thickets when he penned "The Wonderful One-Hoss Shay". Yet, a hundred years later, no sounder logic exists for the designer of rocket cases. In the ideal rocket design, where a pound less weight can mean miles more distance, all sections should be exactly of identical strength. No part should be one iota stronger or weaker than the rest.

Fulfilling Dr. Holmes' "picture of the impossible" to the ultimate degree has been M. W. Kellogg's aim from the time it began designing and fabricating rocket cases for the Navy Department in 1951. Since then the company has continued to participate in the research, development, and production of a wide range of missile and rocket propulsion systems.

Organizations interested in putting the Kellogg team to work on their specific rocket problems are invited to write.

DEFENSE PRODUCTS DIVISION

THE M. W. KELLOGG COMPANY

711 THIRD AVENUE, NEW YORK 17, N. Y.

A SUBSIDIARY OF PULLMAN INCORPORATED

The Canadian Kellogg Company Limited, Toronto • Kellogg International Corporation, London
Companhia Kellogg Brasileira, Rio de Janeiro • Compania Kellogg de Venezuela, Caracas
Kellogg Pan American Corporation, New York • Societe Kellogg, Paris

M KELLOGG W


NIAFRAX® NOZZLES
from 1/2" to 30" φ
last the full burning time without cooling
NIAFRAX® nozzles are available in intricate shapes and can be produced to close tolerances in sizes ranging from ½" to more than 30" in diameter.
In uncooled rocket motors, NIAFRAX silicon-nitride-bonded silicon carbide refractories stand up to extreme temperatures, heat shock and erosion *for the full burning time.* In fact, NIAFRAX nozzles and liners will often last through several firings.
For details, write Dept. T77, Refractories Division, The Carborundum Company, Perth Amboy, New Jersey.
CARBORUNDUM
Registered Trade Mark

Index to Advertisers

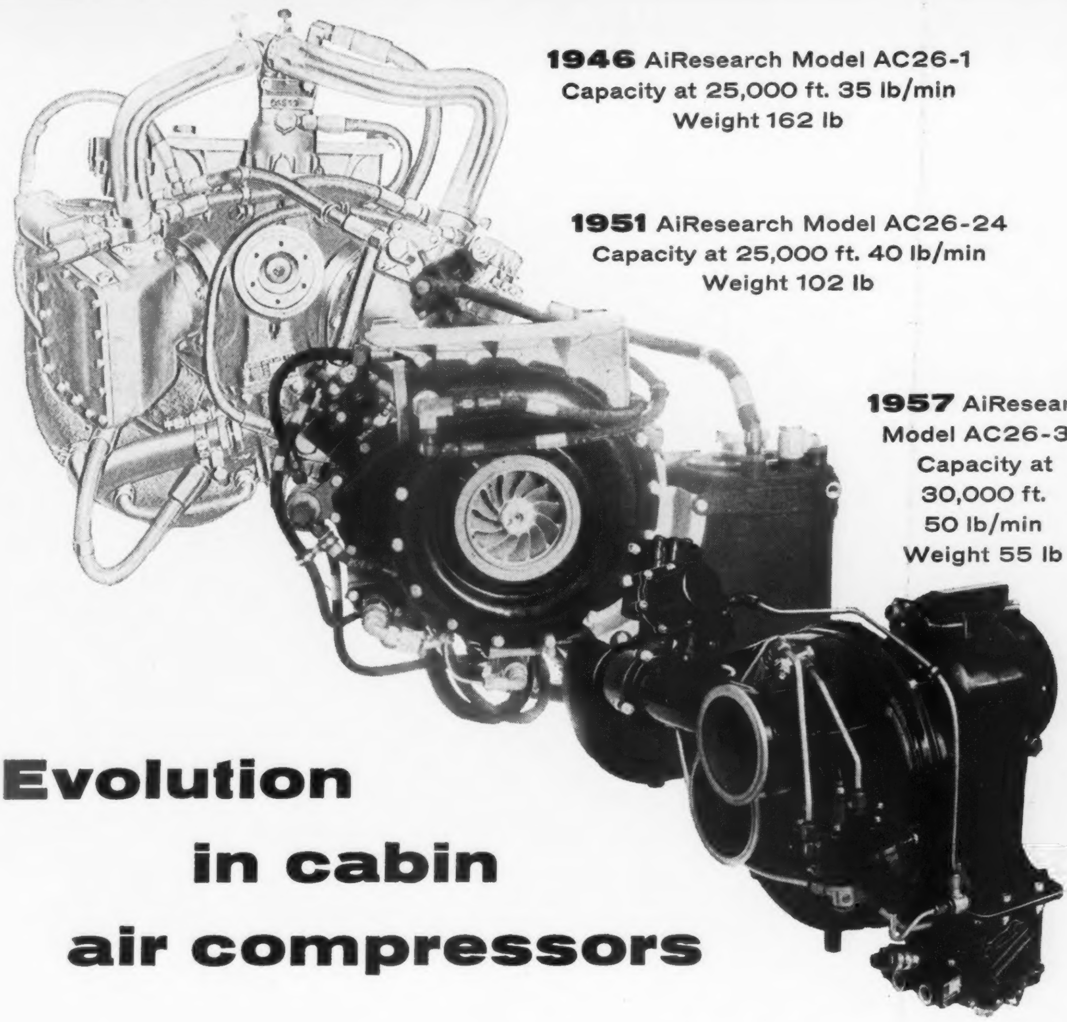

Evolution in cabin air compressors

New AiResearch unit weighs one-third as much, increases performance by 43%

The performance demands on aircraft cabin air compressors are constantly increasing. Yet weight and space limitation on these pressurization components becomes even more critical. Basic design advancement is the only solution.

AiResearch has achieved this in its new, engine-driven compressor for turboprop aircraft. Compared to earlier models, it increases output by 43% while actually cutting weight to one-third. Dependability and durability are assured by the company's extensive experience in the production of all types of cabin air compressors, including units for the latest jet transports.

Superior performance is further assured by our unmatched experience in developing compatible systems. AiResearch has assumed complete system responsibility in the field of pressurization for many of America's finest present and projected airliners. We invite your inquiries.

Outstanding opportunities for qualified engineers are available now. Write for information.

THE GARRETT CORPORATION

AiResearch Manufacturing Divisions

Los Angeles 45, California . . . Phoenix, Arizona

Designers and manufacturers of aircraft and missile systems and components: REFRIGERATION SYSTEMS • PNEUMATIC VALVES AND CONTROLS • TEMPERATURE CONTROLS CABIN AIR COMPRESSORS • TURBINE MOTORS • GAS TURBINE ENGINES • CABIN PRESSURE CONTROLS • HEAT TRANSFER EQUIPMENT • ELECTRO-MECHANICAL EQUIPMENT • ELECTRONIC COMPUTERS AND CONTROLS